ISM Dynamics and Star Formation

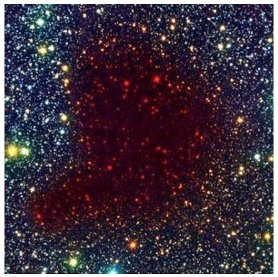
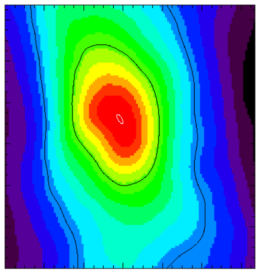

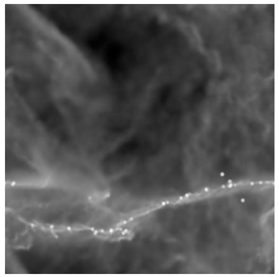

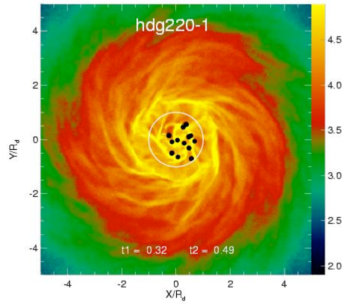

Ralf Klessen

Zentrum für Astronomie der Universität Heidelberg
Institut für Theoretische Astrophysik

thanks to ...

... people in the group in Heidelberg:

Robi Banerjee, Simon Glover, Rahul Shetty, Sharanya Sur, Daniel Seifried, Milica Milosavljevic, Florian Mandl, Christian Baczynski, Rowan Smith, Gustavo Dopcke, Jonathan Downing, Jayanta Dutta, Faviola Molina, Christoph Federrath, Erik Bertram, Lukas Konstandin, Paul Clark, Stefan Schmeja, Ingo Berentzen, Thomas Peters, Hsiang-Hsu Wang

... many collaborators abroad!

Deutsche Forschungsgemeinschaft DFG
Emmy Noether-Programm DFG
ASTRONET
LANDESSTIFTUNG Baden-Württemberg
HGSFP
IMPRS

agenda

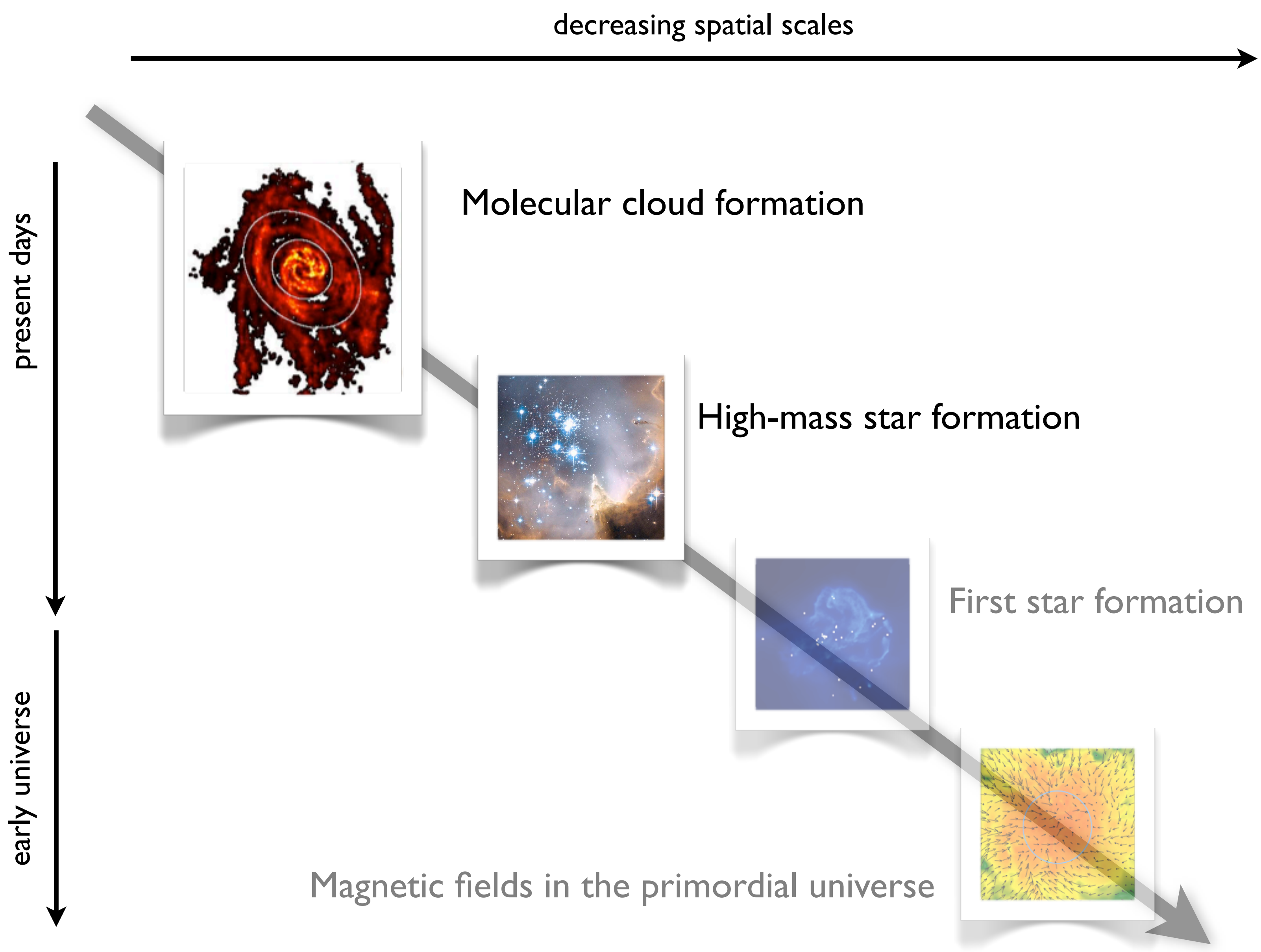
decreasing spatial scales
present days
early universe
Molecular cloud formation
High-mass star formation
First star formation
Magnetic fields in the primordial universe


NGC 602 in the LMC: Hubble Heritage Image

stellar mass fuction

stars seem to follow a universal mass function at birth --> IMF

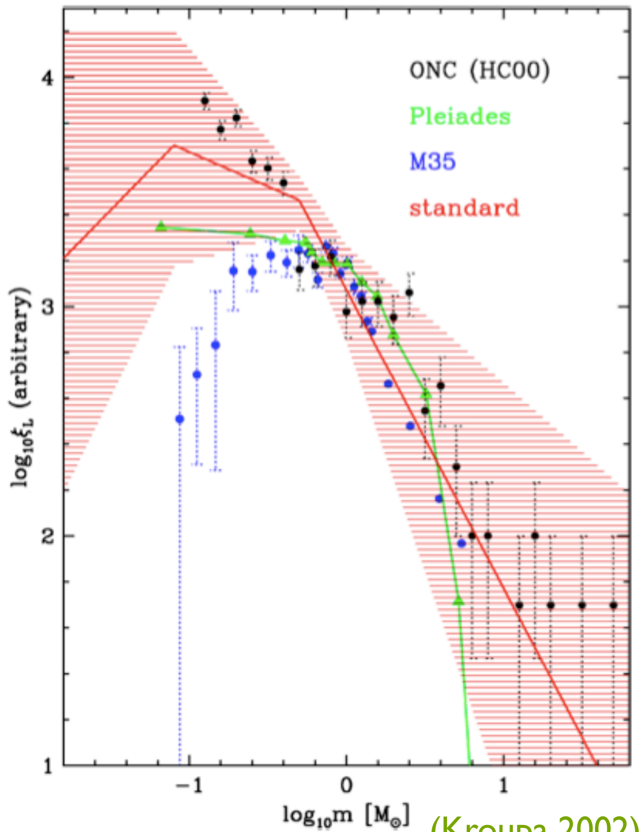

(Kroupa 2002)

Orion, NGC 3603, 30 Doradus
(Zinnecker & Yorke 2007)

nearby molecular clouds

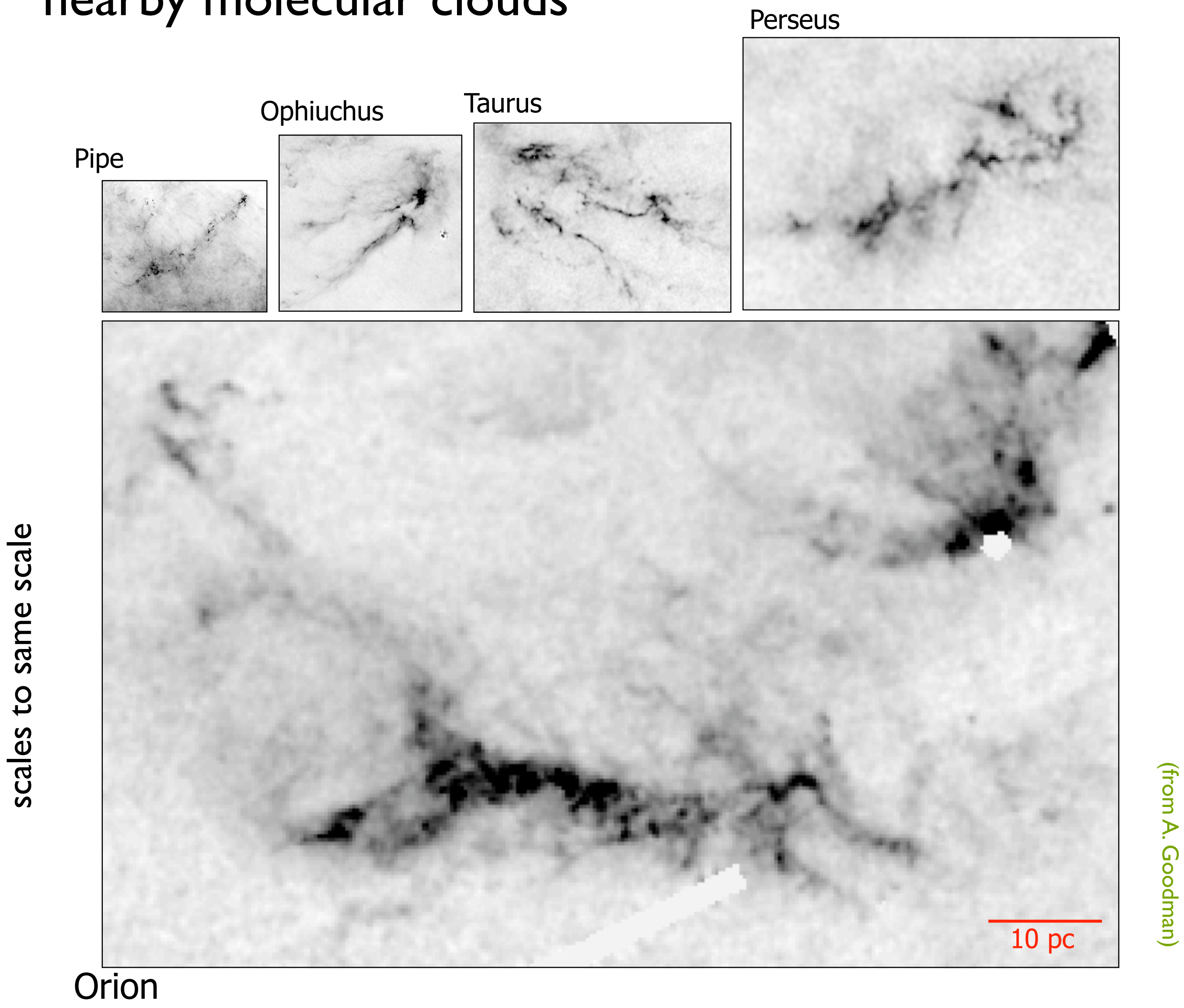

nearby molecular clouds

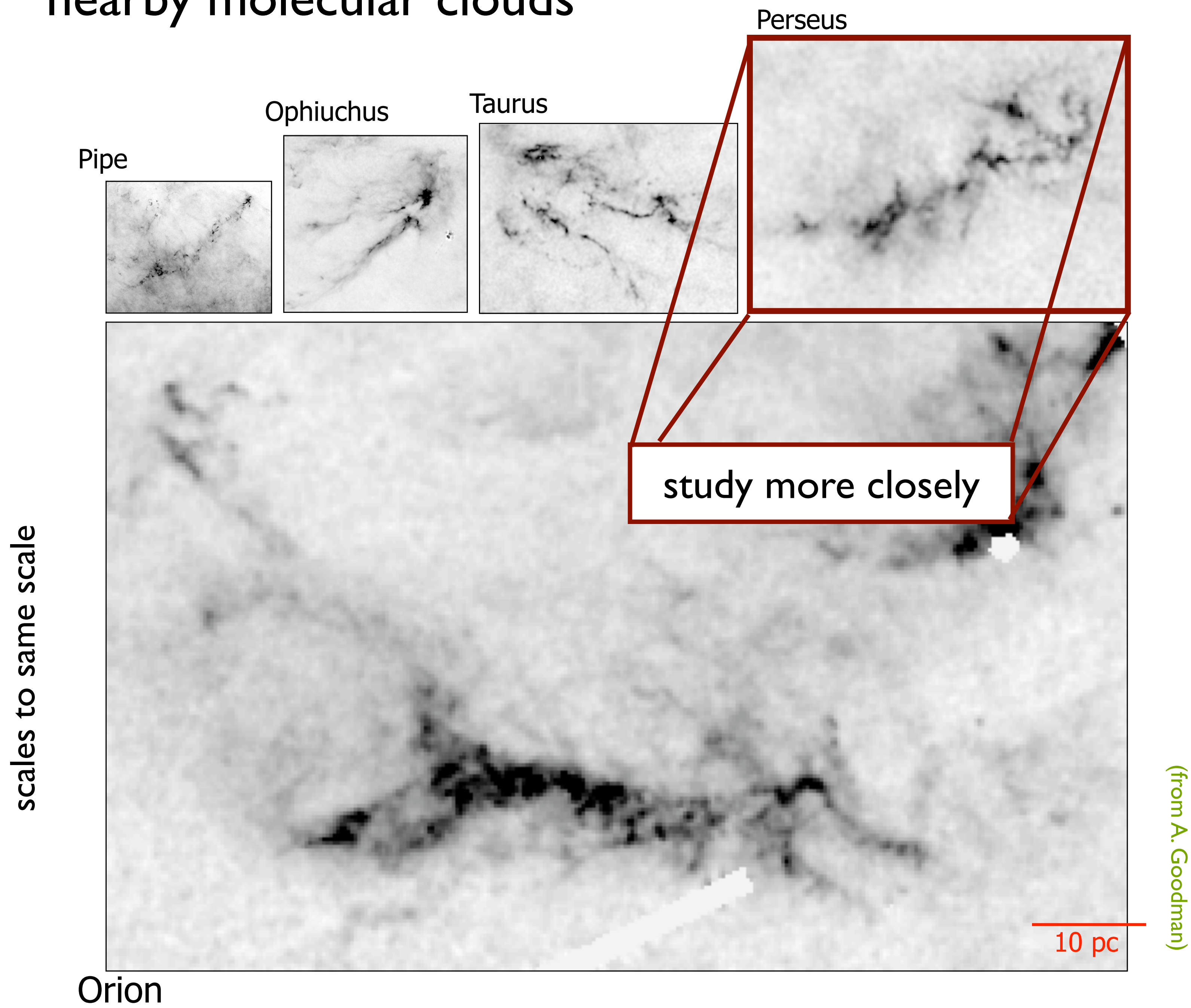

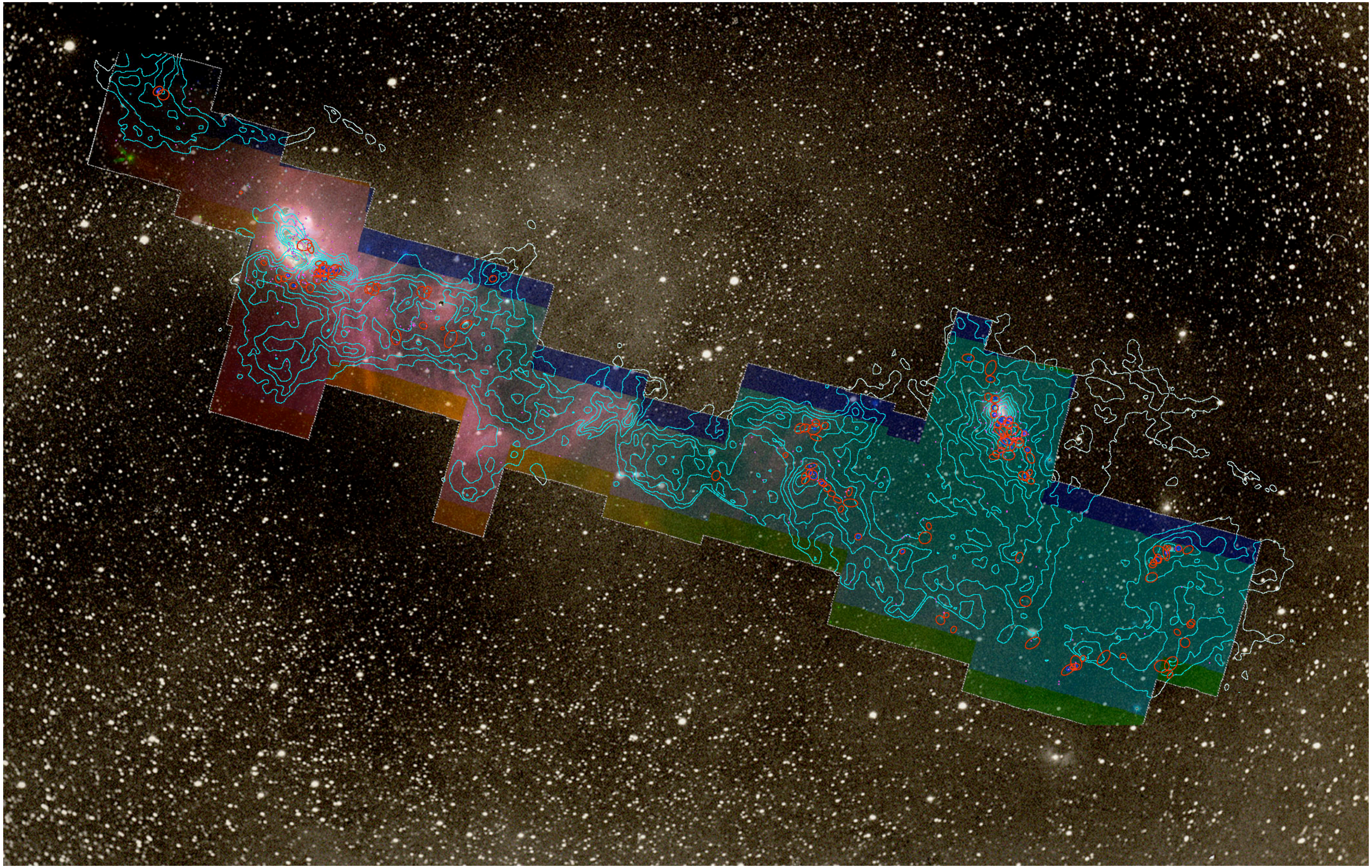

image from Alyssa Goodman: COMPLETE survey

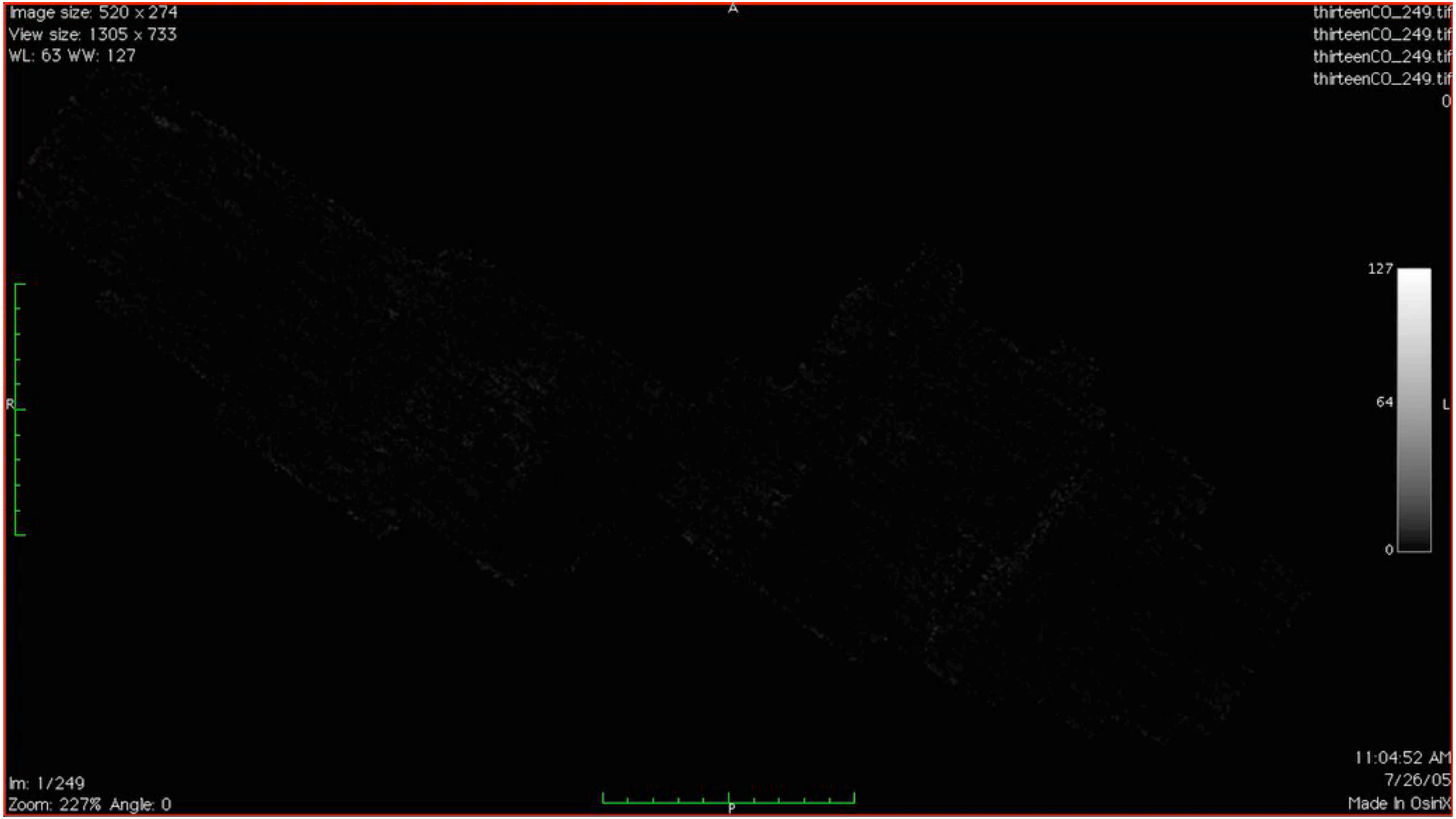

velocity distribution in Perseus

velocity cube from Alyssa Goodman: COMPLETE survey

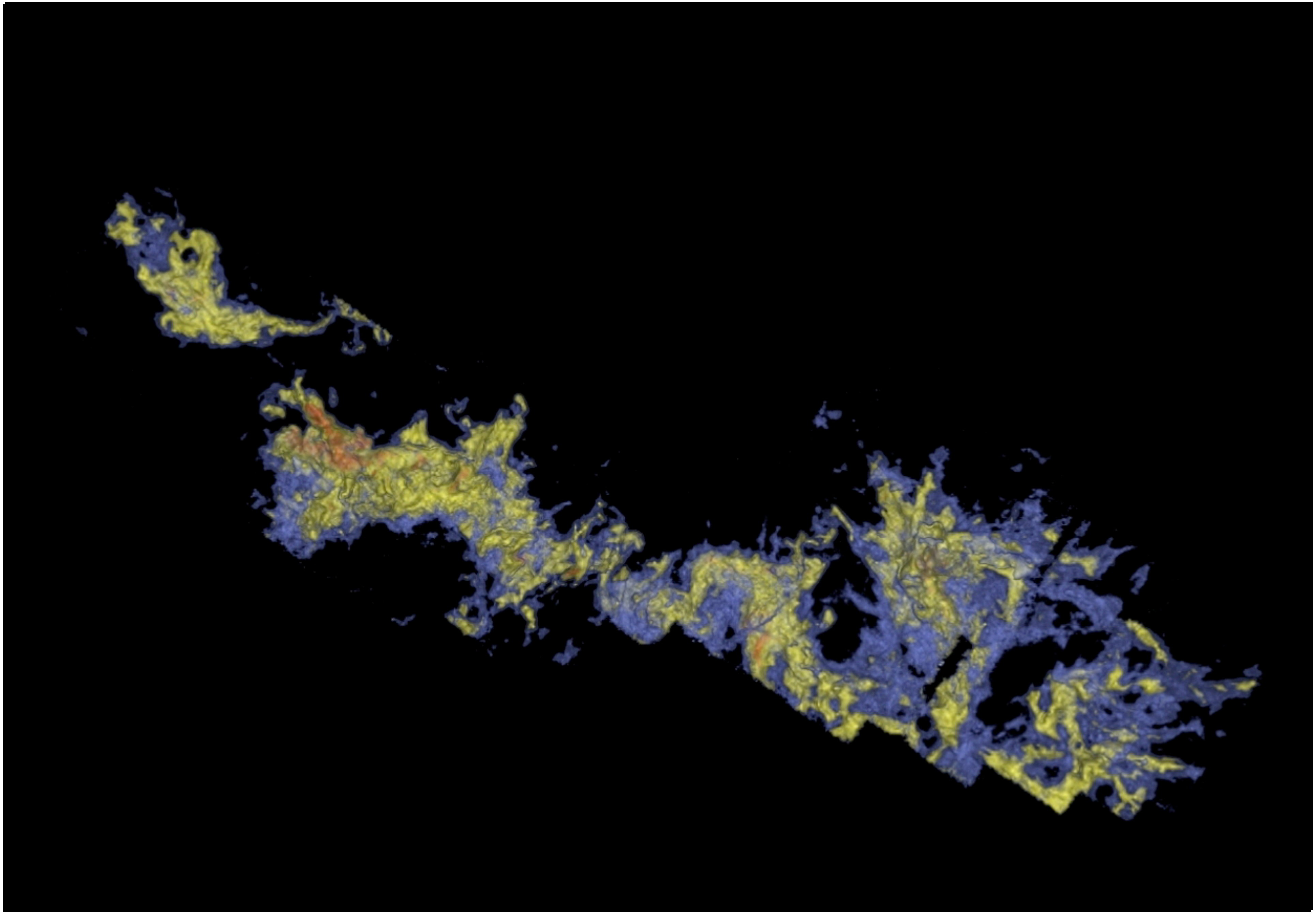

image from Alyssa Goodman: COMPLETE survey

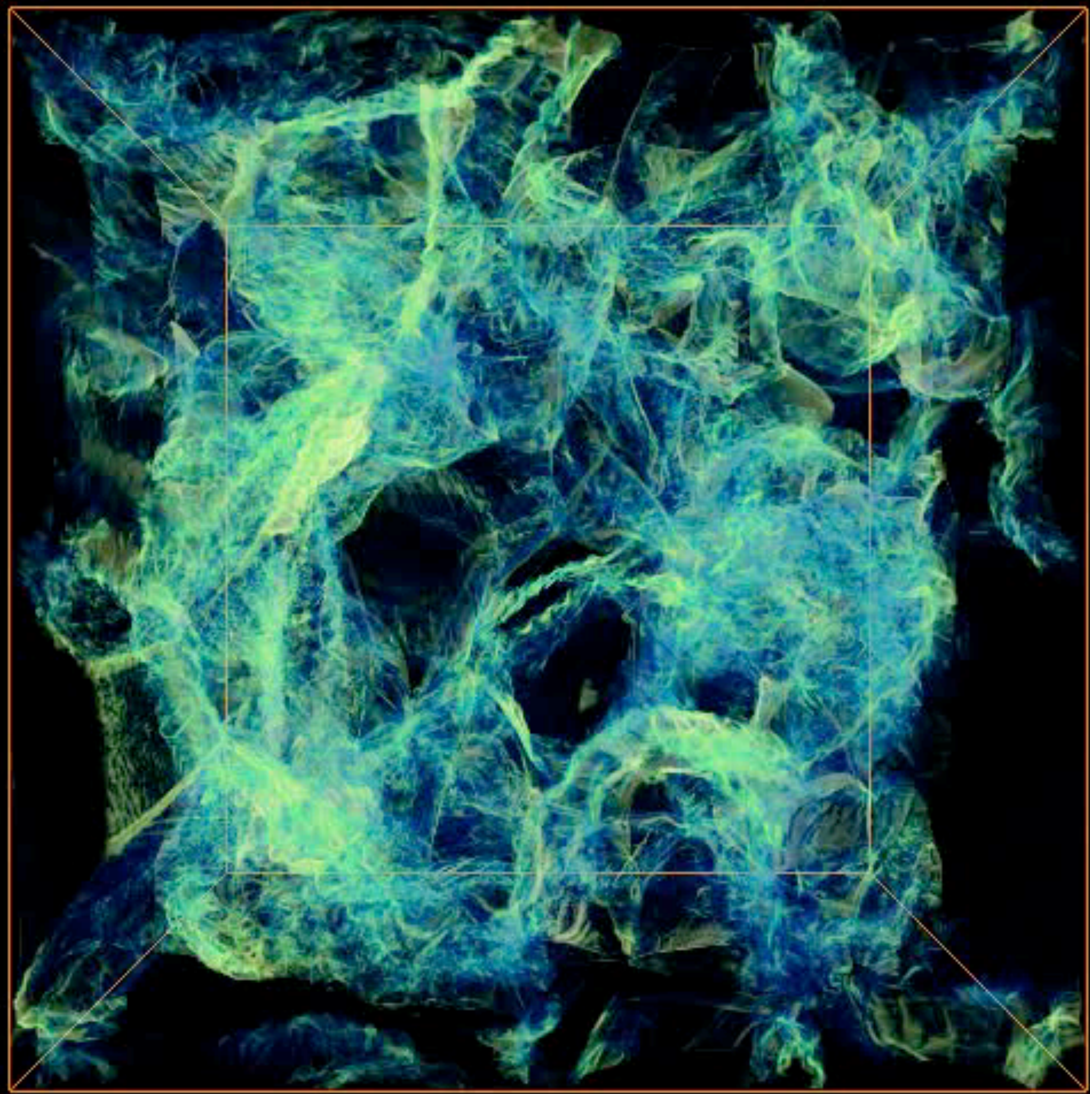

(movie from Christoph Federrath)

Turbulent cascade

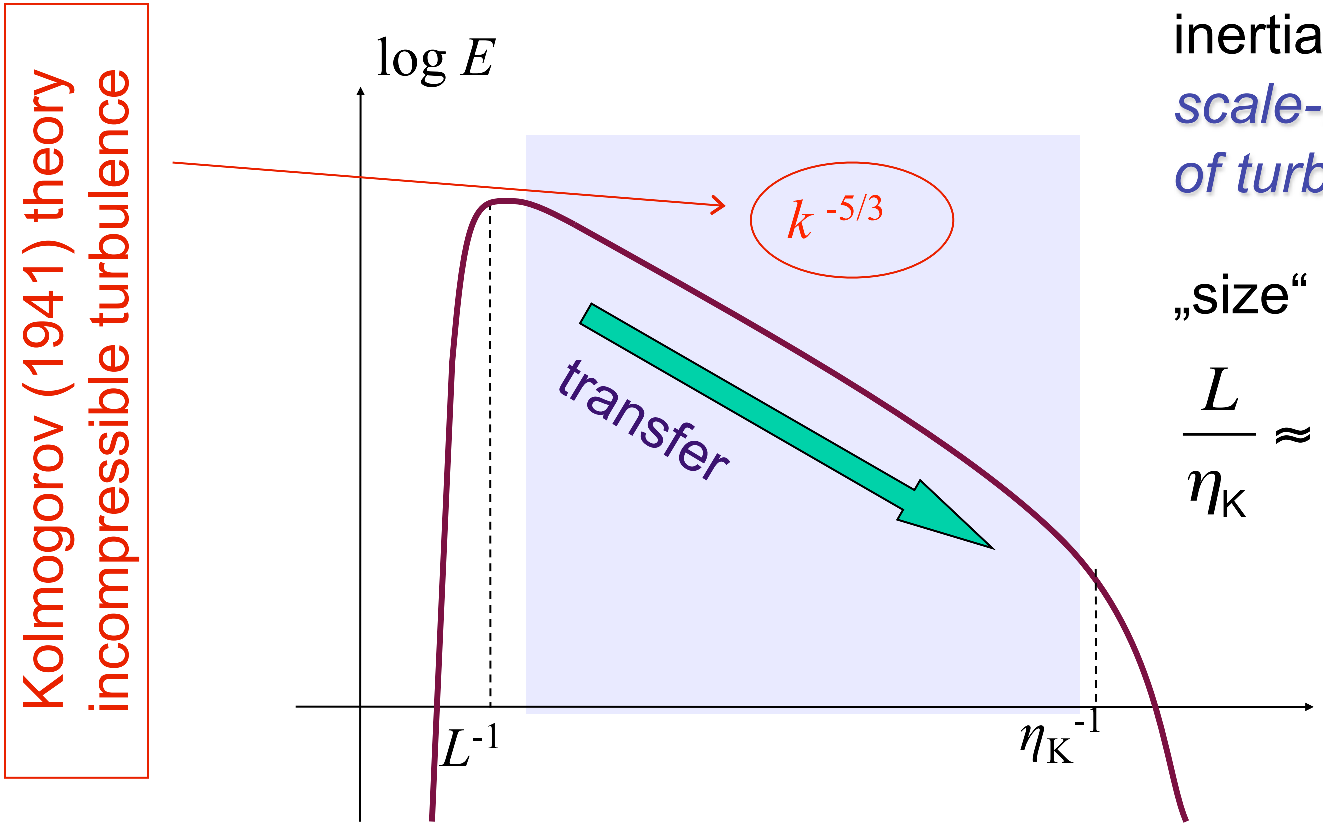

inertial range:
scale-free behavior of turbulence

„size“ of inertial range:

$$\frac{L}{\eta_K} \approx \mathrm{Re}^{3/4}$$

energy input scale

energy dissipation scale

Turbulent cascade

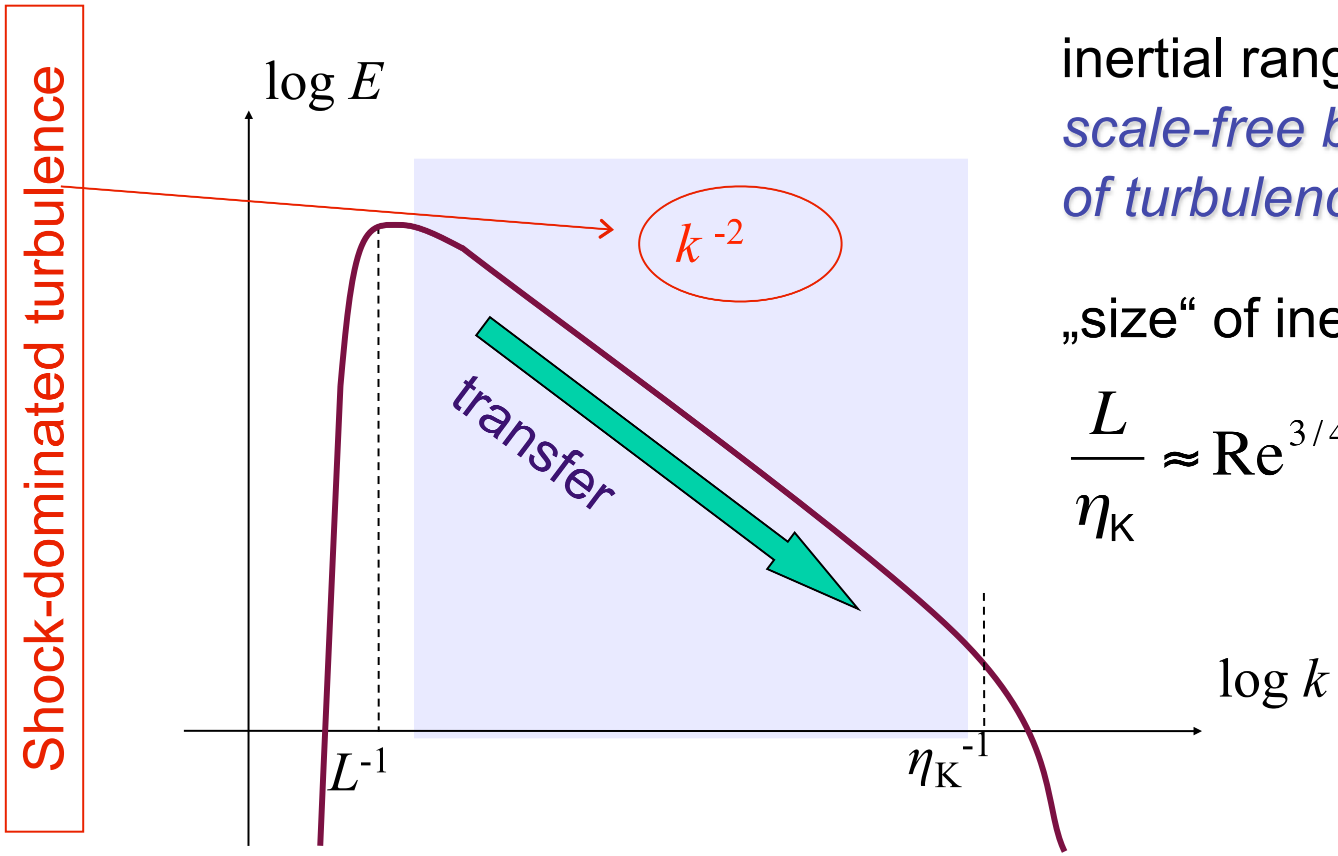

inertial range:
scale-free behavior of turbulence

„size“ of inertial range:

$$\frac{L}{\eta_K} \approx \mathrm{Re}^{3/4}$$

energy input scale

energy dissipation scale

Turbulent cascade in ISM

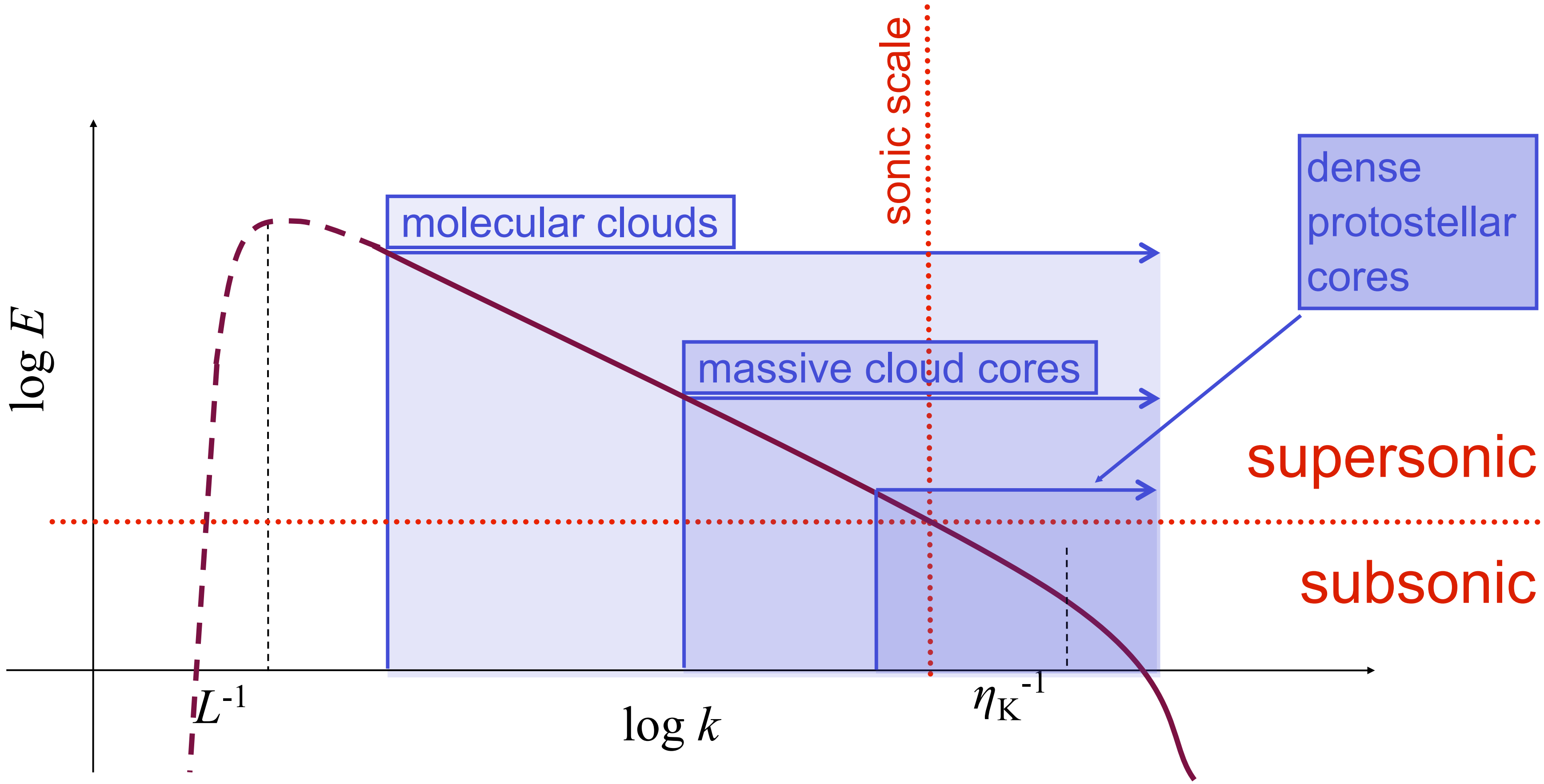

energy source & scale
NOT known
(supernovae, winds,
spiral density waves?)

σ_{rms} << 1 km/s
$M_{rms} \leq 1$
$L \approx 0.1$ pc

dissipation scale not known
(ambipolar diffusion,
molecular diffusion?)

agenda

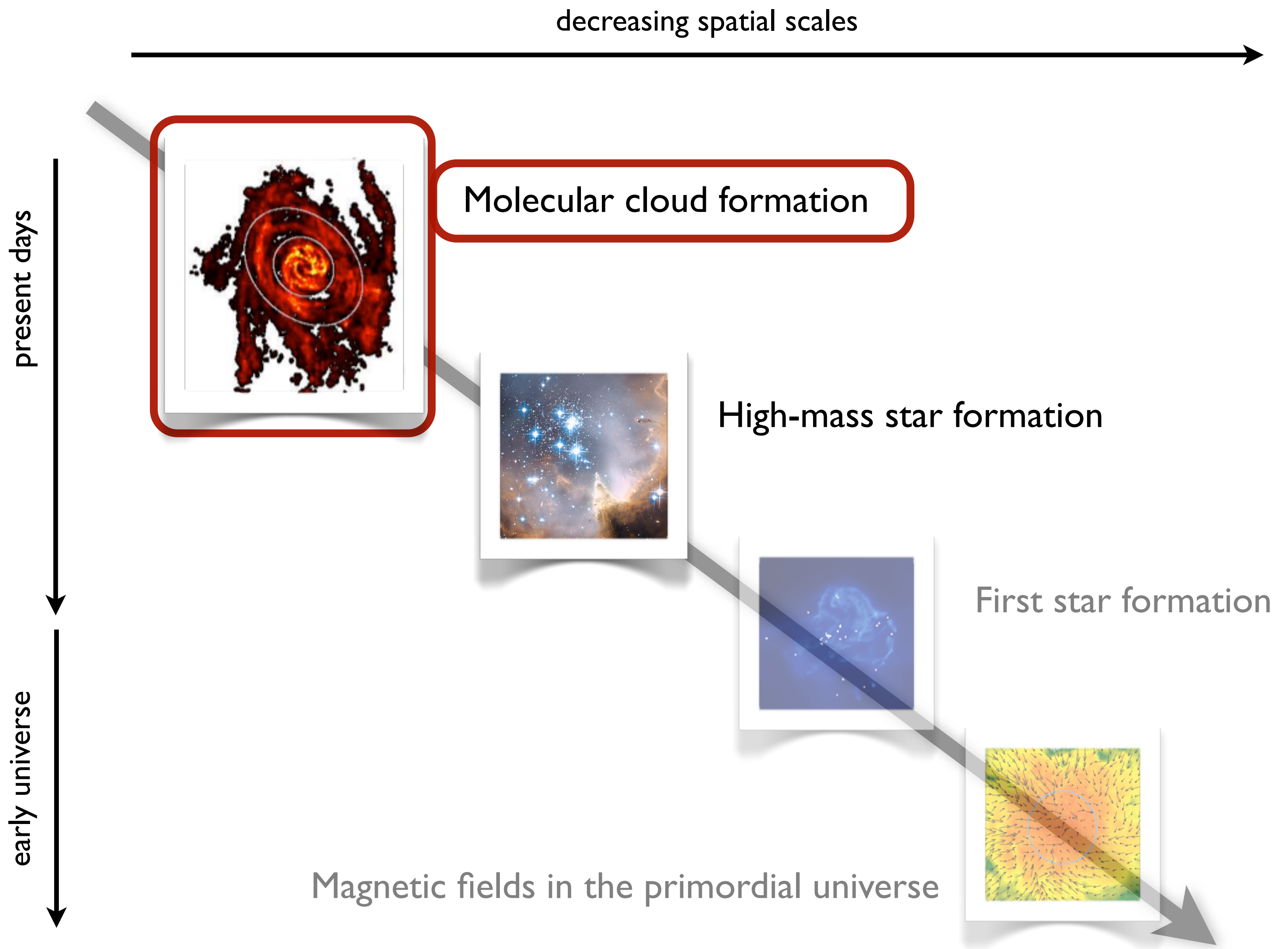

decreasing spatial scales
present days
early universe
Molecular cloud formation
High-mass star formation
First star formation
Magnetic fields in the primordial universe

experimental set-up

6 ray approximation to external radiation field

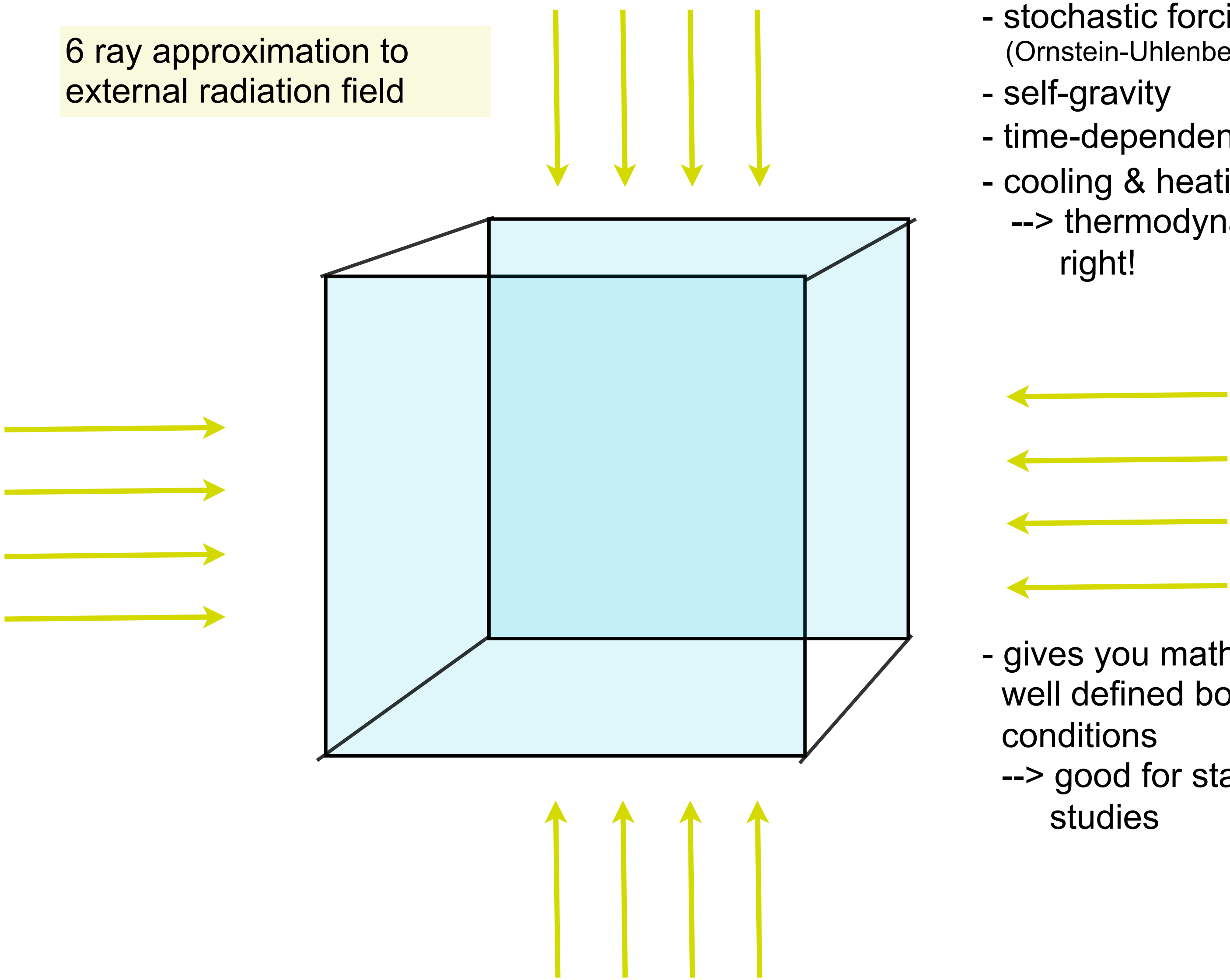

- AMR MHD (B = 2 muG)
- stochastic forcing (Ornstein-Uhlenbeck)
- self-gravity
- time-dependent chemistry
- cooling & heating processes
  --> thermodynamics done right!

- gives you mathematically well defined boundary conditions
  --> good for statistical studies

chemical model 0

- 32 chemical species
  - 17 in instantaneous equilibrium:

H^-, H_2^+, H_3^+, CH^+, CH_2^+, OH^+, H_2O^+, H_3O^+, CO^+, HOC^+, O^-, C^- and O_2^+

  - 19 full non-equilibrium evolution

e^-, H^+, H, H_2, He, He^+, C, C^+, O, O^+, OH, H_2O, CO,

C_2, O_2, HCO^+, CH, CH_2 and CH_3^+

- 218 reactions
- various heating and cooling processes

(Glover, Federrath, Mac Low, Klessen, 2010, MNRS, 404, 2)

chemical model 1

Process	Reference(s)
Cooling:	
C fine structure lines	Atomic data – Silva & Viegas (2002)
	Collisional rates (H) – Abrahamsson, Krems & Dalgarno (2007)
	Collisional rates (H_2) – Schroder et al. (1991)
	Collisional rates (e^-) – Johnson et al. (1987)
	Collisional rates (H^+) – Roueff & Le Bourlot (1990)
C^+ fine structure lines	Atomic data – Silva & Viegas (2002)
	Collisional rates (H_2) – Flower & Launay (1977)
	Collisional rates (H, $T < 2000$ K) – Hollenbach & McKee (1989)
	Collisional rates (H, $T > 2000$ K) – Keenan et al. (1986)
	Collisional rates (e^-) – Wilson & Bell (2002)
O fine structure lines	Atomic data – Silva & Viegas (2002)
	Collisional rates (H) – Abrahamsson, Krems & Dalgarno (2007)
	Collisional rates (H_2) – see Glover & Jappsen (2007)
	Collisional rates (e^-) – Bell, Berrington & Thomas (1998)
	Collisional rates (H^+) – Pequignot (1990, 1996)
H_2 rovibrational lines	Le Bourlot, Pineau des Forêts & Flower (1999)
CO and H_2O rovibrational lines	Neufeld & Kaufman (1993); Neufeld, Lepp & Melnick (1995)
OH rotational lines	Pavlovski et al. (2002)
Gas-grain energy transfer	Hollenbach & McKee (1989)
Recombination on grains	Wolfire et al. (2003)
Atomic resonance lines	Sutherland & Dopita (1993)
H collisional ionization	Abel et al. (1997)
H_2 collisional dissociation	See Table B1
Compton cooling	Cen (1992)
Heating:	
Photoelectric effect	Bakes & Tielens (1994); Wolfire et al. (2003)
H_2 photodissociation	Black & Dalgarno (1977)
UV pumping of H_2	Burton, Hollenbach & Tielens (1990)
H_2 formation on dust grains	Hollenbach & McKee (1989)
Cosmic ray ionization	Goldsmith & Langer (1978)

(Glover, Federrath, Mac Low, Klessen, 2010, MNRS, 404, 2)

chemical model 2

Table B1. List of collisional gas-phase reactions included in our chemical model

No.	Reaction	Rate coefficient	Notes	Ref.
1	$H + e^- \rightarrow H^- + \gamma$	$k_1 = \mathrm{dex}[-17.845 + 0.762 \log T + 0.1523 (\log T)^2$ $- 0.03274 (\log T)^3]$	$T \leqslant 6000$ K	1
		$= \mathrm{dex}[-16.420 + 0.1998 (\log T)^2$ $- 5.447 \times 10^{-3} (\log T)^4$ $+ 4.0415 \times 10^{-5} (\log T)^6]$	$T > 6000$ K	
2	$H^- + H \rightarrow H_2 + e^-$	$k_2 = 1.5 \times 10^{-9}$	$T \leqslant 300$ K	2
		$= 4.0 \times 10^{-9} T^{-0.17}$	$T > 300$ K	
3	$H + H^+ \rightarrow H_2^+ + \gamma$	$k_3 = \mathrm{dex}[-19.38 - 1.523 \log T$ $+ 1.118 (\log T)^2 - 0.1269 (\log T)^3]$		3
4	$H + H_2^+ \rightarrow H_2 + H^+$	$k_4 = 6.4 \times 10^{-10}$		4
5	$H^- + H^+ \rightarrow H + H$	$k_5 = 2.4 \times 10^{-6} T^{-1/2} (1.0 + T/20000)$		5
6	$H_2^+ + e^- \rightarrow H + H$	$k_6 = 1.0 \times 10^{-8}$	$T \leqslant 617$ K	6
		$= 1.32 \times 10^{-6} T^{-0.76}$	$T > 617$ K	
7	$H_2 + H^+ \rightarrow H_2^+ + H$	$k_7 = [-3.3232183 \times 10^{-7}$ $+ 3.3735382 \times 10^{-7} \ln T$ $- 1.4491368 \times 10^{-7} (\ln T)^2$ $+ 3.4172805 \times 10^{-8} (\ln T)^3$ $- 4.7813720 \times 10^{-9} (\ln T)^4$ $+ 3.9731542 \times 10^{-10} (\ln T)^5$ $- 1.8171411 \times 10^{-11} (\ln T)^6$ $+ 3.5311932 \times 10^{-13} (\ln T)^7]$ $\times \exp\left(\frac{-21237.15}{T}\right)$		7
8	$H_2 + e^- \rightarrow H + H + e^-$	$k_8 = 3.73 \times 10^{-9} T^{0.1121} \exp\left(\frac{-99430}{T}\right)$		8
9	$H_2 + H \rightarrow H + H + H$	$k_{9,\mathrm{l}} = 6.67 \times 10^{-12} T^{1/2} \exp\left[-(1 + \frac{63590}{T})\right]$		9
		$k_{9,\mathrm{h}} = 3.52 \times 10^{-9} \exp\left(-\frac{43900}{T}\right)$		10
		$n_{\mathrm{cr,H}} = \mathrm{dex}\left[3.0 - 0.416 \log\left(\frac{T}{10000}\right) - 0.327 \left\{\log\left(\frac{T}{10000}\right)\right\}^2\right]$		10
10	$H_2 + H_2 \rightarrow H_2 + H + H$	$k_{10,\mathrm{l}} = \frac{5.996 \times 10^{-30} T^{4.1881}}{(1.0 + 6.761 \times 10^{-6} T)^{5.6881}} \exp\left(-\frac{54657.4}{T}\right)$		11
		$k_{10,\mathrm{h}} = 1.3 \times 10^{-9} \exp\left(-\frac{53300}{T}\right)$		12
		$n_{\mathrm{cr,H_2}} = \mathrm{dex}\left[4.845 - 1.3 \log\left(\frac{T}{10000}\right) + 1.62 \left\{\log\left(\frac{T}{10000}\right)\right\}^2\right]$		12
11	$H + e^- \rightarrow H^+ + e^- + e^-$	$k_{11} = \exp[-3.271396786 \times 10^1$ $+ 1.35365560 \times 10^1 \ln T_e$ $- 5.73932875 \times 10^0 (\ln T_e)^2$ $+ 1.56315498 \times 10^0 (\ln T_e)^3$ $- 2.87705600 \times 10^{-1} (\ln T_e)^4$ $+ 3.48255977 \times 10^{-2} (\ln T_e)^5$ $- 2.63197617 \times 10^{-3} (\ln T_e)^6$ $+ 1.11954395 \times 10^{-4} (\ln T_e)^7$ $- 2.03914985 \times 10^{-6} (\ln T_e)^8]$		13
12	$H^+ + e^- \rightarrow H + \gamma$	$k_{12,\mathrm{A}} = 1.269 \times 10^{-13} \left(\frac{315614}{T}\right)^{1.503}$ $\times \left[1.0 + \left(\frac{604625}{T}\right)^{0.470}\right]^{-1.923}$	Case A	14
		$k_{12,\mathrm{B}} = 2.753 \times 10^{-14} \left(\frac{315614}{T}\right)^{1.500}$ $\times \left[1.0 + \left(\frac{115188}{T}\right)^{0.407}\right]^{-2.242}$	Case B	14
13	$H^- + e^- \rightarrow H + e^- + e^-$	$k_{13} = \exp[-1.801849334 \times 10^1$ $+ 2.36085220 \times 10^0 \ln T_e$ $- 2.82744300 \times 10^{-1} (\ln T_e)^2$ $+ 1.62331664 \times 10^{-2} (\ln T_e)^3$ $- 3.36501203 \times 10^{-2} (\ln T_e)^4$ $+ 1.17832978 \times 10^{-2} (\ln T_e)^5$ $- 1.65619470 \times 10^{-3} (\ln T_e)^6$ $+ 1.06827520 \times 10^{-4} (\ln T_e)^7$ $- 2.63128581 \times 10^{-6} (\ln T_e)^8]$		13

(Glover, Federrath, Mac Low, Klessen, 2010, MNRS, 404, 2)

chemical model 2

14	$H^- + H \rightarrow H + H + e^-$	$k_{14} = 2.5634 \times 10^{-9} T_e^{1.78186}$	$T_e \leqslant 0.1\,eV$	13
		$= \exp[-2.0372609 \times 10^{1}$		
		$+ 1.13944933 \times 10^{0} \ln T_e$		
		$- 1.4210135 \times 10^{-1} (\ln T_e)^2$		
		$+ 8.4644554 \times 10^{-3} (\ln T_e)^3$		
		$- 1.$[illegible]$7641 \times 10^{-}$[illegible]$(\ln T_e)^4$		
		$+ 2.$[illegible]$(\ln T_e)^5$		
		$+ 8.6639632 \times 10^{-5} (\ln T_e)^6$		
		$- 2.5850097 \times 10^{-5} (\ln T_e)^7$		
		$+ 2.4555012 \times 10^{-6} (\ln T_e)^8$		
		$- 8.0683825 \times 10^{-8} (\ln T_e)^9]$	$T_e > 0.1\,eV$	
15	$H^- + H^+ \rightarrow H_2^+ + e^-$	$k_{15} = 6.9 \times 10^{-9} T^{-0.35}$	$T \leqslant 8000\,K$	15
		$= 9.6 \times 10^{-7} T^{-0.90}$	$T > 8000\,K$	
16	$He + e^- \rightarrow He^+ + e^- + e^-$	$k_{16} = \exp[-4.409864886 \times 10^{1}$		13
		$+ 2.391596563 \times 10^{1} \ln T_e$		
		$- 1.07532302 \times 10^{1} (\ln T_e)^2$		
		$+ 3.05803875 \times 10^{0} (\ln T_e)^3$		
		$- 5.6851189 \times 10^{-1} (\ln T_e)^4$		
		$+ 6.79539123 \times 10^{-2} (\ln T_e)^5$		
		$- 5.0090561 \times 10^{-3} (\ln T_e)^6$		
		$+ 2.06723616 \times 10^{-4} (\ln T_e)^7$		
		$- 3.64916141 \times 10^{-6} (\ln T_e)^8]$		
17	$He^+ + e^- \rightarrow He + \gamma$	$k_{17,rr,A} = 10^{-11} T^{-0.5} [12.72 - 1.615 \log T$	Case A	16
		$- 0.3162 (\log T)^2 + 0.0493 (\log T)^3]$		
		$k_{17,rr,B} = 10^{-11} T^{-0.5} [11.19 - 1.676 \log T$	Case B	16
		$- 0.2852 (\log T)^2 + 0.04433 (\log T)^3]$		
		$k_{17,di} = 1.9 \times 10^{-3} T^{-1.5} \exp\left(-\frac{473421}{T}\right)$		
		$\times \left[1.0 + 0.3 \exp\left(-\frac{94684}{T}\right)\right]$		17
18	$He^+ + H \rightarrow He + H^+$	$k_{18} = 1.25 \times 10^{-15} \left(\frac{T}{300}\right)^{0.25}$		18
19	$He + H^+ \rightarrow He^+ + H$	$k_{19} = 1.26 \times 10^{-9} T^{-0.75} \exp\left(-\frac{127500}{T}\right)$	$T \leqslant 10000\,K$	19
		$= 4.0 \times 10^{-37} T^{4.74}$	$T > 10000\,K$	
20	$C^+ + e^- \rightarrow C + \gamma$	$k_{20} = 4.67 \times 10^{-12} \left(\frac{T}{300}\right)^{-0.6}$	$T \leqslant 7950\,K$	20
		$= 1.23 \times 10^{-17} \left(\frac{T}{300}\right)^{2.49} \exp\left(\frac{21845.6}{T}\right)$	$7950\,K < T \leqslant 21140\,K$	
		$= 9.62 \times 10^{-8} \left(\frac{T}{300}\right)^{-1.37} \exp\left(\frac{-115786.2}{T}\right)$	$T > 21140\,K$	
21	$O^+ + e^- \rightarrow O + \gamma$	$k_{21} = 1.30 \times 10^{-10} T^{-0.64}$	$T \leqslant 400\,K$	21
		$= 1.41 \times 10^{-10} T^{-0.66} + 7.4 \times 10^{-4} T^{-1.5}$		
		$\times \exp\left(-\frac{175000}{T}\right) [1.0 + 0.062 \times \exp\left(-\frac{145000}{T}\right)]$	$T > 400\,K$	
22	$C + e^- \rightarrow C^+ + e^- + e^-$	$k_{22} = 6.85 \times 10^{-8} (0.193 + u)^{-1} u^{0.25} e^{-u}$	$u = 11.26/T_e$	22
23	$O + e^- \rightarrow O^+ + e^- + e^-$	$k_{23} = 3.59 \times 10^{-8} (0.073 + u)^{-1} u^{0.34} e^{-u}$	$u = 13.6/T_e$	22
24	$O^+ + H \rightarrow O + H^+$	$k_{24} = 4.99 \times 10^{-11} T^{0.405} + 7.54 \times 10^{-10} T^{-0.458}$		23
25	$O + H^+ \rightarrow O^+ + H$	$k_{25} = [1.08 \times 10^{-11} T^{0.517}$		24
		$+ 4.00 \times 10^{-10} T^{0.00669}] \exp\left(-\frac{227}{T}\right)$		
26	$O + He^+ \rightarrow O^+ + He$	$k_{26} = 4.991 \times 10^{-15} \left(\frac{T}{10000}\right)^{0.3794} \exp\left(-\frac{T}{1121000}\right)$		25
		$+ 2.780 \times 10^{-15} \left(\frac{T}{10000}\right)^{-0.2163} \exp\left(\frac{T}{815800}\right)$		
27	$C + H^+ \rightarrow C^+ + H$	$k_{27} = 3.9 \times 10^{-16} T^{0.213}$		24
28	$C^+ + H \rightarrow C + H^+$	$k_{28} = 6.08 \times 10^{-14} \left(\frac{T}{10000}\right)^{1.96} \exp\left(-\frac{170000}{T}\right)$		24
29	$C + He^+ \rightarrow C^+ + He$	$k_{29} = 8.58 \times 10^{-17} T^{0.757}$	$T \leqslant 200\,K$	26
		$= 3.25 \times 10^{-17} T^{0.968}$	$200 < T \leqslant 2000\,K$	
		$= 2.77 \times 10^{-19} T^{1.597}$	$T > 2000\,K$	
30	$H_2 + He \rightarrow H + H + He$	$k_{30,l} = \mathrm{dex}[-27.029 + 3.801 \log(T) - 29487/T]$		27
		$k_{30,h} = \mathrm{dex}[-2.729 - 1.75 \log(T) - 23474/T]$		
		$n_{cr,He} = \mathrm{dex}\left[5.0792(1.0 - 1.23 \times 10^{-5}(T - 2000)\right]$		27
31	$OH + H \rightarrow O + H + H$	$k_{31} = 6.0 \times 10^{-9} \exp\left(-\frac{50900}{T}\right)$		28
32	$HOC^+ + H_2 \rightarrow HCO^+ + H_2$	$k_{32} = 3.8 \times 10^{-10}$		29
33	$HOC^+ + CO \rightarrow HCO^+ + CO$	$k_{33} = 4.0 \times 10^{-10}$		30
34	$C + H_2 \rightarrow CH + H$	$k_{34} = 6.64 \times 10^{-10} \exp\left(-\frac{11700}{T}\right)$		31
35	$CH + H \rightarrow C + H_2$	$k_{35} = 1.31 \times 10^{-10} \exp\left(-\frac{80}{T}\right)$		32

Table B1. [illegible]

No.	Rea[illegible]
1	$H +$
2	H^-
3	$H +$
4	$H +$
5	H^-
6	H_2^+
7	H_2
8	H_2
9	H_2
10	H_2
11	$H +$
12	H^+
13	H^-

(Glover, Federrath, Mac Low, Klessen, 2010, MNRAS, 404, 2)

chemical model 2

Table B1.

No.	Reaction	Rate coefficient	Notes	Reference
14	$H^- + H \to H + H + e^-$	$k_{14} = 2.5634 \times 10^{-9} T_e^{1.78186}$	$T_e \leqslant 0.1$ eV	13

36	$CH + H_2 \to CH_2 + H$	$k_{36} = 5.46 \times 10^{-10} \exp\left(-\frac{1943}{T}\right)$		33
37	$CH + C \to C_2 + H$	$k_{37} = 6.59 \times 10^{-11}$		34
38	$CH + O \to CO + H$	$k_{38} = 6.6 \times 10^{-11}$	$T \leqslant 2000$ K	35
		$= 1.02 \times 10^{-10} \exp\left(-\frac{[illegible]}{T}\right)$	$T > 2000$ K	36
39	[illegible] $\to CH + H_2$	$k_{39} = $ [illegible] $\times 10^{-11}$		37
40	$CH_2 + O \to CO + H + H$	$k_{40} = 1.33 \times 10^{-10}$		38
41	$CH_2 + O \to CO + H_2$	$k_{41} = 8.0 \times 10^{-11}$		39
42	$C_2 + O \to CO + C$	$k_{42} = 5.0 \times 10^{-11} \left(\frac{T}{300}\right)^{0.5}$	$T \leqslant 300$ K	40
		$= 5.0 \times 10^{-11} \left(\frac{T}{300}\right)^{0.757}$	$T > 300$ K	41
43	$O + H_2 \to OH + H$	$k_{43} = 3.14 \times 10^{-13} \left(\frac{T}{300}\right)^{2.7} \exp\left(-\frac{3150}{T}\right)$		42
44	$OH + H \to O + H_2$	$k_{44} = 6.99 \times 10^{-14} \left(\frac{T}{300}\right)^{2.8} \exp\left(-\frac{1950}{T}\right)$		43
45	$OH + H_2 \to H_2O + H$	$k_{45} = 2.05 \times 10^{-12} \left(\frac{T}{300}\right)^{1.52} \exp\left(-\frac{1736}{T}\right)$		44
46	$OH + C \to CO + H$	$k_{46} = 1.0 \times 10^{-10}$		34
47	$OH + O \to O_2 + H$	$k_{47} = 3.50 \times 10^{-11}$	$T \leqslant 261$ K	45
		$= 1.77 \times 10^{-11} \exp\left(\frac{178}{T}\right)$	$T > 261$ K	33
48	$OH + OH \to H_2O + H$	$k_{48} = 1.65 \times 10^{-12} \left(\frac{T}{300}\right)^{1.14} \exp\left(-\frac{50}{T}\right)$		34
49	$H_2O + H \to H_2 + OH$	$k_{49} = 1.59 \times 10^{-11} \left(\frac{T}{300}\right)^{1.2} \exp\left(-\frac{9610}{T}\right)$		46
50	$O_2 + H \to OH + O$	$k_{50} = 2.61 \times 10^{-10} \exp\left(-\frac{8156}{T}\right)$		33
51	$O_2 + H_2 \to OH + OH$	$k_{51} = 3.16 \times 10^{-10} \exp\left(-\frac{21890}{T}\right)$		47
52	$O_2 + C \to CO + O$	$k_{52} = 4.7 \times 10^{-11} \left(\frac{T}{300}\right)^{-0.34}$	$T \leqslant 295$ K	34
		$= 2.48 \times 10^{-12} \left(\frac{T}{300}\right)^{1.54} \exp\left(\frac{613}{T}\right)$	$T > 295$ K	33
53	$CO + H \to C + OH$	$k_{53} = 1.1 \times 10^{-10} \left(\frac{T}{300}\right)^{0.5} \exp\left(-\frac{77700}{T}\right)$		28
54	$H_2^+ + H_2 \to H_3^+ + H$	$k_{54} = 2.24 \times 10^{-9} \left(\frac{T}{300}\right)^{0.042} \exp\left(-\frac{T}{46600}\right)$		48
55	$H_3^+ + H \to H_2^+ + H_2$	$k_{55} = 7.7 \times 10^{-9} \exp\left(-\frac{17560}{T}\right)$		49
56	$C + H_2^+ \to CH^+ + H$	$k_{56} = 2.4 \times 10^{-9}$		28
57	$C + H_3^+ \to CH^+ + H_2$	$k_{57} = 2.0 \times 10^{-9}$		28
58	$C^+ + H_2 \to CH^+ + H$	$k_{58} = 1.0 \times 10^{-10} \exp\left(-\frac{4640}{T}\right)$		50
59	$CH^+ + H \to C^+ + H_2$	$k_{59} = 7.5 \times 10^{-10}$		51
60	$CH^+ + H_2 \to CH_2^+ + H$	$k_{60} = 1.2 \times 10^{-9}$		51
61	$CH^+ + O \to CO^+ + H$	$k_{61} = 3.5 \times 10^{-10}$		52
62	$CH_2 + H^+ \to CH^+ + H_2$	$k_{62} = 1.4 \times 10^{-9}$		28
63	$CH_2^+ + H \to CH^+ + H_2$	$k_{63} = 1.0 \times 10^{-9} \exp\left(-\frac{7080}{T}\right)$		28
64	$CH_2^+ + H_2 \to CH_3^+ + H$	$k_{64} = 1.6 \times 10^{-9}$		53
65	$CH_2^+ + O \to HCO^+ + H$	$k_{65} = 7.5 \times 10^{-10}$		28
66	$CH_3^+ + H \to CH_2^+ + H_2$	$k_{66} = 7.0 \times 10^{-10} \exp\left(-\frac{10560}{T}\right)$		28
67	$CH_3^+ + O \to HCO^+ + H_2$	$k_{67} = 4.0 \times 10^{-10}$		54
68	$C_2 + O^+ \to CO^+ + C$	$k_{68} = 4.8 \times 10^{-10}$		28
69	$O^+ + H_2 \to OH^+ + H$	$k_{69} = 1.7 \times 10^{-9}$		55
70	$O + H_2^+ \to OH^+ + H$	$k_{70} = 1.5 \times 10^{-9}$		28
71	$O + H_3^+ \to OH^+ + H_2$	$k_{71} = 8.4 \times 10^{-10}$		56
72	$OH + H_3^+ \to H_2O^+ + H_2$	$k_{72} = 1.3 \times 10^{-9}$		28
73	$OH + C^+ \to CO^+ + H$	$k_{73} = 7.7 \times 10^{-10}$		28
74	$OH^+ + H_2 \to H_2O^+ + H$	$k_{74} = 1.01 \times 10^{-9}$		57
75	$H_2O^+ + H_2 \to H_3O^+ + H$	$k_{75} = 6.4 \times 10^{-10}$		58
76	$H_2O + H_3^+ \to H_3O^+ + H_2$	$k_{76} = 5.9 \times 10^{-9}$		59
77	$H_2O + C^+ \to HCO^+ + H$	$k_{77} = 9.0 \times 10^{-10}$		60
78	$H_2O + C^+ \to HOC^+ + H$	$k_{78} = 1.8 \times 10^{-9}$		60
79	$H_3O^+ + C \to HCO^+ + H_2$	$k_{79} = 1.0 \times 10^{-11}$		28
80	$O_2 + C^+ \to CO^+ + O$	$k_{80} = 3.8 \times 10^{-10}$		53
81	$O_2 + C^+ \to CO + O^+$	$k_{81} = 6.2 \times 10^{-10}$		53
82	$O_2 + CH_2^+ \to HCO^+ + OH$	$k_{82} = 9.1 \times 10^{-10}$		53
83	$O_2^+ + C \to CO^+ + O$	$k_{83} = 5.2 \times 10^{-11}$		28
84	$CO + H_3^+ \to HOC^+ + H_2$	$k_{84} = 2.7 \times 10^{-11}$		61
85	$CO + H_3^+ \to HCO^+ + H_2$	$k_{85} = 1.7 \times 10^{-9}$		61
86	$HCO^+ + C \to CO + CH^+$	$k_{86} = 1.1 \times 10^{-9}$		28
87	$HCO^+ + H_2O \to CO + H_3O^+$	$k_{87} = 2.5 \times 10^{-9}$		62

(Glover, Federrath, Mac Low, Klessen, 2010, MNRAS, 404, 2)

chemical model 2

(Glover, Federrath, Mac Low, Klessen, 2010, MNRS, 404, 2)

88	$H_2 + He^+ \rightarrow He + H_2^+$	$k_{88} = 7.2 \times 10^{-15}$	63
89	$H_2 + He^+ \rightarrow He + H + H^+$	$k_{89} = 3.7 \times 10^{-14} \exp\left(\frac{35}{T}\right)$	63
90	$CH + H^+ \rightarrow CH^+ + H$	$k_{90} = 1.9 \times 10^{-9}$	28
91	$CH_2 + H^+ \rightarrow CH_2^+ + H$	$k_{91} = 1.4 \times 10^{-9}$	28
92	$CH_2 + He^+ \rightarrow C^+ + He + H_2$	$k_{92} =$ [illegible]	28
93	$C_2 + He^+ \rightarrow C^+ + C + He$	$k_{93} =$ [illegible] 6×10^{-9}	28
94	$OH + H^+ \rightarrow OH^+ + H$	$k_{94} = 2.1 \times 10^{-9}$	28
95	$OH + He^+ \rightarrow O^+ + He + H$	$k_{95} = 1.1 \times 10^{-9}$	28
96	$H_2O + H^+ \rightarrow H_2O^+ + H$	$k_{96} = 6.9 \times 10^{-9}$	64
97	$H_2O + He^+ \rightarrow OH + He + H^+$	$k_{97} = 2.04 \times 10^{-10}$	65
98	$H_2O + He^+ \rightarrow OH^+ + He + H$	$k_{98} = 2.86 \times 10^{-10}$	65
99	$H_2O + He^+ \rightarrow H_2O^+ + He$	$k_{99} = 6.05 \times 10^{-11}$	65
100	$O_2 + H^+ \rightarrow O_2^+ + H$	$k_{100} = 2.0 \times 10^{-9}$	64
101	$O_2 + He^+ \rightarrow O_2^+ + He$	$k_{101} = 3.3 \times 10^{-11}$	66
102	$O_2 + He^+ \rightarrow O^+ + O + He$	$k_{102} = 1.1 \times 10^{-9}$	66
103	$O_2^+ + C \rightarrow O_2 + C^+$	$k_{103} = 5.2 \times 10^{-11}$	28
104	$CO + He^+ \rightarrow C^+ + O + He$	$k_{104} = 1.4 \times 10^{-9} \left(\frac{T}{300}\right)^{-0.5}$	67
105	$CO + He^+ \rightarrow C + O^+ + He$	$k_{105} = 1.4 \times 10^{-16} \left(\frac{T}{300}\right)^{-0.5}$	67
106	$CO^+ + H \rightarrow CO + H^+$	$k_{106} = 7.5 \times 10^{-10}$	68
107	$C^- + H^+ \rightarrow C + H$	$k_{107} = 2.3 \times 10^{-7} \left(\frac{T}{300}\right)^{-0.5}$	28
108	$O^- + H^+ \rightarrow O + H$	$k_{108} = 2.3 \times 10^{-7} \left(\frac{T}{300}\right)^{-0.5}$	28
109	$He^+ + H^- \rightarrow He + H$	$k_{109} = 2.32 \times 10^{-7} \left(\frac{T}{300}\right)^{-0.52} \exp\left(\frac{T}{22400}\right)$	69
110	$H_3^+ + e^- \rightarrow H_2 + H$	$k_{110} = 2.34 \times 10^{-8} \left(\frac{T}{300}\right)^{-0.52}$	70
111	$H_3^+ + e^- \rightarrow H + H + H$	$k_{111} = 4.36 \times 10^{-8} \left(\frac{T}{300}\right)^{-0.52}$	70
112	$CH^+ + e^- \rightarrow C + H$	$k_{112} = 7.0 \times 10^{-8} \left(\frac{T}{300}\right)^{-0.5}$	71
113	$CH_2^+ + e^- \rightarrow CH + H$	$k_{113} = 1.6 \times 10^{-7} \left(\frac{T}{300}\right)^{-0.6}$	72
114	$CH_2^+ + e^- \rightarrow C + H + H$	$k_{114} = 4.03 \times 10^{-7} \left(\frac{T}{300}\right)^{-0.6}$	72
115	$CH_2^+ + e^- \rightarrow C + H_2$	$k_{115} = 7.68 \times 10^{-8} \left(\frac{T}{300}\right)^{-0.6}$	72
116	$CH_3^+ + e^- \rightarrow CH_2 + H$	$k_{116} = 7.75 \times 10^{-8} \left(\frac{T}{300}\right)^{-0.5}$	73
117	$CH_3^+ + e^- \rightarrow CH + H_2$	$k_{117} = 1.95 \times 10^{-7} \left(\frac{T}{300}\right)^{-0.5}$	73
118	$CH_3^+ + e^- \rightarrow CH + H + H$	$k_{118} = 2.0 \times 10^{-7} \left(\frac{T}{300}\right)^{-0.4}$	28
119	$OH^+ + e^- \rightarrow O + H$	$k_{119} = 6.3 \times 10^{-9} \left(\frac{T}{300}\right)^{-0.48}$	74
120	$H_2O^+ + e^- \rightarrow O + H + H$	$k_{120} = 3.05 \times 10^{-7} \left(\frac{T}{300}\right)^{-0.5}$	75
121	$H_2O^+ + e^- \rightarrow O + H_2$	$k_{121} = 3.9 \times 10^{-8} \left(\frac{T}{300}\right)^{-0.5}$	75
122	$H_2O^+ + e^- \rightarrow OH + H$	$k_{122} = 8.6 \times 10^{-8} \left(\frac{T}{300}\right)^{-0.5}$	75
123	$H_3O^+ + e^- \rightarrow H + H_2O$	$k_{123} = 1.08 \times 10^{-7} \left(\frac{T}{300}\right)^{-0.5}$	76
124	$H_3O^+ + e^- \rightarrow OH + H_2$	$k_{124} = 6.02 \times 10^{-8} \left(\frac{T}{300}\right)^{-0.5}$	76
125	$H_3O^+ + e^- \rightarrow OH + H + H$	$k_{125} = 2.58 \times 10^{-7} \left(\frac{T}{300}\right)^{-0.5}$	76
126	$H_3O^+ + e^- \rightarrow O + H + H_2$	$k_{126} = 5.6 \times 10^{-9} \left(\frac{T}{300}\right)^{-0.5}$	76
127	$O_2^+ + e^- \rightarrow O + O$	$k_{127} = 1.95 \times 10^{-7} \left(\frac{T}{300}\right)^{-0.7}$	77
128	$CO^+ + e^- \rightarrow C + O$	$k_{128} = 2.75 \times 10^{-7} \left(\frac{T}{300}\right)^{-0.55}$	78
129	$HCO^+ + e^- \rightarrow CO + H$	$k_{129} = 2.76 \times 10^{-7} \left(\frac{T}{300}\right)^{-0.64}$	79
130	$HCO^+ + e^- \rightarrow OH + C$	$k_{130} = 2.4 \times 10^{-8} \left(\frac{T}{300}\right)^{-0.64}$	79
131	$HOC^+ + e^- \rightarrow CO + H$	$k_{131} = 1.1 \times 10^{-7} \left(\frac{T}{300}\right)^{-1.0}$	28
132	$H^- + C \rightarrow CH + e^-$	$k_{132} = 1.0 \times 10^{-9}$	28
133	$H^- + O \rightarrow OH + e^-$	$k_{133} = 1.0 \times 10^{-9}$	28
134	$H^- + OH \rightarrow H_2O + e^-$	$k_{134} = 1.0 \times 10^{-10}$	28
135	$C^- + H \rightarrow CH + e^-$	$k_{135} = 5.0 \times 10^{-10}$	28
136	$C^- + H_2 \rightarrow CH_2 + e^-$	$k_{136} = 1.0 \times 10^{-13}$	28
137	$C^- + O \rightarrow CO + e^-$	$k_{137} = 5.0 \times 10^{-10}$	28
138	$O^- + H \rightarrow OH + e^-$	$k_{138} = 5.0 \times 10^{-10}$	28
139	$O^- + H_2 \rightarrow H_2O + e^-$	$k_{139} = 7.0 \times 10^{-10}$	28
140	$O^- + C \rightarrow CO + e^-$	$k_{140} = 5.0 \times 10^{-10}$	28
87	$HCO^+ + H_2O \rightarrow CO + H_3O^+$	$k_{87} = 2.5 \times 10^{-9}$	62

chemical model 2

88	$H_2 + He^+ \rightarrow He + H_2^+$	$k_{88} = 7.2 \times 10^{-15}$	63
89	$H_2 + He^+ \rightarrow He + H + H^+$	$k_{89} = 3.7 \times 10^{-14} \exp\left(\frac{35}{T}\right)$	63
90	$CH + H^+ \rightarrow CH^+ + H$	$k_{90} = 1.9 \times 10^{-9}$	28
91	$CH_2 + H^+ \rightarrow CH_2^+ + H$	$k_{91} = 1.4 \times 10^{-9}$	28
94	$OH + H^+ \rightarrow OH^+ + H$	$k_{94} = 2.1 \times 10^{-9}$	28
95	$OH + He^+ \rightarrow O^+ + He + H$	$k_{95} = 1.1 \times 10^{-9}$	28
96	$H_2O + H^+ \rightarrow H_2O^+ + H$	$k_{96} = 6.9 \times 10^{-9}$	64
97	$H_2O + He^+ \rightarrow OH + He + H^+$	$k_{97} = 2.04 \times 10^{-10}$	65

142	$C + e^- \rightarrow C^- + \gamma$	$k_{142} = 2.25 \times 10^{-15}$		81
143	$C + H \rightarrow CH + \gamma$	$k_{143} = 1.0 \times 10^{-17}$		82
144	$C + H_2 \rightarrow CH_2 + \gamma$	$k_{144} = 1.0 \times 10^{-17}$		82
145	$C + C \rightarrow C_2 + \gamma$	$k_{145} = 4.36 \times 10^{-18} \left(\frac{T}{300}\right)^{0.35} \exp\left(-\frac{161.3}{T}\right)$		83
146	$C + O \rightarrow CO + \gamma$	$k_{146} = 2.1 \times 10^{-19}$	$T \leqslant 300$ K	84
		$= 3.09 \times 10^{-17} \left(\frac{T}{300}\right)^{0.33} \exp\left(-\frac{1629}{T}\right)$	$T > 300$ K	85
147	$C^+ + H \rightarrow CH^+ + \gamma$	$k_{147} = 4.46 \times 10^{-16} T^{-0.5} \exp\left(-\frac{4.93}{T^{2/3}}\right)$		86
148	$C^+ + H_2 \rightarrow CH_2^+ + \gamma$	$k_{148} = 4.0 \times 10^{-16} \left(\frac{T}{300}\right)^{-0.2}$		87
149	$C^+ + O \rightarrow CO^+ + \gamma$	$k_{149} = 2.5 \times 10^{-18}$	$T \leqslant 300$ K	84
		$= 3.14 \times 10^{-18} \left(\frac{T}{300}\right)^{-0.15} \exp\left(\frac{68}{T}\right)$	$T > 300$ K	
150	$O + e^- \rightarrow O^- + \gamma$	$k_{150} = 1.5 \times 10^{-15}$		28
151	$O + H \rightarrow OH + \gamma$	$k_{151} = 9.9 \times 10^{-19} \left(\frac{T}{300}\right)^{-0.38}$		28
152	$O + O \rightarrow O_2 + \gamma$	$k_{152} = 4.9 \times 10^{-20} \left(\frac{T}{300}\right)^{1.58}$		82
153	$OH + H \rightarrow H_2O + \gamma$	$k_{153} = 5.26 \times 10^{-18} \left(\frac{T}{300}\right)^{-5.22} \exp\left(-\frac{90}{T}\right)$		88
154	$H + H + H \rightarrow H_2 + H$	$k_{154} = 1.32 \times 10^{-32} \left(\frac{T}{300}\right)^{-0.38}$	$T \leqslant 300$ K	89
		$= 1.32 \times 10^{-32} \left(\frac{T}{300}\right)^{-1.0}$	$T > 300$ K	90
155	$H + H + H_2 \rightarrow H_2 + H_2$	$k_{155} = 2.8 \times 10^{-31} T^{-0.6}$		91
156	$H + H + He \rightarrow H_2 + He$	$k_{156} = 6.9 \times 10^{-32} T^{-0.4}$		92
157	$C + C + M \rightarrow C_2 + M$	$k_{157} = 5.99 \times 10^{-33} \left(\frac{T}{5000}\right)^{-1.6}$	$T \leqslant 5000$ K	93
		$= 5.99 \times 10^{-33} \left(\frac{T}{5000}\right)^{-0.64} \exp\left(\frac{5255}{T}\right)$	$T > 5000$ K	94
158	$C + O + M \rightarrow CO + M$	$k_{158} = 6.16 \times 10^{-29} \left(\frac{T}{300}\right)^{-3.08}$	$T \leqslant 2000$ K	35
		$= 2.14 \times 10^{-29} \left(\frac{T}{300}\right)^{-3.08} \exp\left(\frac{2114}{T}\right)$	$T > 2000$ K	67
159	$C^+ + O + M \rightarrow CO^+ + M$	$k_{159} = 100 \times k_{210}$		67
160	$C + O^+ + M \rightarrow CO^+ + M$	$k_{160} = 100 \times k_{210}$		67
161	$O + H + M \rightarrow OH + M$	$k_{161} = 4.33 \times 10^{-32} \left(\frac{T}{300}\right)^{-1.0}$		43
162	$OH + H + M \rightarrow H_2O + M$	$k_{162} = 2.56 \times 10^{-31} \left(\frac{T}{300}\right)^{-2.0}$		35
163	$O + O + M \rightarrow O_2 + M$	$k_{163} = 9.2 \times 10^{-34} \left(\frac{T}{300}\right)^{-1.0}$		37
164	$O + CH \rightarrow HCO^+ + e^-$	$k_{164} = 2.0 \times 10^{-11} \left(\frac{T}{300}\right)^{0.44}$		95
165	$H + H(s) \rightarrow H_2$	$k_{165} = 3.0 \times 10^{-18} T^{0.5} f_A [1.0 + 0.04 (T + T_d)^{0.5} + 0.002\,T + 8 \times 10^{-6} T^2]^{-1}$	$f_A = \left[1.0 + 10^4 \exp\left(-\frac{600}{T_d}\right)\right]^{-1}$	96

129	$HCO^+ + e^- \rightarrow CO + H$	$k_{129} = 2.76 \times 10^{-7} \left(\frac{T}{300}\right)^{-0.64}$	79
130	$HCO^+ + e^- \rightarrow OH + C$	$k_{130} = 2.4 \times 10^{-8} \left(\frac{T}{300}\right)^{-0.64}$	79
131	$HOC^+ + e^- \rightarrow CO + H$	$k_{131} = 1.1 \times 10^{-7} \left(\frac{T}{300}\right)^{-1.0}$	28
132	$H^- + C \rightarrow CH + e^-$	$k_{132} = 1.0 \times 10^{-9}$	28
133	$H^- + O \rightarrow OH + e^-$	$k_{133} = 1.0 \times 10^{-9}$	28
134	$H^- + OH \rightarrow H_2O + e^-$	$k_{134} = 1.0 \times 10^{-10}$	28
135	$C^- + H \rightarrow CH + e^-$	$k_{135} = 5.0 \times 10^{-10}$	28
136	$C^- + H_2 \rightarrow CH_2 + e^-$	$k_{136} = 1.0 \times 10^{-13}$	28
137	$C^- + O \rightarrow CO + e^-$	$k_{137} = 5.0 \times 10^{-10}$	28
138	$O^- + H \rightarrow OH + e^-$	$k_{138} = 5.0 \times 10^{-10}$	28
139	$O^- + H_2 \rightarrow H_2O + e^-$	$k_{139} = 7.0 \times 10^{-10}$	28
140	$O^- + C \rightarrow CO + e^-$	$k_{140} = 5.0 \times 10^{-10}$	28

(Glover, Federrath, Mac Low, Klessen, 2010, MNRS, 404, 2)

chemical model 2

Table B2. List of photochemical reactions included in our chemical model

No.	Reaction	Optically thin rate (s^{-1})	γ	Ref.
166	$H^- + \gamma \rightarrow H + e^-$	$R_{166} = 7.1 \times 10^{-7}$	0.5	1
167	$H_2^+ + \gamma \rightarrow H + H^+$	$R_{167} = 1.1 \times 10^{-9}$	1.9	2
168	$H_2 + \gamma \rightarrow H + H$	$R_{168} = 5.6 \times 10^{-11}$	See §2.2	3
169	$H_3^+ + \gamma \rightarrow H_2 + H^+$	$R_{169} = 4.9 \times 10^{-13}$	1.8	4
170	$H_3^+ + \gamma \rightarrow H_2^+ + H$	$R_{170} = 4.9 \times 10^{-13}$	2.3	4
171	$C + \gamma \rightarrow C^+ + e^-$	$R_{171} = 3.1 \times 10^{-10}$	3.0	5
172	$C^- + \gamma \rightarrow C + e^-$	$R_{172} = 2.4 \times 10^{-7}$	0.9	6
173	$CH + \gamma \rightarrow C + H$	$R_{173} = 8.7 \times 10^{-10}$	1.2	7
174	$CH + \gamma \rightarrow CH^+ + e^-$	$R_{174} = 7.7 \times 10^{-10}$	2.8	8
175	$CH^+ + \gamma \rightarrow C + H^+$	$R_{175} = 2.6 \times 10^{-10}$	2.5	7
176	$CH_2 + \gamma \rightarrow CH + H$	$R_{176} = 7.1 \times 10^{-10}$	1.7	7
177	$CH_2 + \gamma \rightarrow CH_2^+ + e^-$	$R_{177} = 5.9 \times 10^{-10}$	2.3	6
178	$CH_2^+ + \gamma \rightarrow CH^+ + H$	$R_{178} = 4.6 \times 10^{-10}$	1.7	9
179	$CH_3^+ + \gamma \rightarrow CH_2^+ + H$	$R_{179} = 1.0 \times 10^{-9}$	1.7	6
180	$CH_3^+ + \gamma \rightarrow CH^+ + H_2$	$R_{180} = 1.0 \times 10^{-9}$	1.7	6
181	$C_2 + \gamma \rightarrow C + C$	$R_{181} = 1.5 \times 10^{-10}$	2.1	7
182	$O^- + \gamma \rightarrow O + e^-$	$R_{182} = 2.4 \times 10^{-7}$	0.5	6
183	$OH + \gamma \rightarrow O + H$	$R_{183} = 3.7 \times 10^{-10}$	1.7	10
184	$OH + \gamma \rightarrow OH^+ + e^-$	$R_{184} = 1.6 \times 10^{-12}$	3.1	6
185	$OH^+ + \gamma \rightarrow O + H^+$	$R_{185} = 1.0 \times 10^{-12}$	1.8	4
186	$H_2O + \gamma \rightarrow OH + H$	$R_{186} = 6.0 \times 10^{-10}$	1.7	11
187	$H_2O + \gamma \rightarrow H_2O^+ + e^-$	$R_{187} = 3.2 \times 10^{-11}$	3.9	8
188	$H_2O^+ + \gamma \rightarrow H_2^+ + O$	$R_{188} = 5.0 \times 10^{-11}$	See §2.2	12
189	$H_2O^+ + \gamma \rightarrow H^+ + OH$	$R_{189} = 5.0 \times 10^{-11}$	See §2.2	12
190	$H_2O^+ + \gamma \rightarrow O^+ + H_2$	$R_{190} = 5.0 \times 10^{-11}$	See §2.2	12
191	$H_2O^+ + \gamma \rightarrow OH^+ + H$	$R_{191} = 1.5 \times 10^{-10}$	See §2.2	12
192	$H_3O^+ + \gamma \rightarrow H^+ + H_2O$	$R_{192} = 2.5 \times 10^{-11}$	See §2.2	12
193	$H_3O^+ + \gamma \rightarrow H_2^+ + OH$	$R_{193} = 2.5 \times 10^{-11}$	See §2.2	12
194	$H_3O^+ + \gamma \rightarrow H_2O^+ + H$	$R_{194} = 7.5 \times 10^{-12}$	See §2.2	12
195	$H_3O^+ + \gamma \rightarrow OH^+ + H_2$	$R_{195} = 2.5 \times 10^{-11}$	See §2.2	12
196	$O_2 + \gamma \rightarrow O_2^+ + e^-$	$R_{196} = 5.6 \times 10^{-11}$	3.7	7
197	$O_2 + \gamma \rightarrow O + O$	$R_{197} = 7.0 \times 10^{-10}$	1.8	7
198	$CO + \gamma \rightarrow C + O$	$R_{198} = 2.0 \times 10^{-10}$	See §2.2	13

(Glover, Federrath, Mac Low, Klessen, 2010, MNRS, 404, 2)

chemical model 2

88	$H_2 + He^+ \rightarrow He + H_2^+$	$k_{88} = 7.2 \times 10^{-15}$	63
89	$H_2 + He^+ \rightarrow He + H + H^+$	$k_{89} = 3.7 \times 10^{-14} \exp\left(\frac{35}{T}\right)$	63
90	$CH + H^+ \rightarrow CH^+ + H$	$k_{90} = 1.9 \times 10^{-9}$	28
94	$OH + H^+ \rightarrow OH^+ + H$	$k_{94} = 2.1 \times 10^{-9}$	28
95	$OH + He^+ \rightarrow O^+ + He + H$	$k_{95} = 1.1 \times 10^{-9}$	28
96	$H_2O + H^+ \rightarrow H_2O^+ + H$	$k_{96} = 6.9 \times 10^{-9}$	64
97	$H_2O + He^+ \rightarrow OH + He + H^+$	$k_{97} = 2.04 \times 10^{-10}$	65

Table B2. List of photochemical reactions included in our chemical model

No.	Reaction	Optically thin rate (s^{-1})	γ	Ref.
166	$H^- + \gamma \rightarrow H + e^-$	$R_{166} = 7.1 \times 10^{-7}$	0.5	1
167	$H_2^+ + \gamma \rightarrow H + H^+$	$R_{167} = 1.1 \times 10^{-9}$	1.9	2
168	$H_2 + \gamma \rightarrow H + H$	$R_{168} = 5.6 \times 10^{-11}$	See §2.2	3
169	$H_3^+ + \gamma \rightarrow H_2 + H^+$	$R_{169} = 4.9 \times 10^{-13}$	1.8	4
170	$H_3^+ + \gamma \rightarrow H_2^+ + H$	$R_{170} = 4.9 \times 10^{-13}$	2.3	4
171	$C + \gamma \rightarrow$ …	…	…	…
172	$C^- + \gamma$ …			
173	$CH + \gamma$ …			
174	$CH + \gamma$ …			
175	$CH^+ + \gamma$ …			
176	$CH_2 + \gamma$ …			
177	$CH_2 + \gamma$ …			
178	$CH_2^+ + \gamma$ …			
179	$CH_3^+ + \gamma$ …			
180	$CH_3^+ + \gamma$ …			
181	$C_2 + \gamma \rightarrow$ …			
182	$O^- + \gamma$ …			
183	$OH + \gamma$ …			
184	$OH + \gamma$ …			
185	$OH^+ + \gamma$ …			
186	$H_2O + \gamma$ …			
187	$H_2O + \gamma$ …			
188	$H_2O^+ + \gamma$ …			
189	$H_2O^+ + \gamma$ …			
190	$H_2O^+ + \gamma$ …			
191	$H_2O^+ + \gamma$ …			
192	$H_3O^+ + \gamma$ …			
193	$H_3O^+ + \gamma$ …			
194	$H_3O^+ + \gamma$ …			
195	$H_3O^+ + \gamma$ …			
196	$O_2 + \gamma \rightarrow$ …			
197	$O_2 + \gamma \rightarrow O + O$	$R_{197} = 7.0 \times 10^{-10}$	1.8	7
198	$CO + \gamma \rightarrow C + O$	$R_{198} = 2.0 \times 10^{-10}$	See §2.2	13

Table B3. List of reactions included in our chemical model that involve cosmic rays or cosmic-ray induced UV emission

No.	Reaction	Rate ($s^{-1}\zeta_H^{-1}$)	Ref.
199	$H + c.r. \rightarrow H^+ + e^-$	$R_{199} = 1.0$	—
200	$He + c.r. \rightarrow He^+ + e^-$	$R_{200} = 1.1$	1
201	$H_2 + c.r. \rightarrow H^+ + H + e^-$	$R_{201} = 0.037$	1
202	$H_2 + c.r. \rightarrow H + H$	$R_{202} = 0.22$	1
203	$H_2 + c.r. \rightarrow H^+ + H^-$	$R_{203} = 6.5 \times 10^{-4}$	1
204	$H_2 + c.r. \rightarrow H_2^+ + e^-$	$R_{204} = 2.0$	1
205	$C + c.r. \rightarrow C^+ + e^-$	$R_{205} = 3.8$	1
206	$O + c.r. \rightarrow O^+ + e^-$	$R_{206} = 5.7$	1
207	$CO + c.r. \rightarrow CO^+ + e^-$	$R_{207} = 6.5$	1
208	$C + \gamma_{c.r.} \rightarrow C^+ + e^-$	$R_{208} = 2800$	2
209	$CH + \gamma_{c.r.} \rightarrow C + H$	$R_{209} = 4000$	3
210	$CH^+ + \gamma_{c.r.} \rightarrow C^+ + H$	$R_{210} = 960$	3
211	$CH_2 + \gamma_{c.r.} \rightarrow CH_2^+ + e^-$	$R_{211} = 2700$	1
212	$CH_2 + \gamma_{c.r.} \rightarrow CH + H$	$R_{212} = 2700$	1
213	$C_2 + \gamma_{c.r.} \rightarrow C + C$	$R_{213} = 1300$	3
214	$OH + \gamma_{c.r.} \rightarrow O + H$	$R_{214} = 2800$	3
215	$H_2O + \gamma_{c.r.} \rightarrow OH + H$	$R_{215} = 5300$	3
216	$O_2 + \gamma_{c.r.} \rightarrow O + O$	$R_{216} = 4100$	3
217	$O_2 + \gamma_{c.r.} \rightarrow O_2^+ + e^-$	$R_{217} = 640$	3
218	$CO + \gamma_{c.r.} \rightarrow C + O$	$R_{218} = 0.21 T^{1/2} x_{H_2} x_{CO}^{-1/2}$	4

(Glover, Federrath, Mac Low, Klessen, 2010, MNRS, 404, 2)

HI to H2 conversion rate

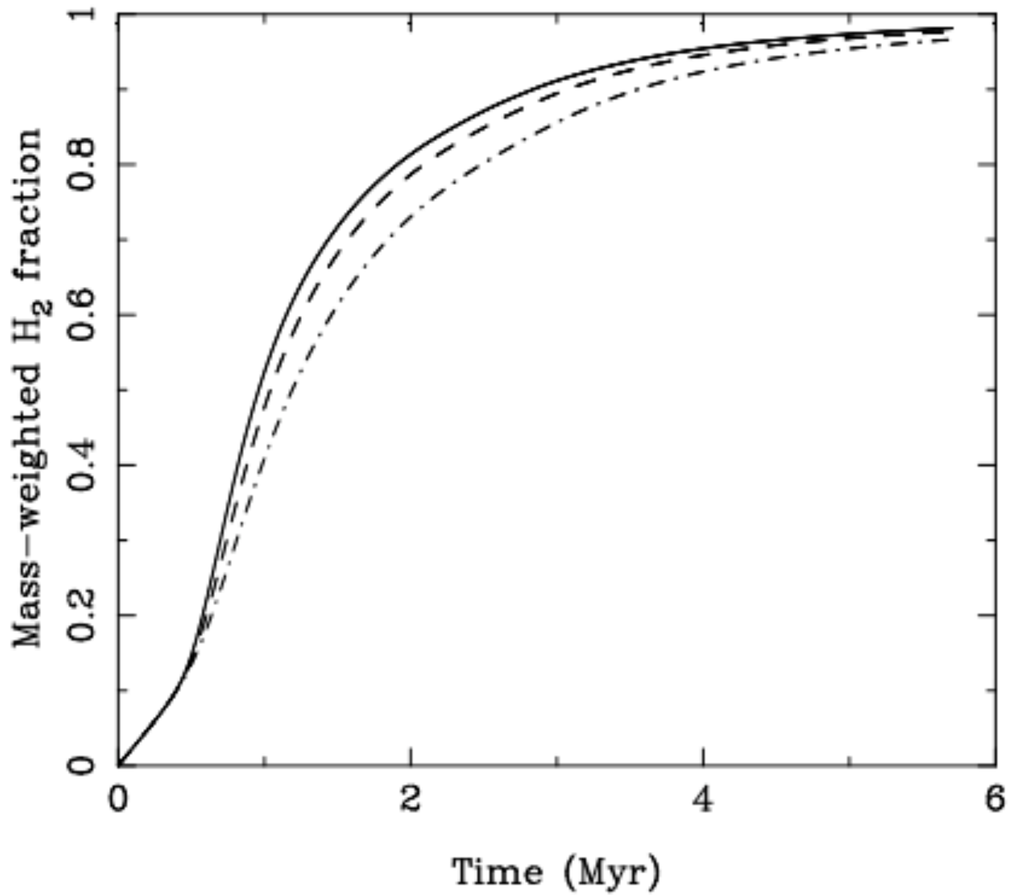

Figure 4. Time evolution of the mass-weighted H_2 abundance in simulations R1, R2 and R3, which have numerical resolutions of 64^3 zones (dot-dashed), 128^3 zones (dashed) and 256^3 zones (solid), respectively.

(Glover, Federrath, Mac Low, Klessen, 2010)

HI to H2 conversion rate

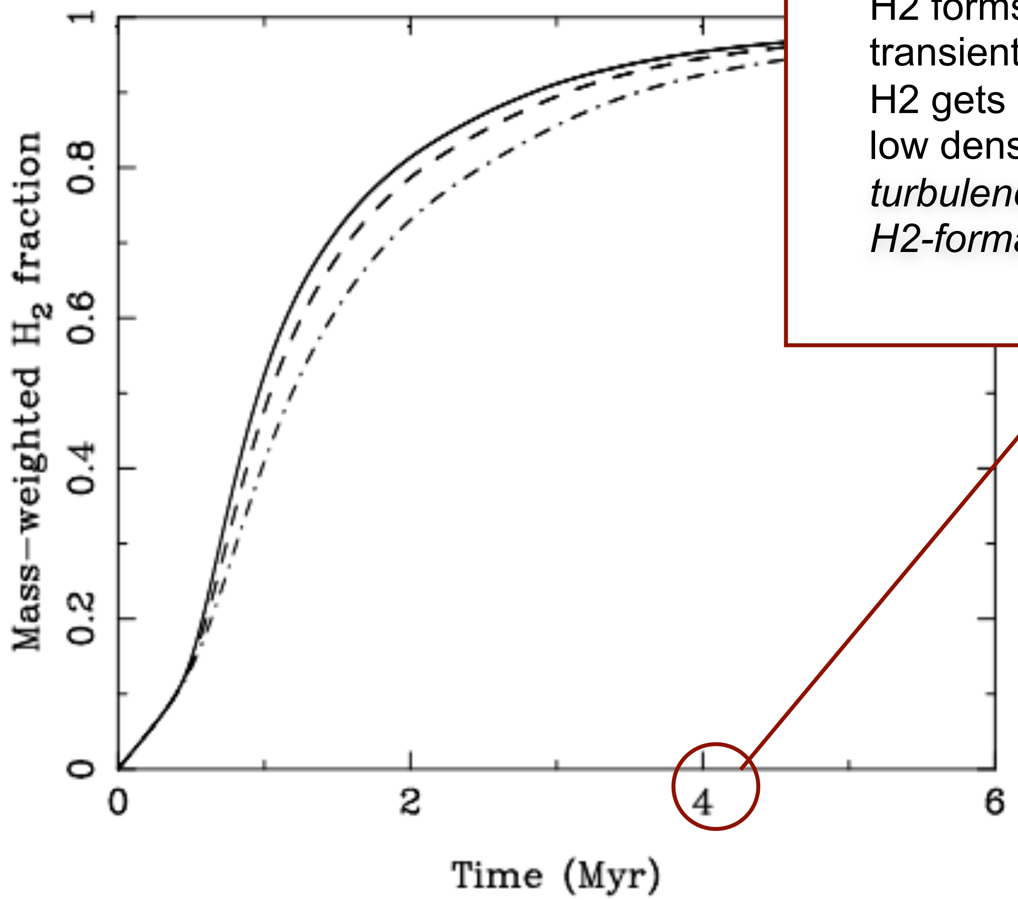

Figure 4. Time evolution of the mass-weighted H_2 abundance in simulations R1, R2 and R3, which have numerical resolutions of 64^3 zones (dot-dashed), 128^3 zones (dashed) and 256^3 zones (solid), respectively.

H2 forms rapidly in shocks / transient density fluctuations / H2 gets destroyed slowly in low density regions / *result: turbulence greatly enhances H2-formation rate*

(Glover, Federrath, Mac Low, Klessen, 2010)

HI to H2 conversion rate

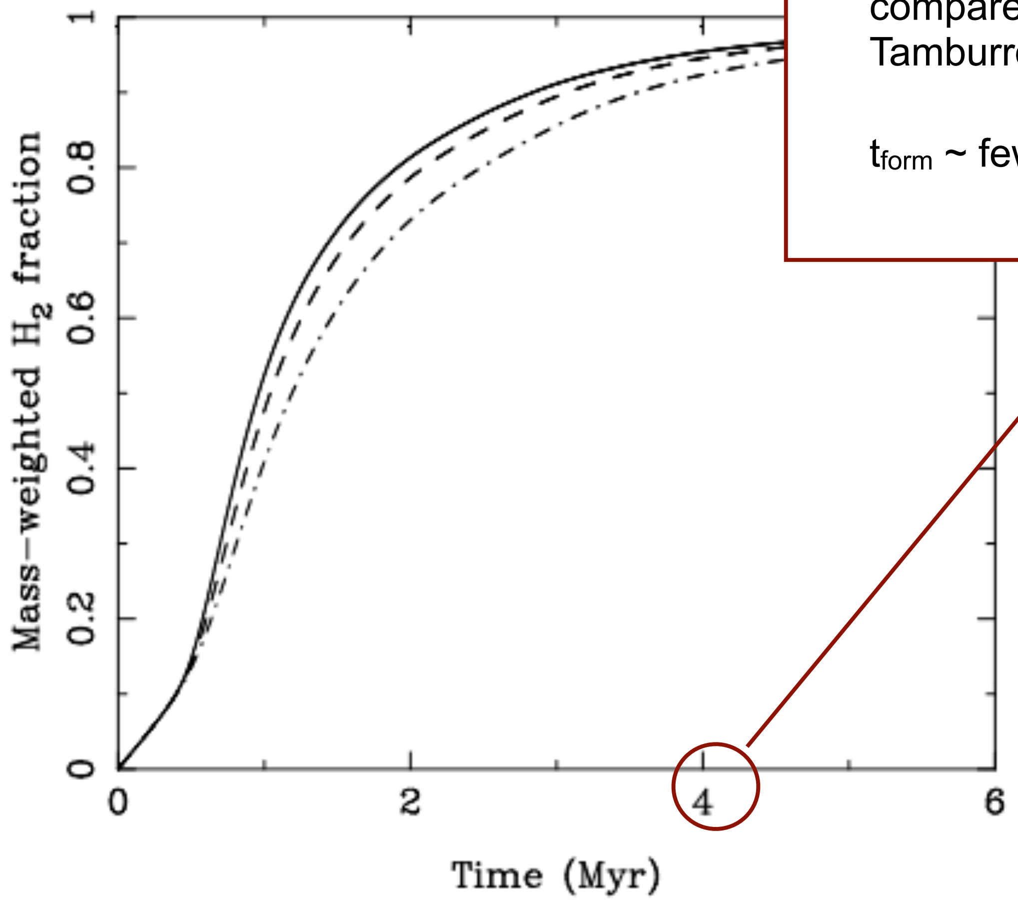

compare to data from Tamburro et al. (2008) study:

t_{form} ~ few x 10^6 years

Figure 4. Time evolution of the mass-weighted H_2 abundance in simulations R1, R2 and R3, which have numerical resolutions of 64^3 zones (dot-dashed), 128^3 zones (dashed) and 256^3 zones (solid), respectively.

(Glover, Federrath, Mac Low, Klessen, 2010)

CO, C^+ formation rates

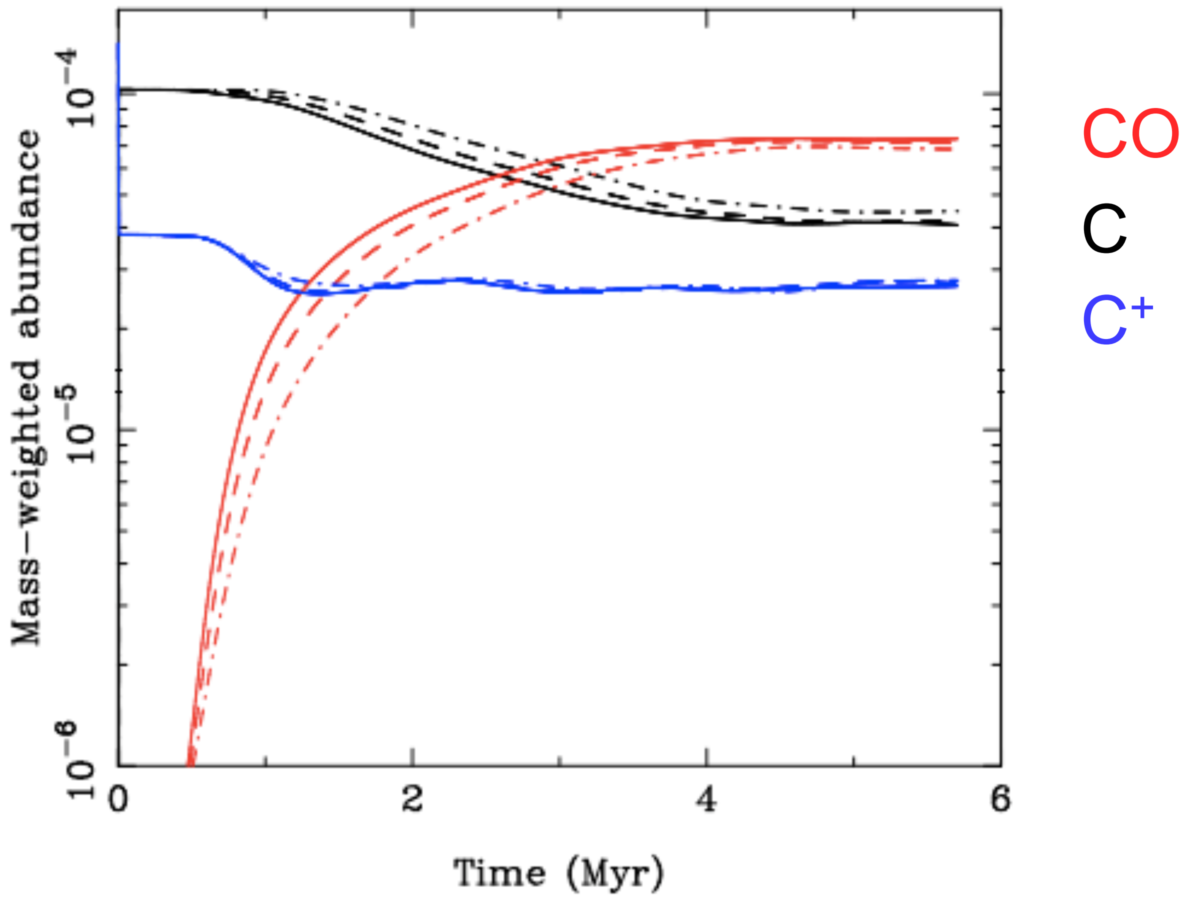

Figure 5. Time evolution of the mass-weighted abundances of atomic carbon (black lines), CO (red lines), and C^+ (blue lines) in simulations with numerical resolutions of 64^3 zones (dot-dashed), 128^3 zones (dashed) and 256^3 zones (solid).

(Glover, Federrath, Mac Low, Klessen, 2010)

effects of chemistry 1

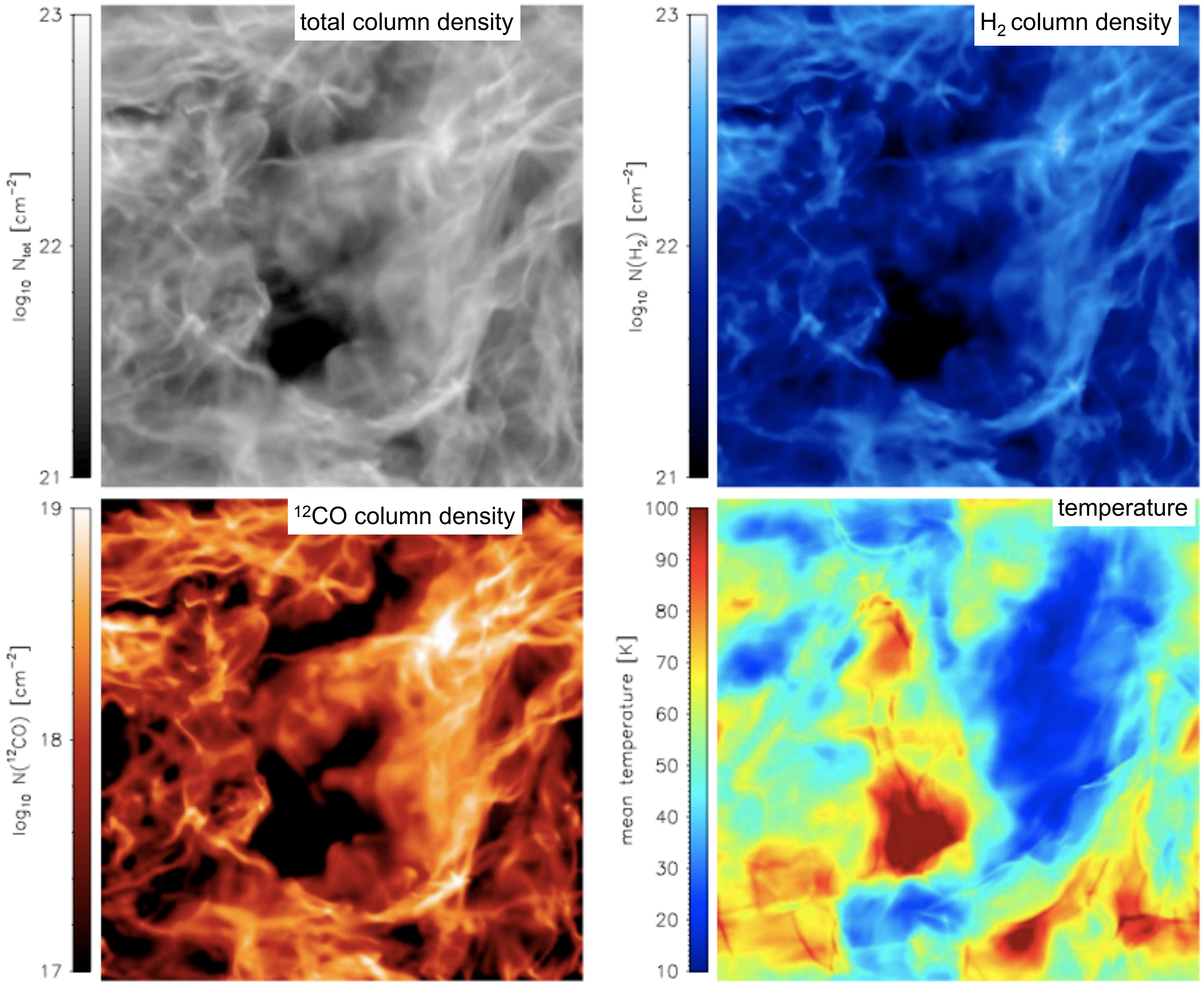

(Glover, Federrath, Mac Low, Klessen, 2010)

effects of chemistry 2

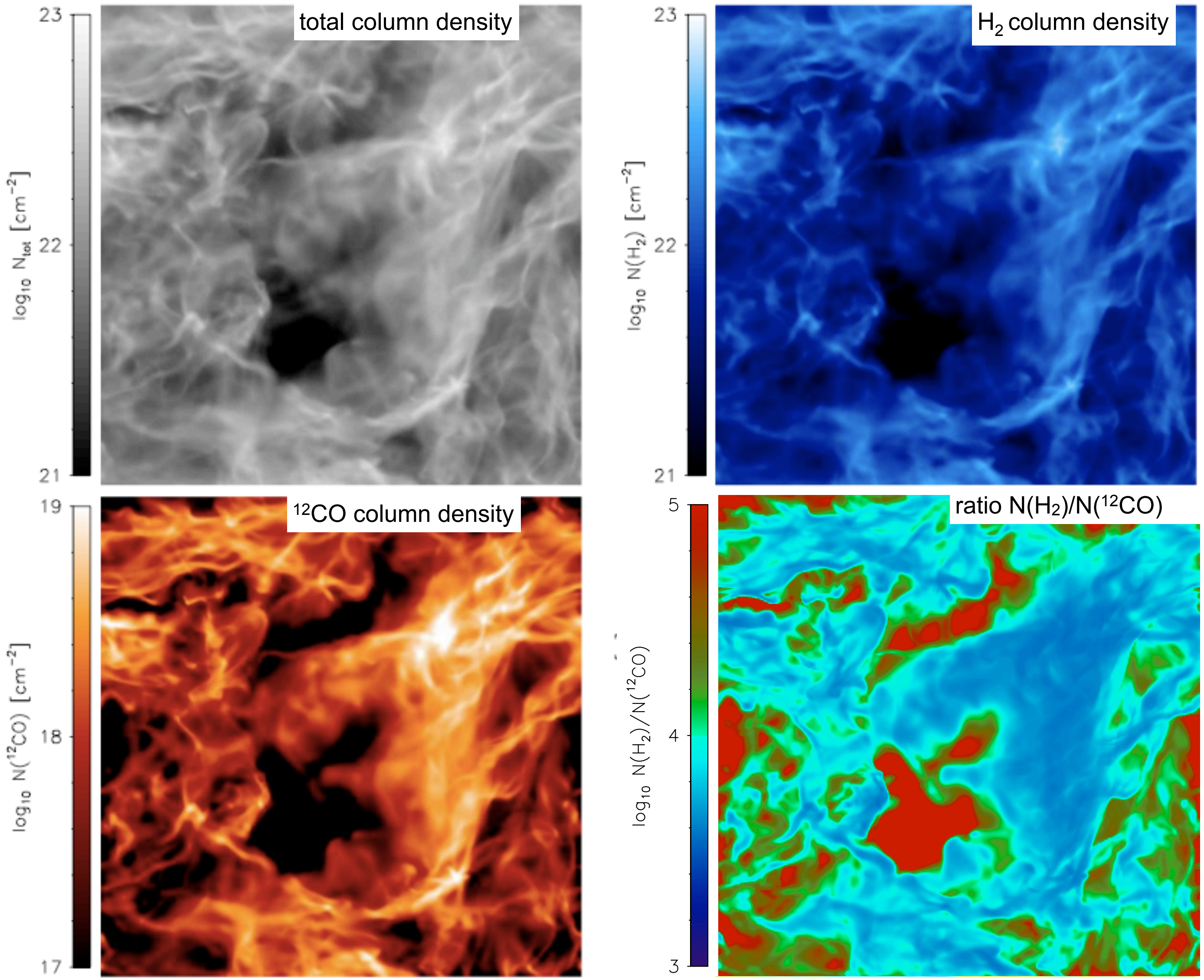

(Glover, Federrath, Mac Low, Klessen, 2010)

effects of chemistry 4

- deliverables / predictions:
  - x-factor estimates (as function of environmental conditions)
  - synthetic line emission maps (in combination with line transfer)
  - pdf's of density, velocity, emissivity / structure functions (to directly connect to observational regime)
  - *COMMENT:* density pdf is *NOT* lognormal!
    --> implications for analytical IMF theories

the x-factor

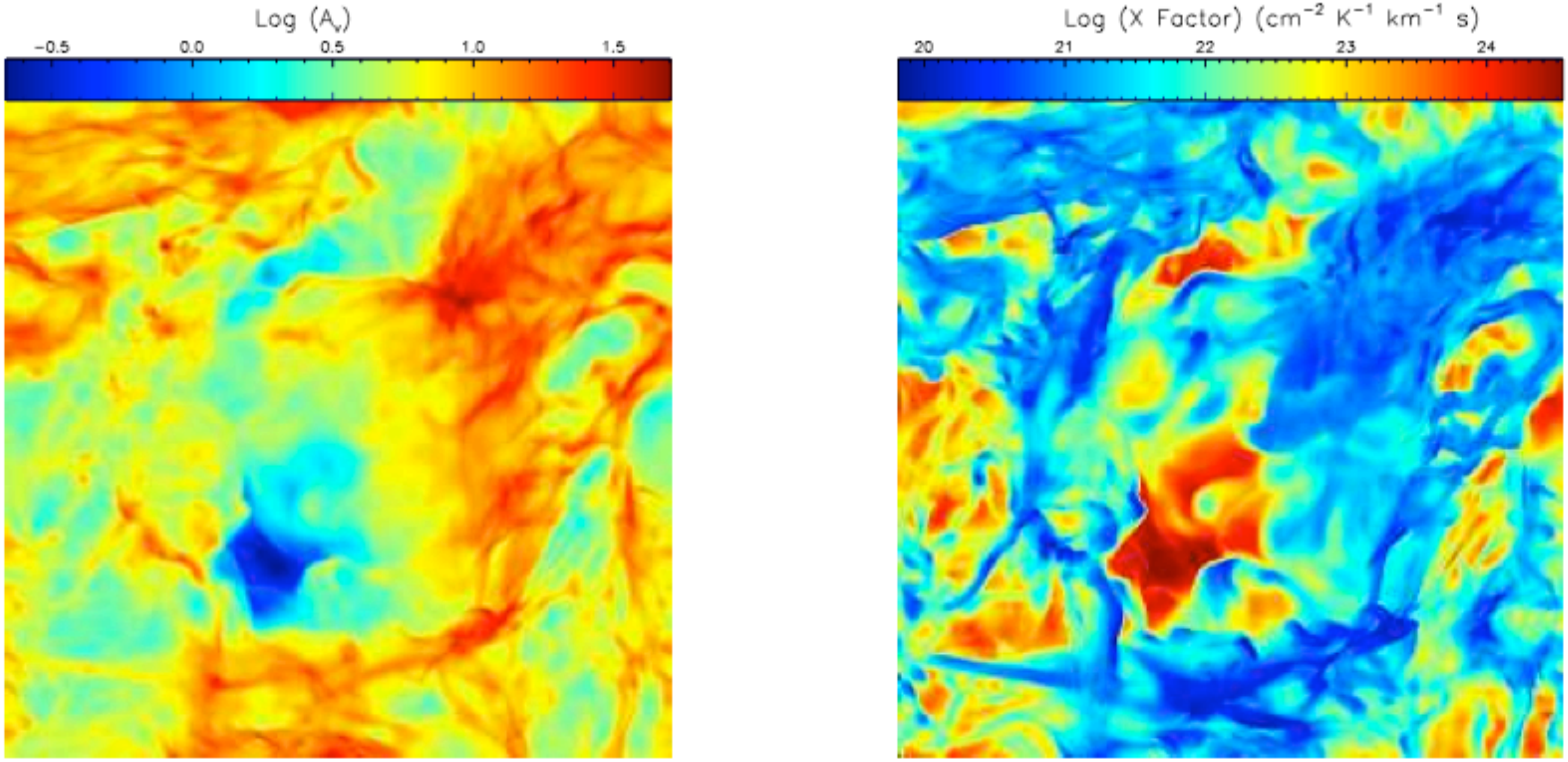

Images of A_v (left) and the X factor (right) of model n300-Z03.

(Shetty, Glover, Dullemond, Klessen 2011)

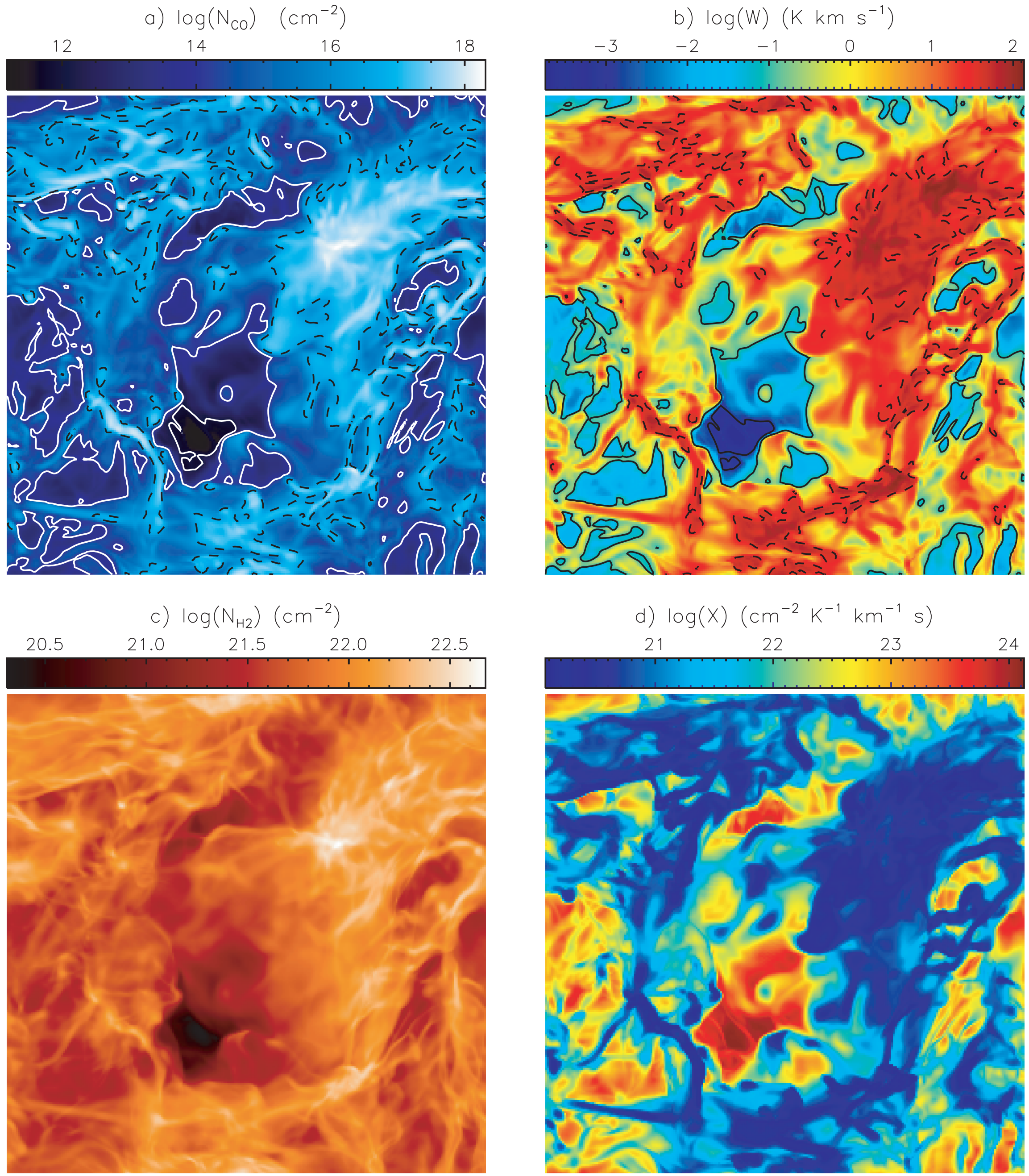

(Shetty, Glover, Dullemond, Klessen 2011)

Figure 4. Images of (a) N_{CO}, (b) W, (c) $N_{\mathrm{H_2}}$ and (d) the X factor of model n300-Z03. Each side has a length of 20 pc. In (a) and (b), solid contours indicate $\log(N_{\mathrm{CO}}) = 12, 14$ and $\log(W) = -3, -1$; dashed contours are $\log(N_{\mathrm{CO}}) = 16.5$ and $\log(W) = 1.5$ (see the text and Fig. 2d).

the x-factor

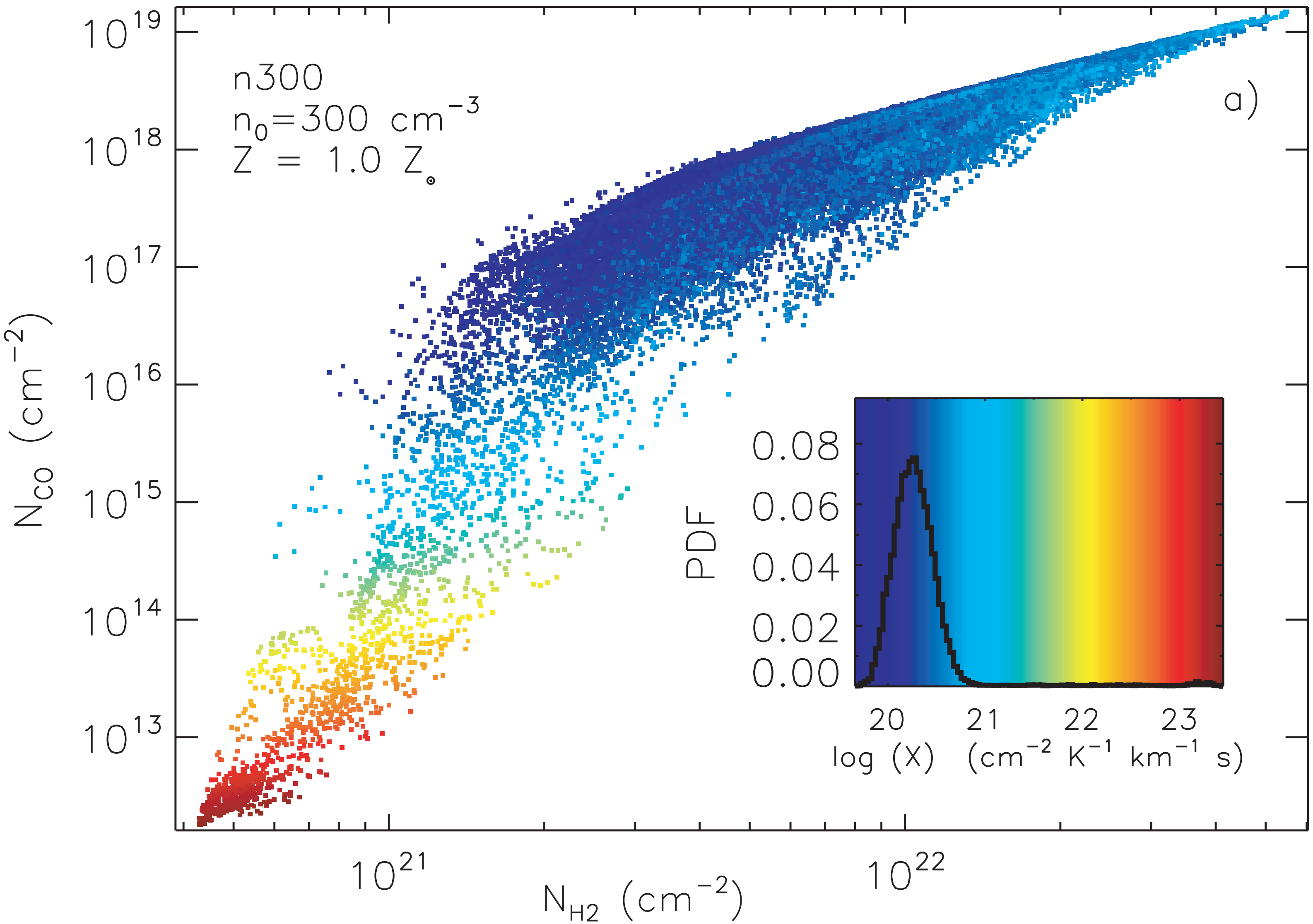

(Shetty, Glover, Dullemond, Klessen 2011)

different metallicities

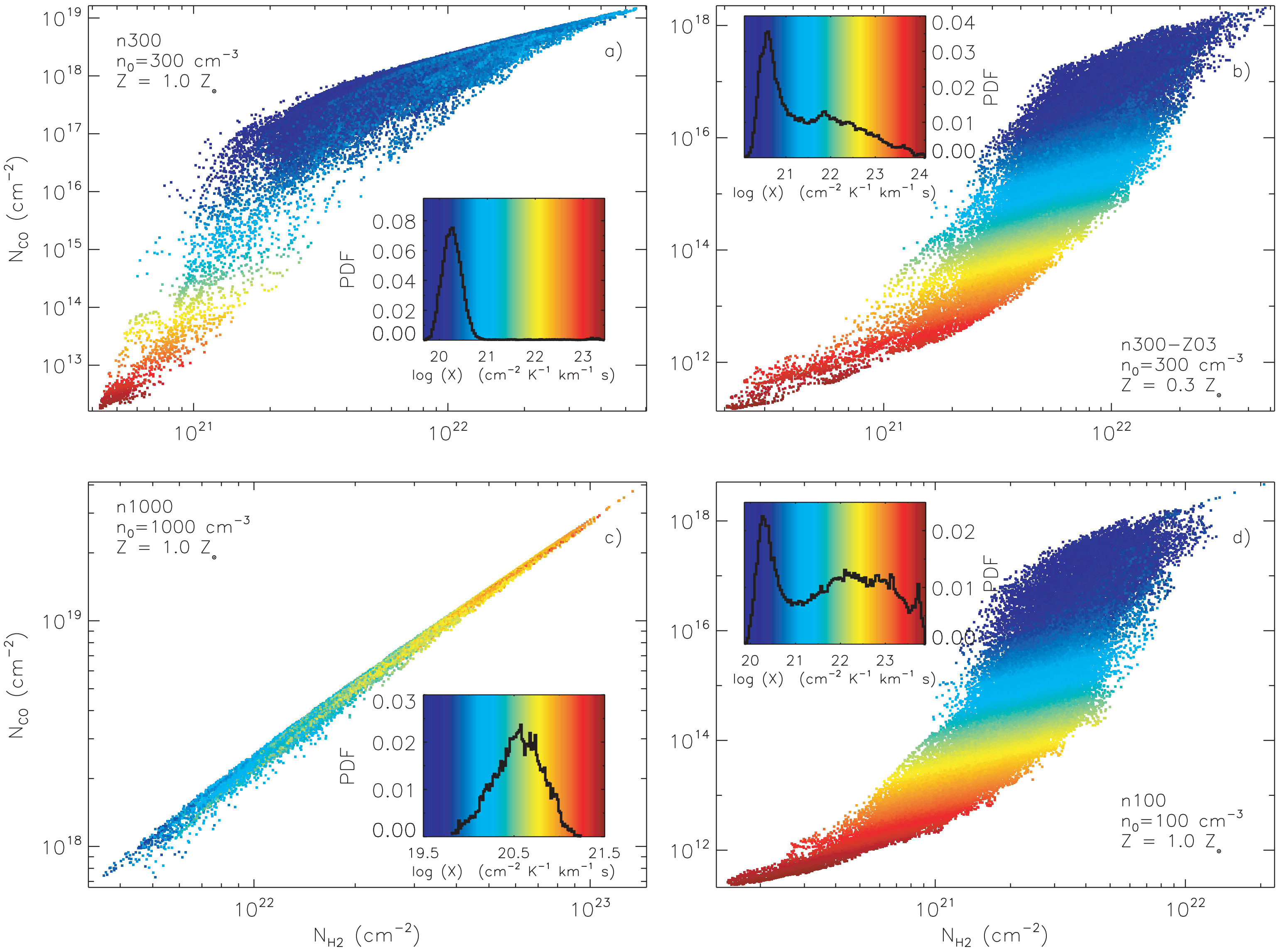

(Shetty, Glover, Dullemond, Klessen 2011)

Figure 5. *X* factor for four models. N_{CO} is plotted as a function of N_{H_2}. The colour of each point indicates the *X* factor. Inset figures show the colour scale and PDF of the *X* factor. The corresponding maps of N_{H_2}, N_{CO} and the *X* factor from model n300-Z03 are shown in Fig. 4.

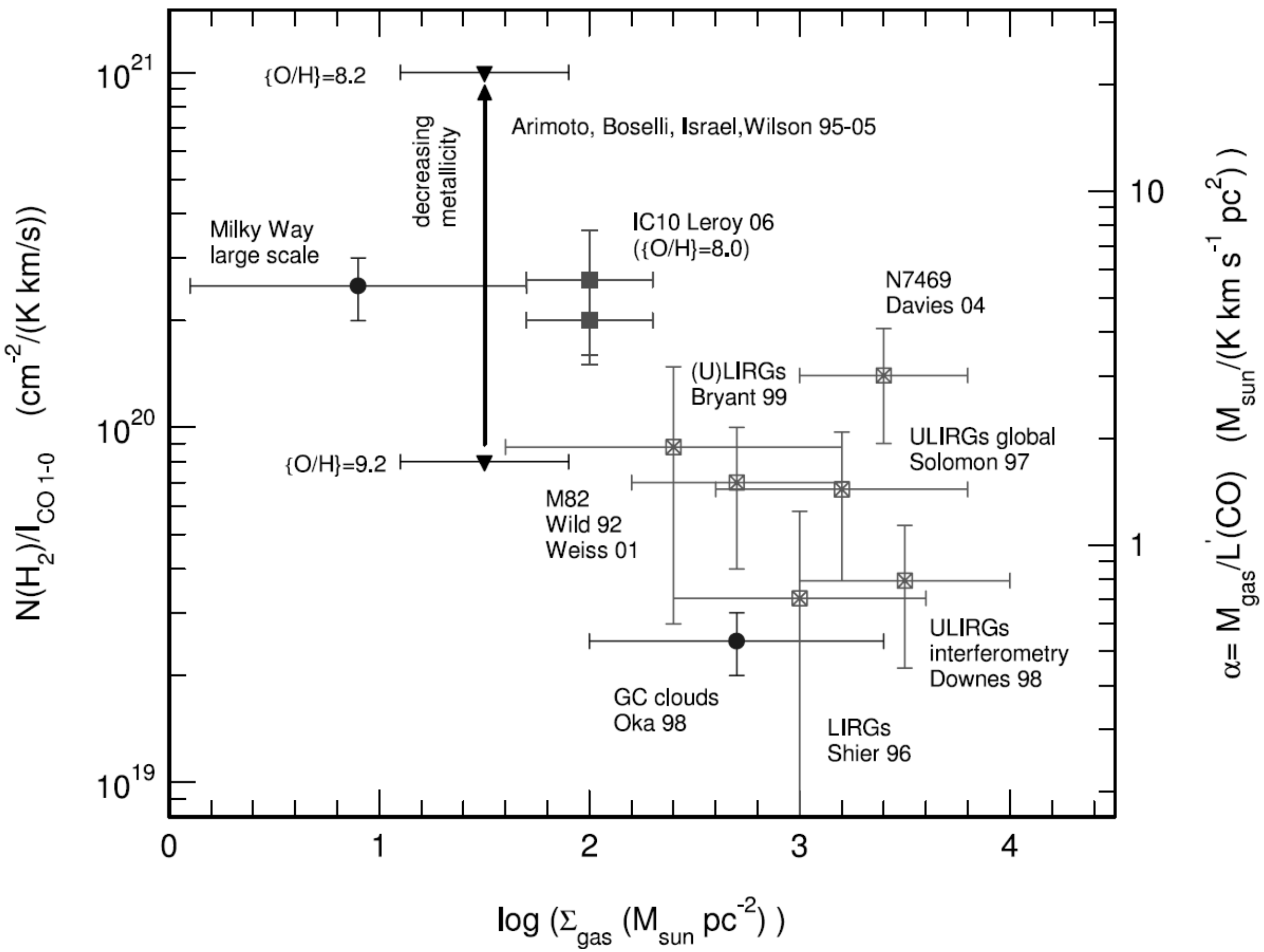

Tacconi et al. (2008)

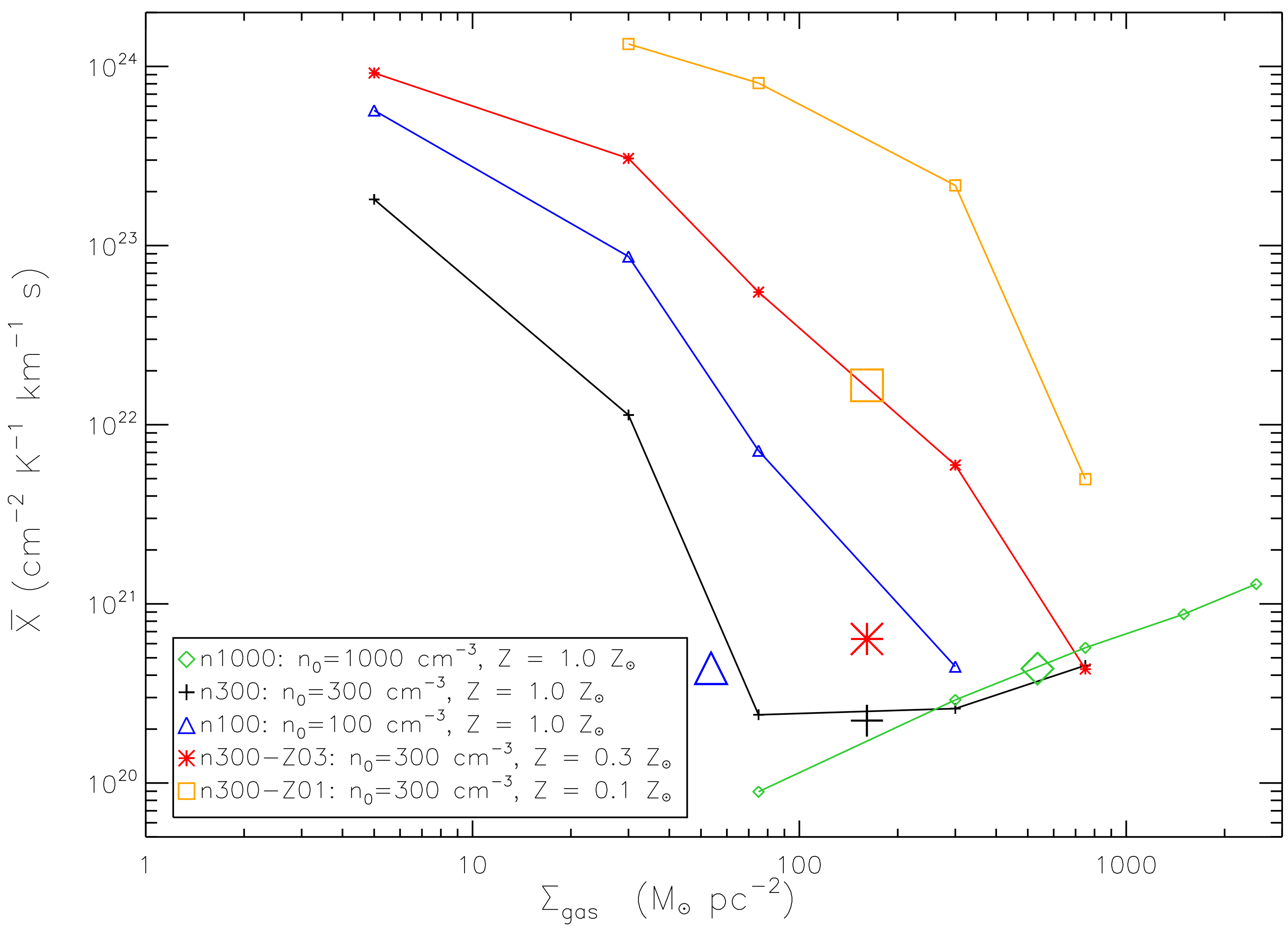

(Shetty, Glover, Dullemond, Klessen, in prep.)

line ratios

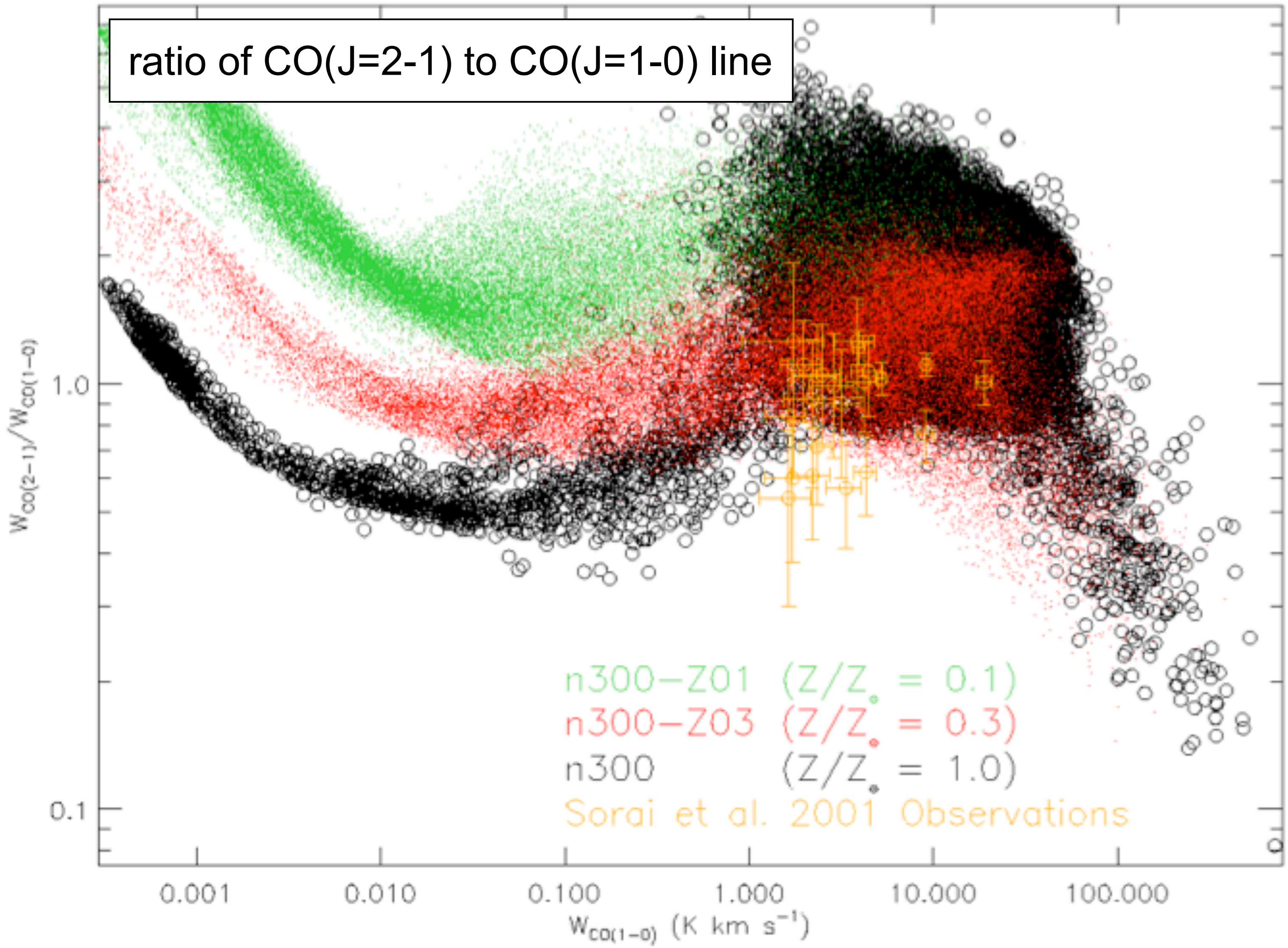

(Shetty, Glover, Dullemond, Klessen, in prep.)

X-factor

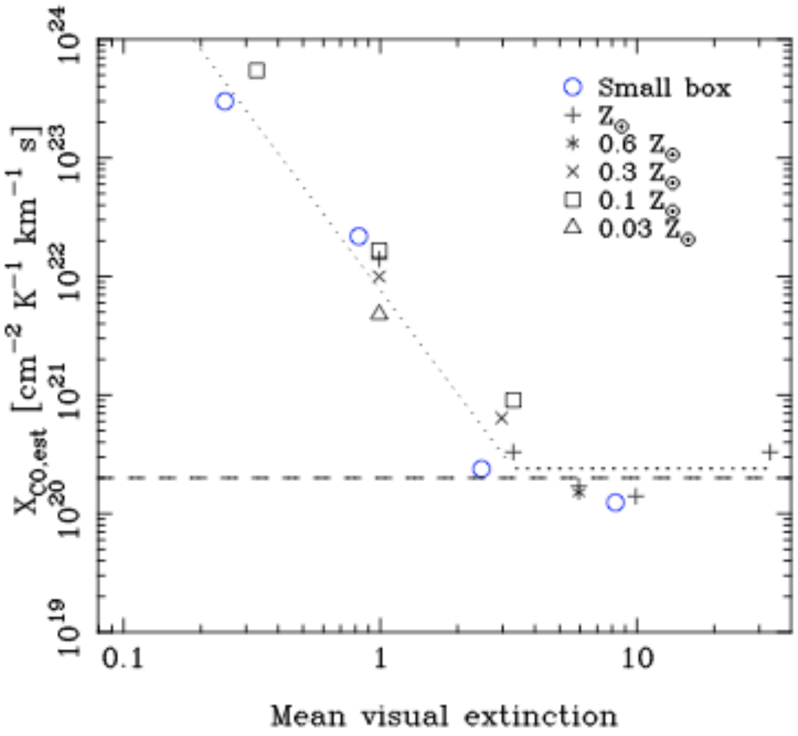

from Glover & Mac Low (2010, ApJ, submitted)

Figure 8. Estimate of the CO-to-H_2 conversion factor $X_{CO,est}$, plotted as a function of the mean visual extinction of the gas, $\langle A_V \rangle$. The simplifications made in our modelling mean that each value of $X_{CO,est}$ is uncertain by at least a factor of two. At $\langle A_V \rangle > 3$, the values we find are consistent with the value of $X_{CO} = 2 \times 10^{20} \mathrm{cm}^{-2}\,\mathrm{K}^{-1}\,\mathrm{km}^{-1}\,\mathrm{s}$ determined observationally for the Milky Way by Dame et al. (2001), indicated in the plot by the horizontal dashed line. At $\langle A_V \rangle < 3$, we find evidence for a strong dependence of $X_{CO,est}$ on $\langle A_V \rangle$. The empirical fit given by Equation 11 is indicated as the dotted line in the Figure, and demonstrates that at low $\langle A_V \rangle$, the CO-to-H_2 conversion factor increases roughly as $X_{CO,est} \propto A_V^{-2.8}$. It should also be noted that at any particular $\langle A_V \rangle$, the dependence of $X_{CO,est}$ on metallicity is relatively small. Previous claims of a strong metallicity dependence likely reflect the fact that there is a strong dependence on the mean extinction, which varies as $\langle A_V \rangle \propto Z$ given fixed mean cloud density and cloud size.

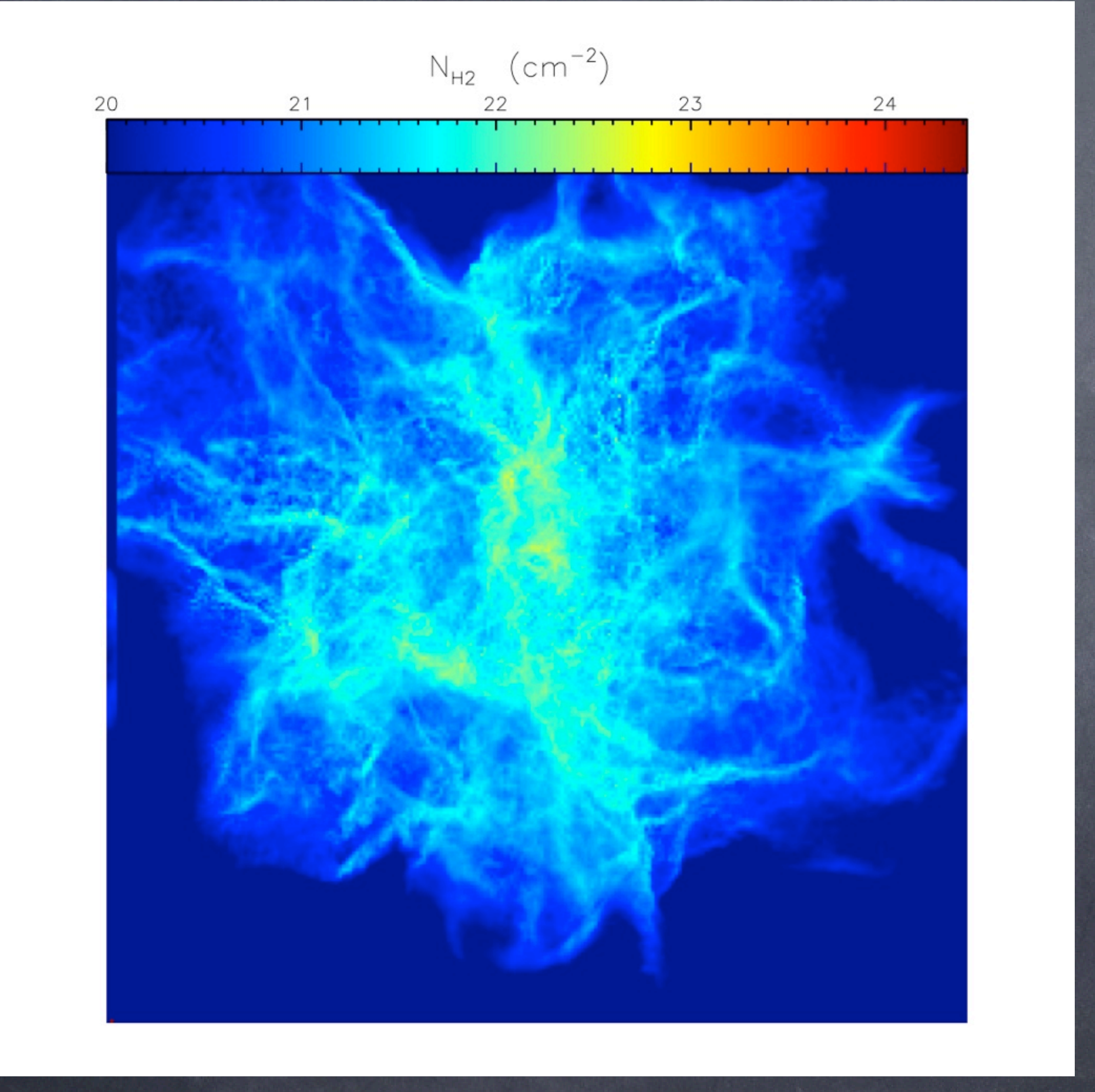
N_{H2} (cm^{-2})
20
21
22
23
24

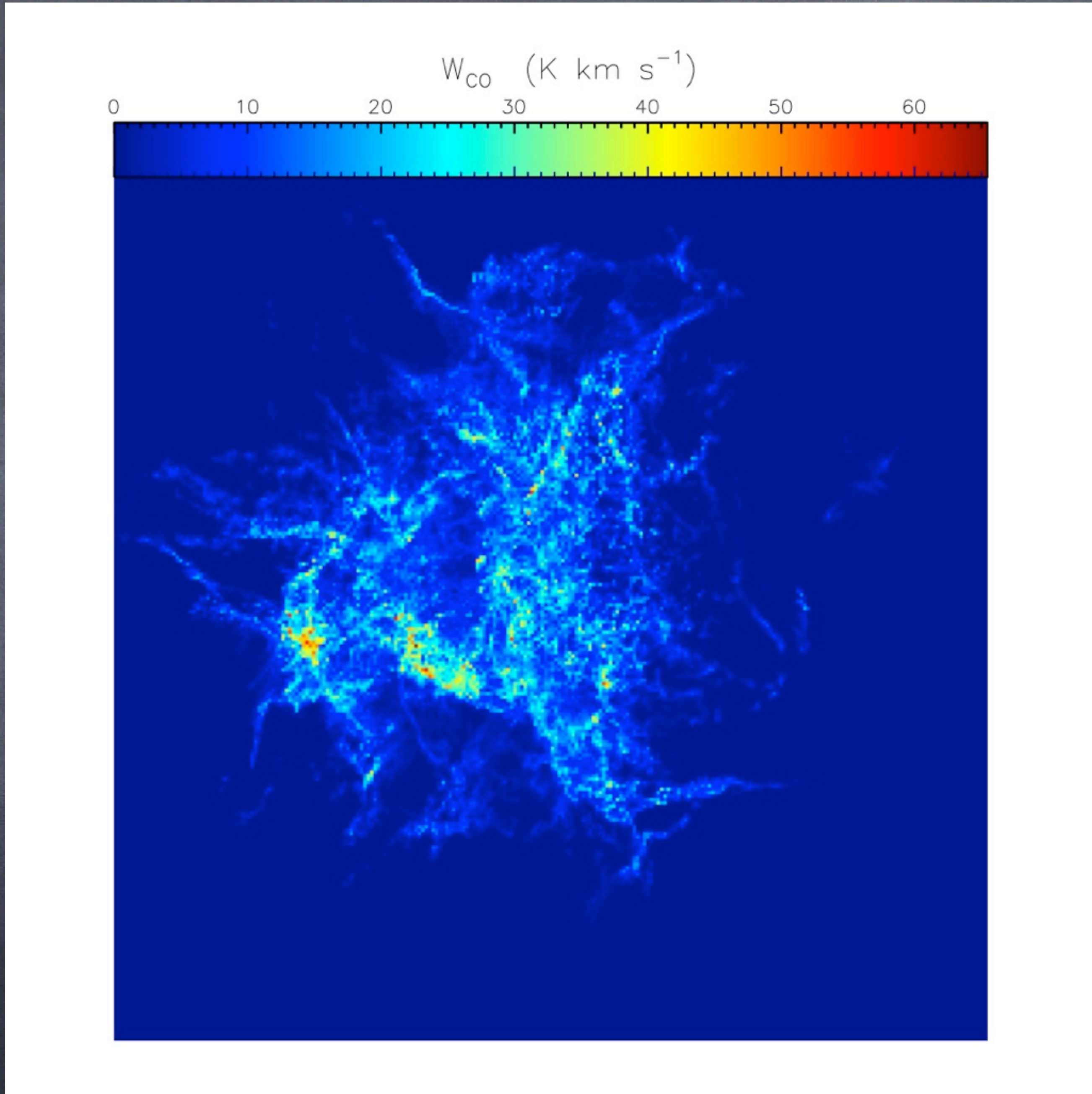

W_CO (K km s^-1)
0
10
20
30
40
50
60

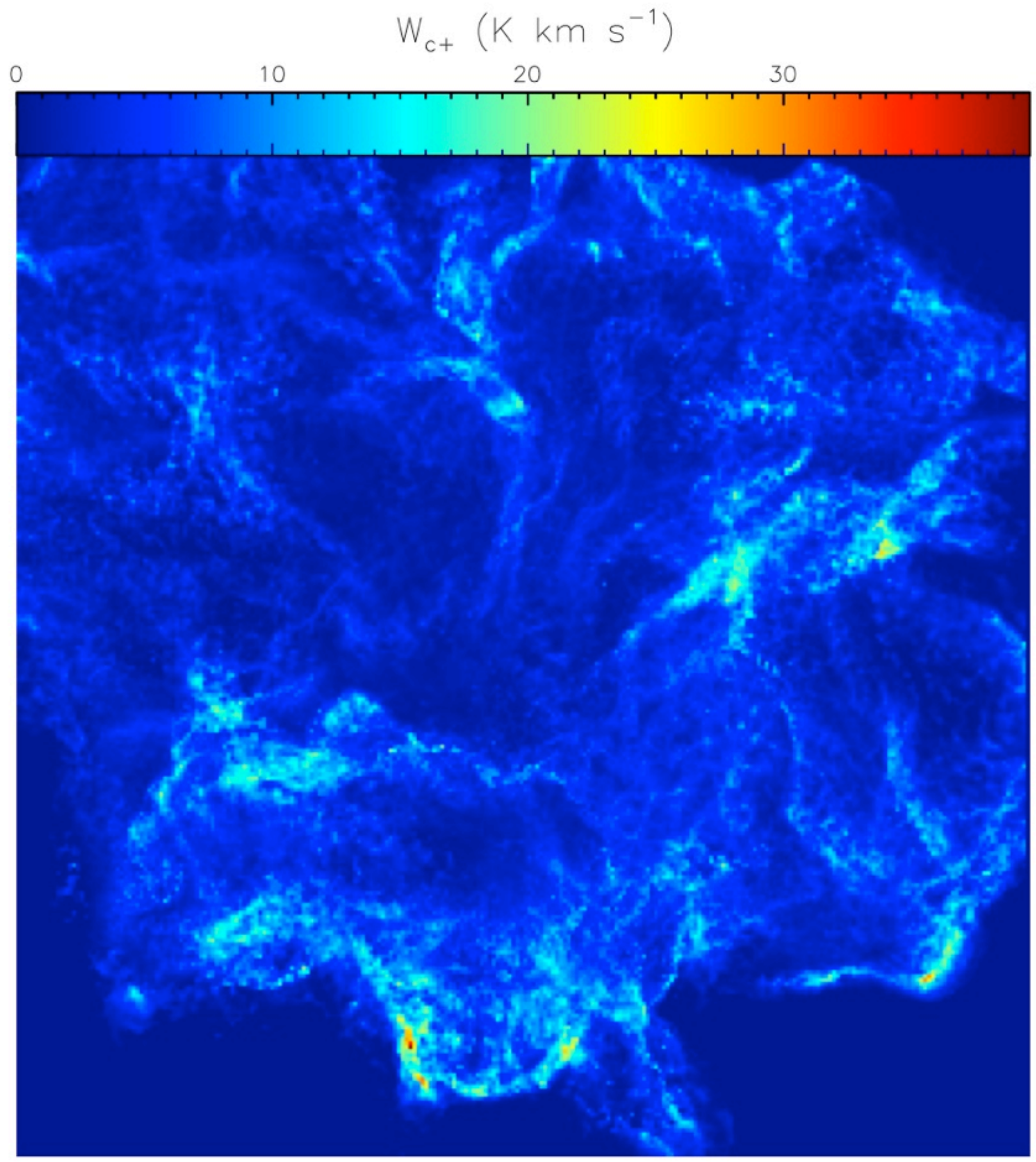

W_{c+} (K km s^{-1})
0
10
20
30

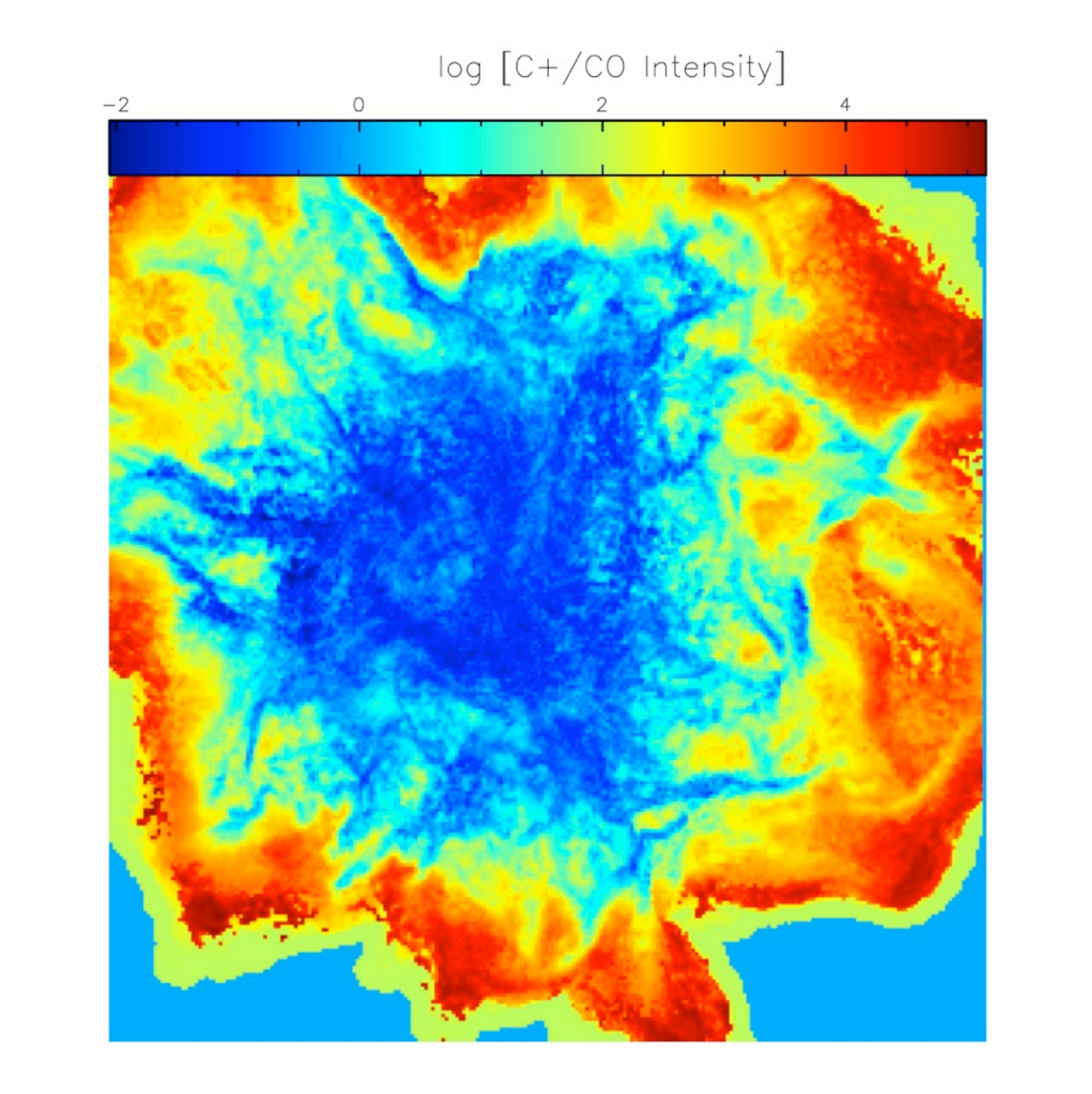
log [C+/CO Intensity]
−2
0
2
4

agenda

decreasing spatial scales

present days

early universe

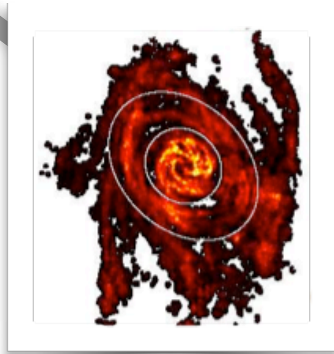

Molecular cloud formation

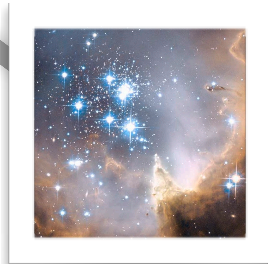

High-mass star formation

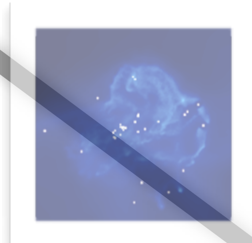

First star formation

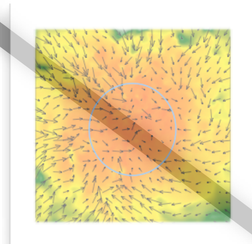

Magnetic fields in the primordial universe

We want to address the following questions:

- how do massive stars (and their associated clusters) form?
- what determines the upper stellar mass limit?
- what is the physics behind observed HII regions?

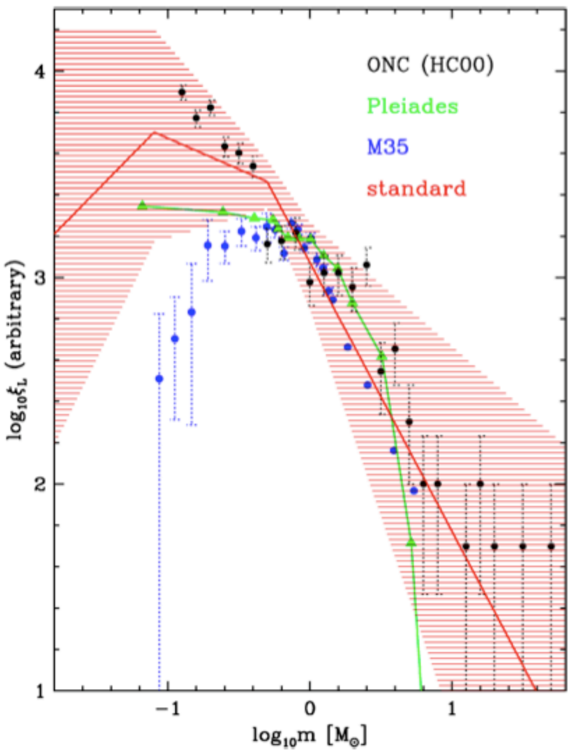

IMF (Kroupa 2002)

Rosetta nebula (NGC 2237)

(proto)stellar feedback processes

- radiation pressure on dust particles
- ionizing radiation
- stellar winds
- jets and outflows

- radiation pressure on dust particles
  - has gained most attention in the literature (see e.g. Krumholz et al. 2007, 2008, 2009)
- ionization
  - few numerical studies so far (e.g. Dale 2007, Gritschneder et al. 2009), detailed collapse calculations with ionizing and non-ionizing feedback still missing
  - HII regions around massive stars are directly observable --> direct comparison between theory and observations

our (numerical) approach

- focus on collapse of individual high-mass cores...
  - massive core with 1,000 $M_\odot$
  - Bonnor-Ebert type density profile
    (flat inner core with 0.5 pc and rho ~ $r^{-3/2}$ further out)
  - initial m=2 perturbation, rotation with β = 0.05
  - sink particle with radius 600 AU and threshold density of 7×10^{-16} g cm^{-3}
  - cell size 100 AU

Peters et al. (2010a, ApJ, 711, 1017), Peters et al. (2010b, ApJ, 719, 831), Peters et al. (2010c, ApJ, 725, 134)

our (numerical) approach

- method:
  - FLASH with ionizing and non-ionizing radiation using raytracing based on hybrid-characteristics
  - protostellar model from Hosokawa & Omukai
  - rate equation for ionization fraction
  - relevant heating and cooling processes
  - some models include magnetic fields
  - *first 3D MHD calculations that consistently treat both ionizing and non-ionizing radiation in the context of high-mass star formation*

Peters et al. (2010a,b,c)

model of high mass star formation

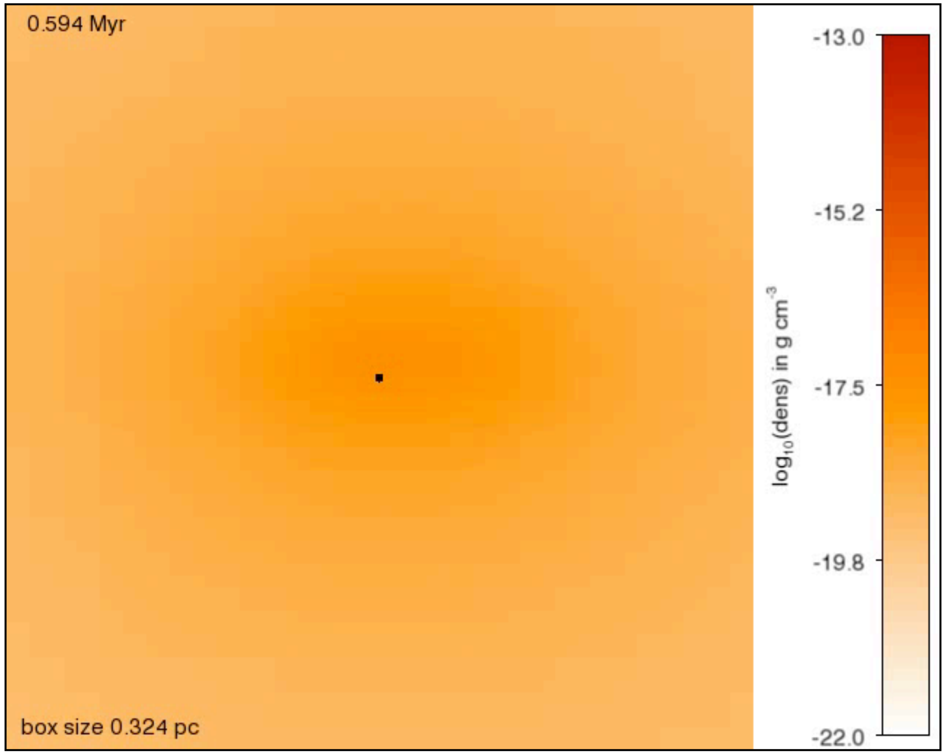

Disk edge on

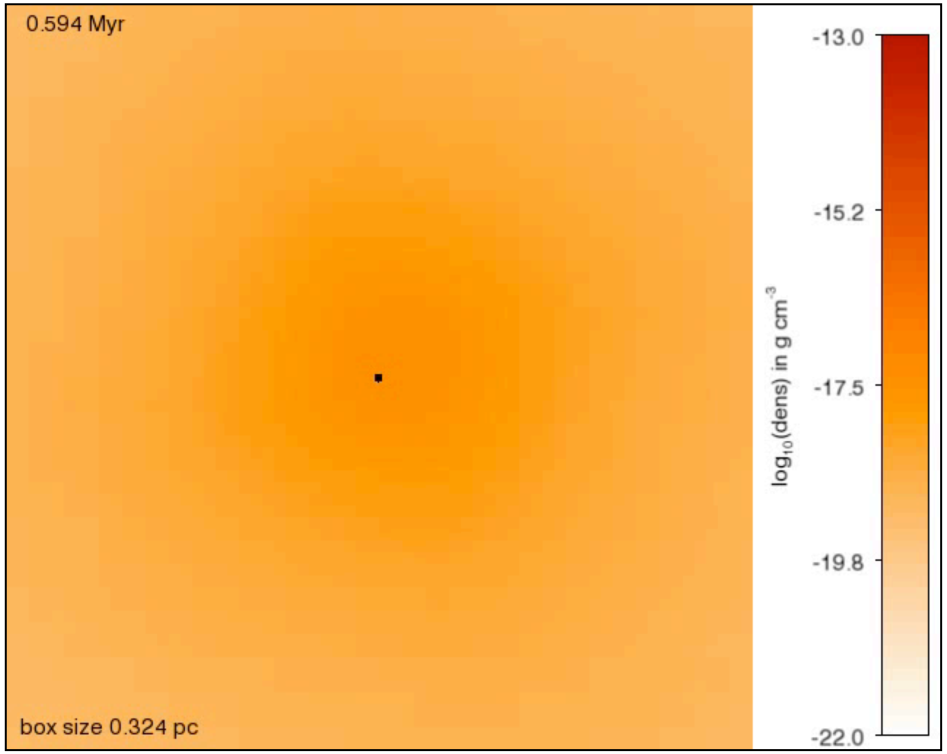

Disk plane

Peters et al. (2010a, ApJ, 711, 1017), Peters et al. (2010b, ApJ, 719, 831), Peters et al. (2010c, ApJ, 725, 134)

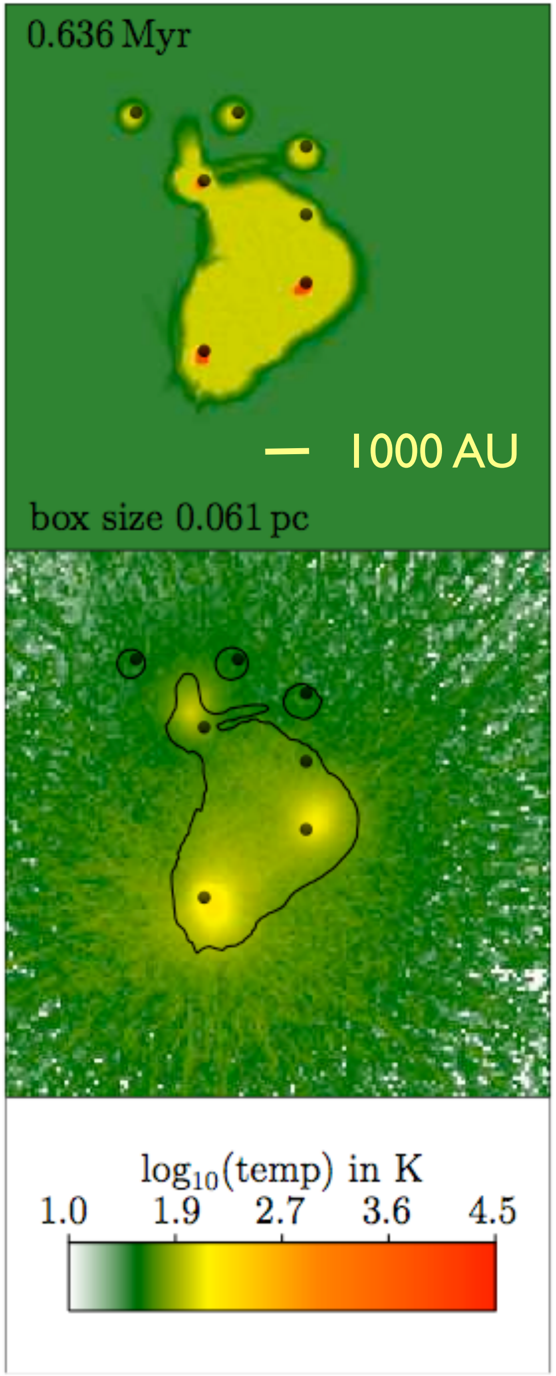

ray tracing method
(hydrid characteristics)

Monte Carlo: full RT
(with scattered radiation)

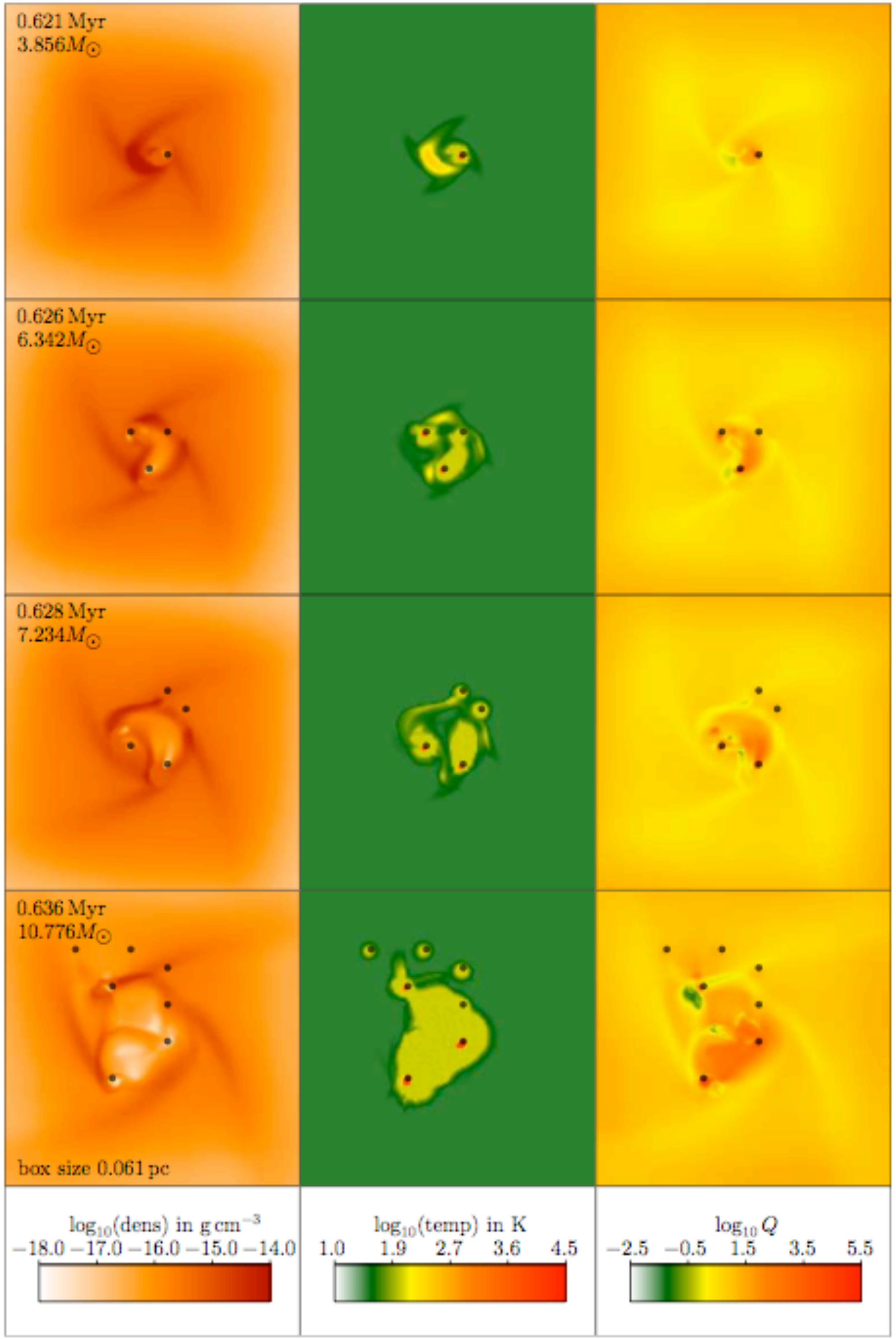

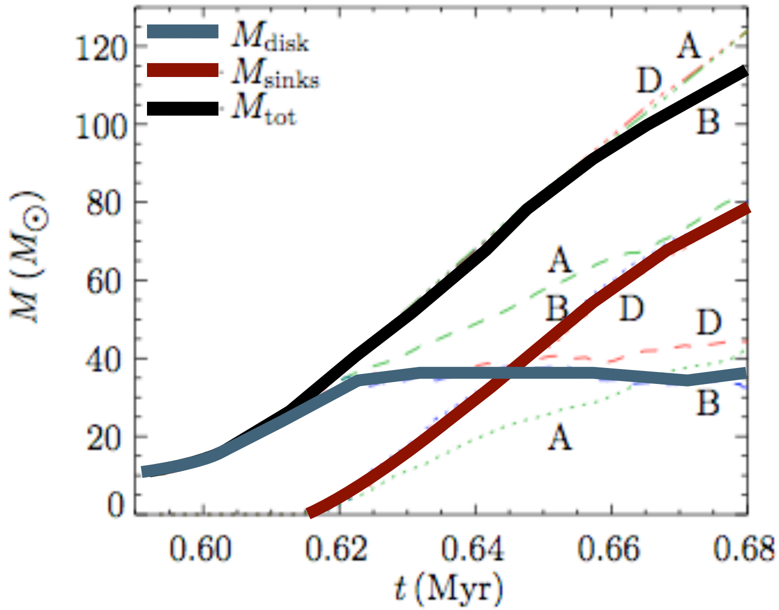

mass load onto the disk exceeds inward transport
--> becomes gravitationally unstable (see also Kratter & Matzner 2006, Kratter et al. 2010)

fragments to form multiple stars --> explains why high-mass stars are seen in clusters

Peters et al. (2010a, ApJ, 711, 1017),
Peters et al. (2010b, ApJ, 719, 831),
Peters et al. (2010c, ApJ, 725, 134)

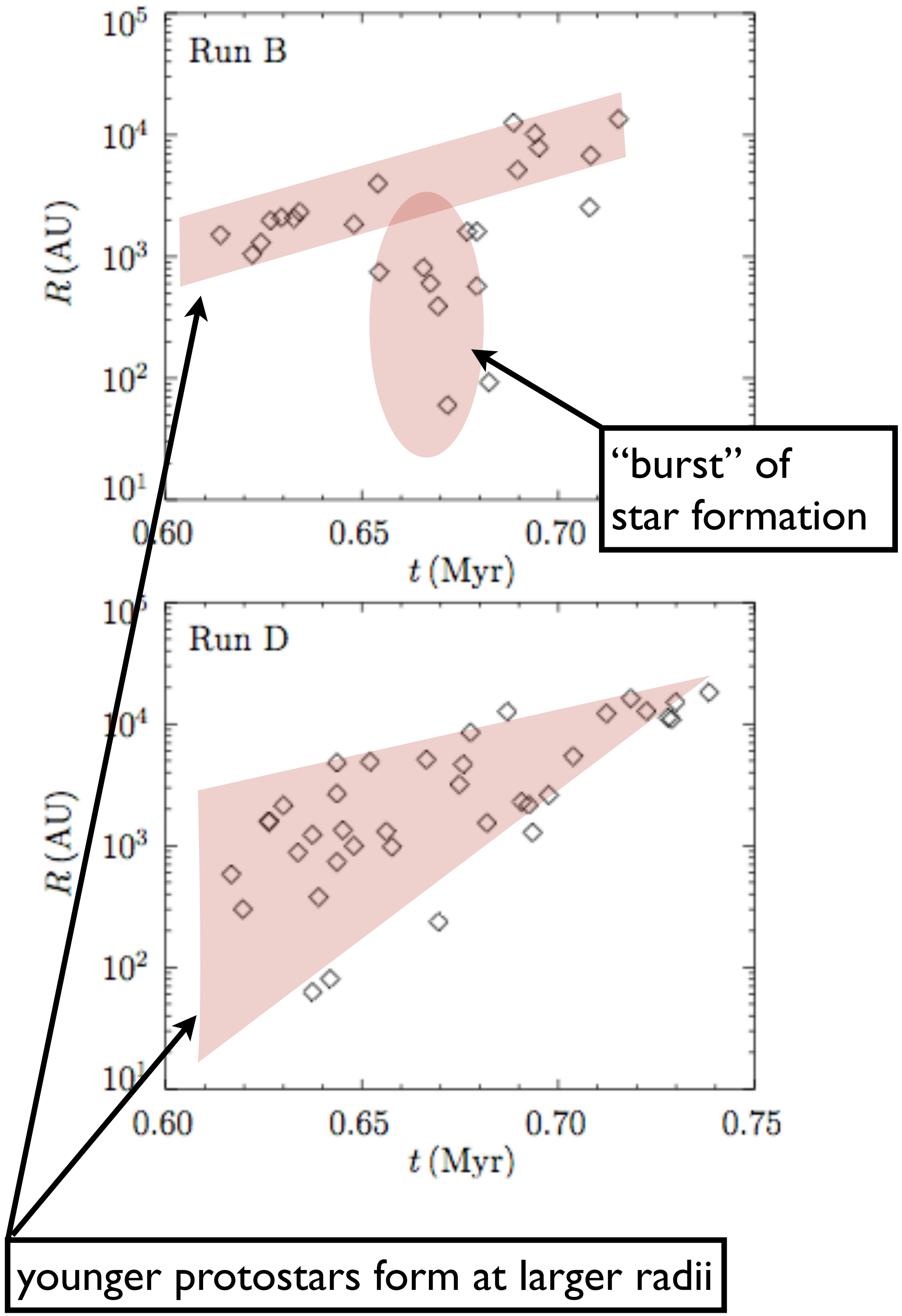

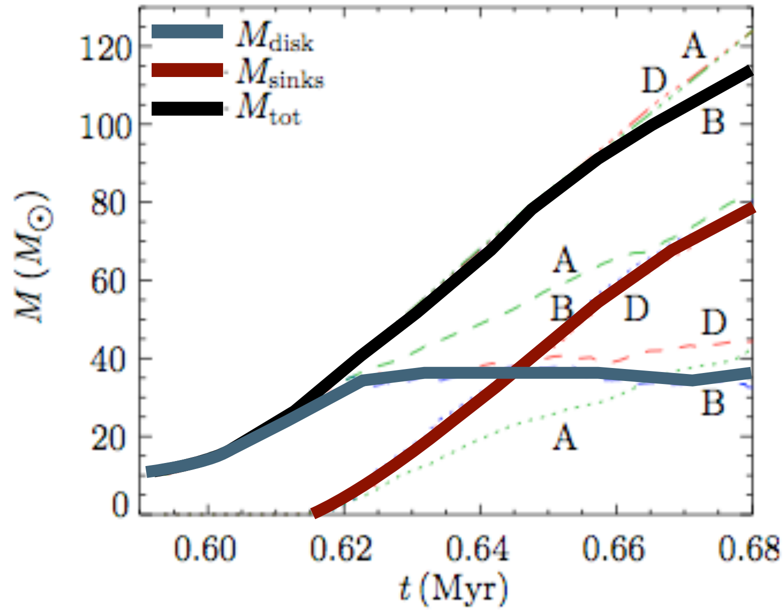

mass load onto the disk exceeds inward transport
--> becomes gravitationally unstable (see also Kratter & Matzner 2006, Kratter et al. 2010)

fragments to form multiple stars --> explains why high-mass stars are seen in clusters

Peters et al. (2010a, ApJ, 711, 1017),
Peters et al. (2010b, ApJ, 719, 831),
Peters et al. (2010c, ApJ, 725, 134)

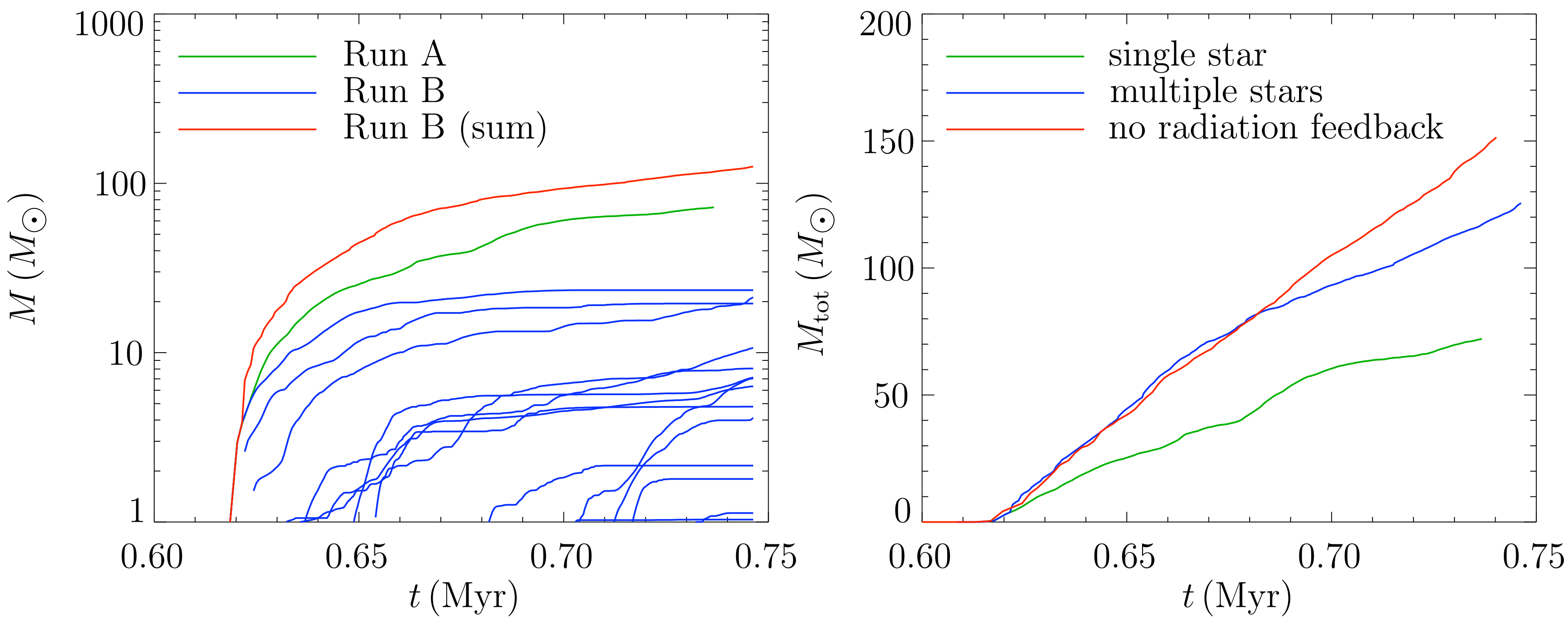

- compare with control run without radiation feedback
- total accretion rate does not change with accretion heating
- expansion of ionized bubble causes turn-off
- no triggered star formation by expanding bubble

Peters et al. (2010a, ApJ, 711, 1017), Peters et al. (2010b, ApJ, 719, 831), Peters et al. (2010c, ApJ, 725, 134)

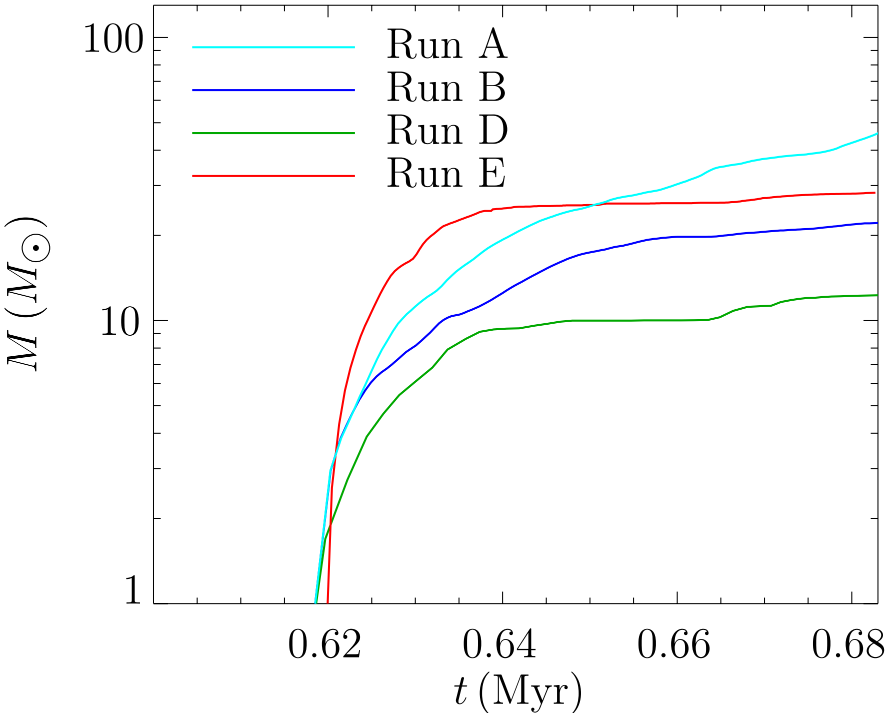

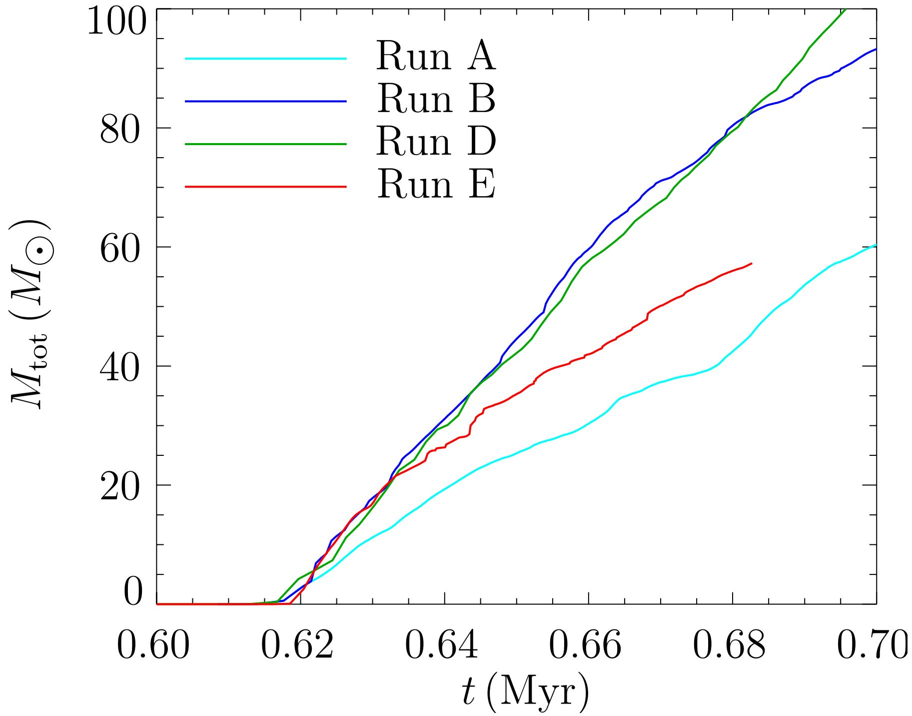

- magnetic fields lead to weaker fragmentation
- central star becomes more massive (magnetic breaking

Peters et al. (2010a, ApJ, 711, 1017), Peters et al. (2010b, ApJ, 719, 831), Peters et al. (2010c, ApJ, 725, 134), Peters et al. (2011, ApJ, 729, 72

Fragmentation-induced starvation in a complex cluster

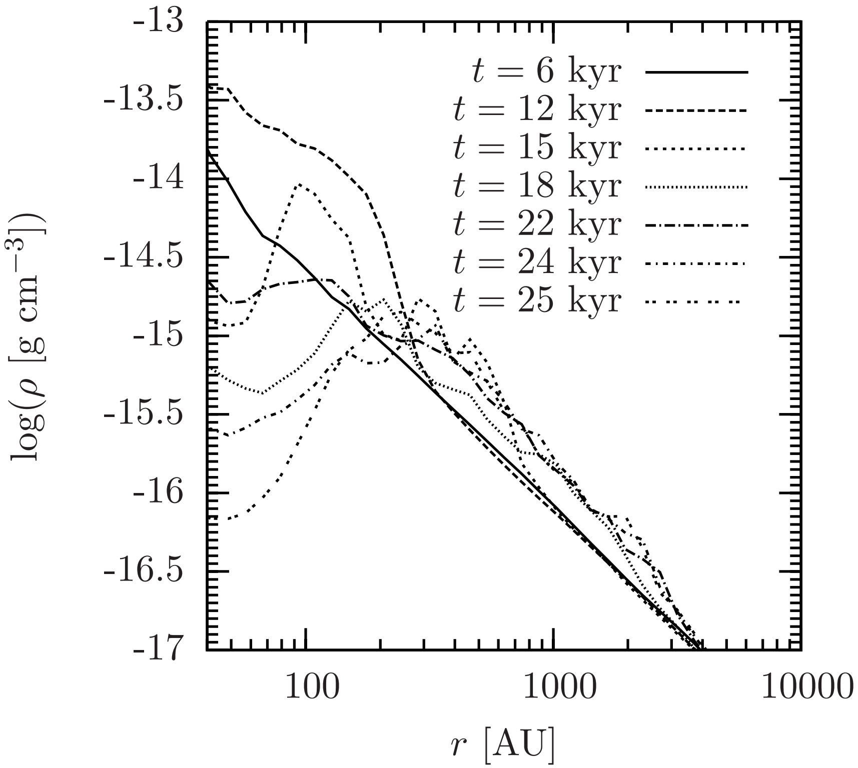

gas density as function of radius at different times

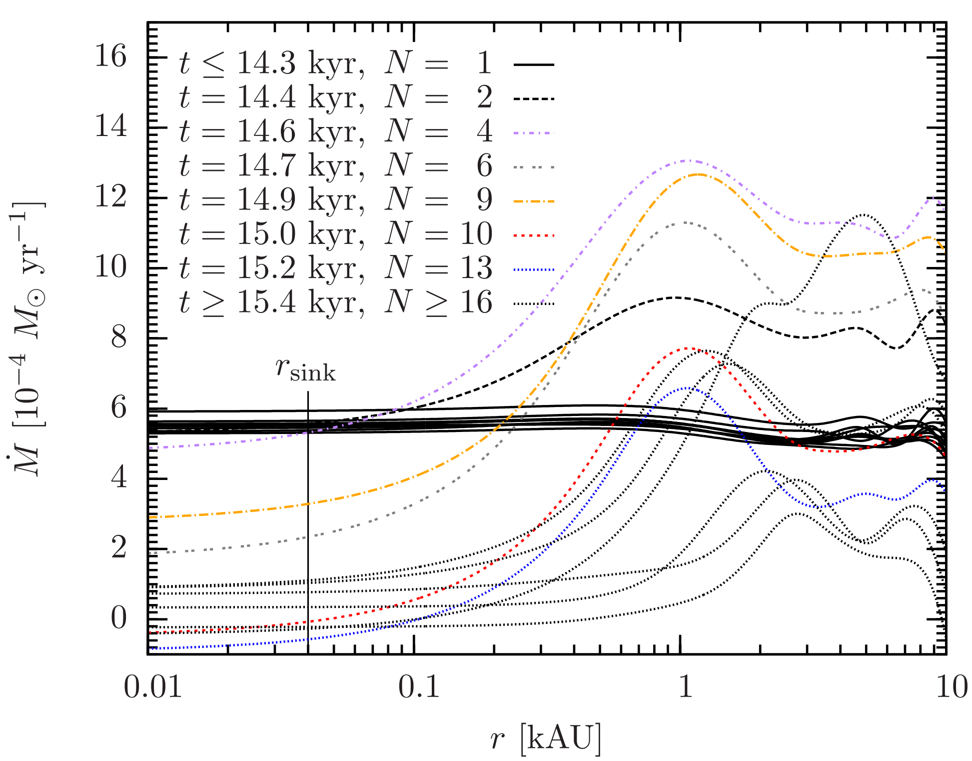

mass flow towards the center as function of radius at different times

Girichidis et al. (2011a,b)

- numerical data can be used to generate continuum maps
- calculate free-free absorption coefficient for every cell
- integrate radiative transfer equation (neglecting scattering)
- convolve resulting image with beam width
- VLA parameters:
  - distance $2.65\,\mathrm{kpc}$
  - wavelength $2\,\mathrm{cm}$
  - FWHM $0\farcs14$
  - noise $10^{-3}\,\mathrm{Jy}$

Peters et al. (2010a, ApJ, 711, 1017), Peters et al. (2010b, ApJ, 719, 831), Peters et al. (2010c, ApJ, 725, 134)

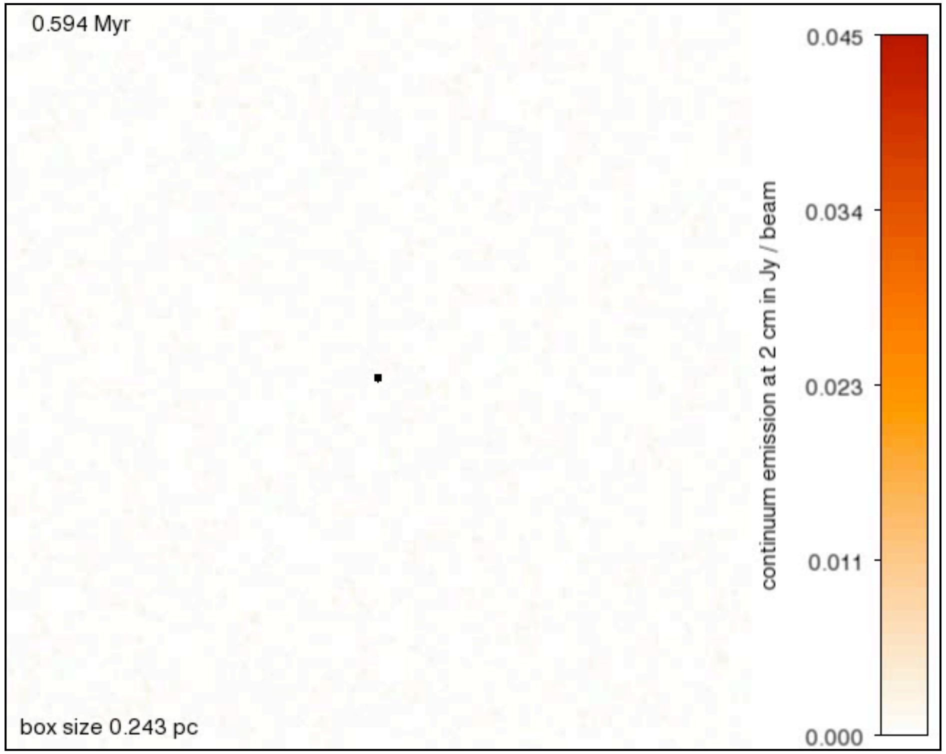

Disk face on

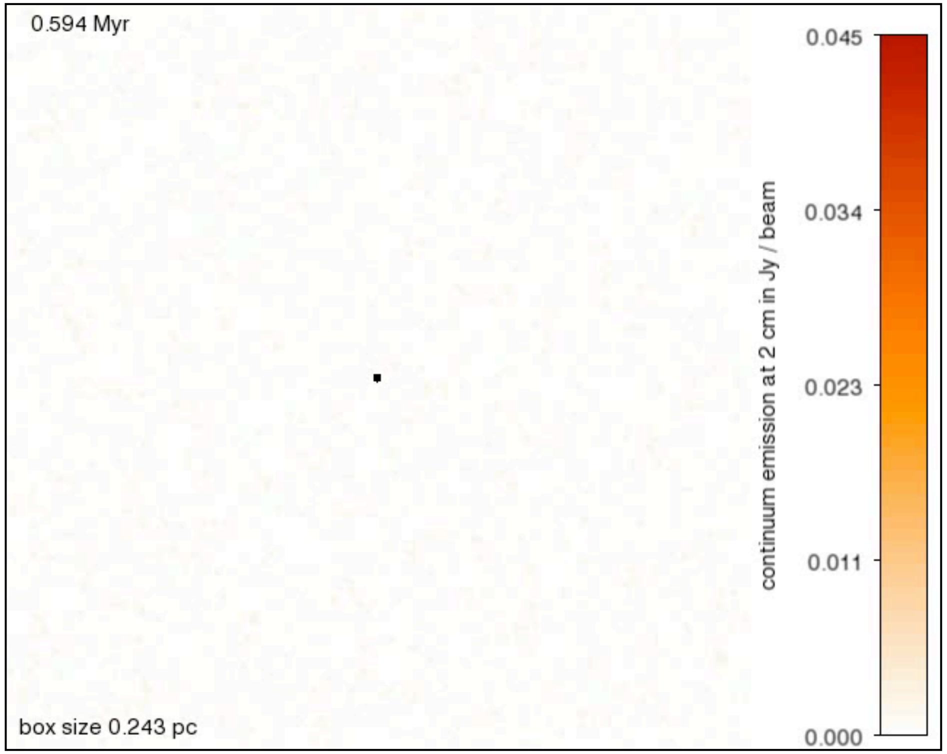

Disk edge on

Peters et al. (2010a, ApJ, 711, 1017), Peters et al. (2010b, ApJ, 719, 831), Peters et al. (2010c, ApJ, 725, 134)

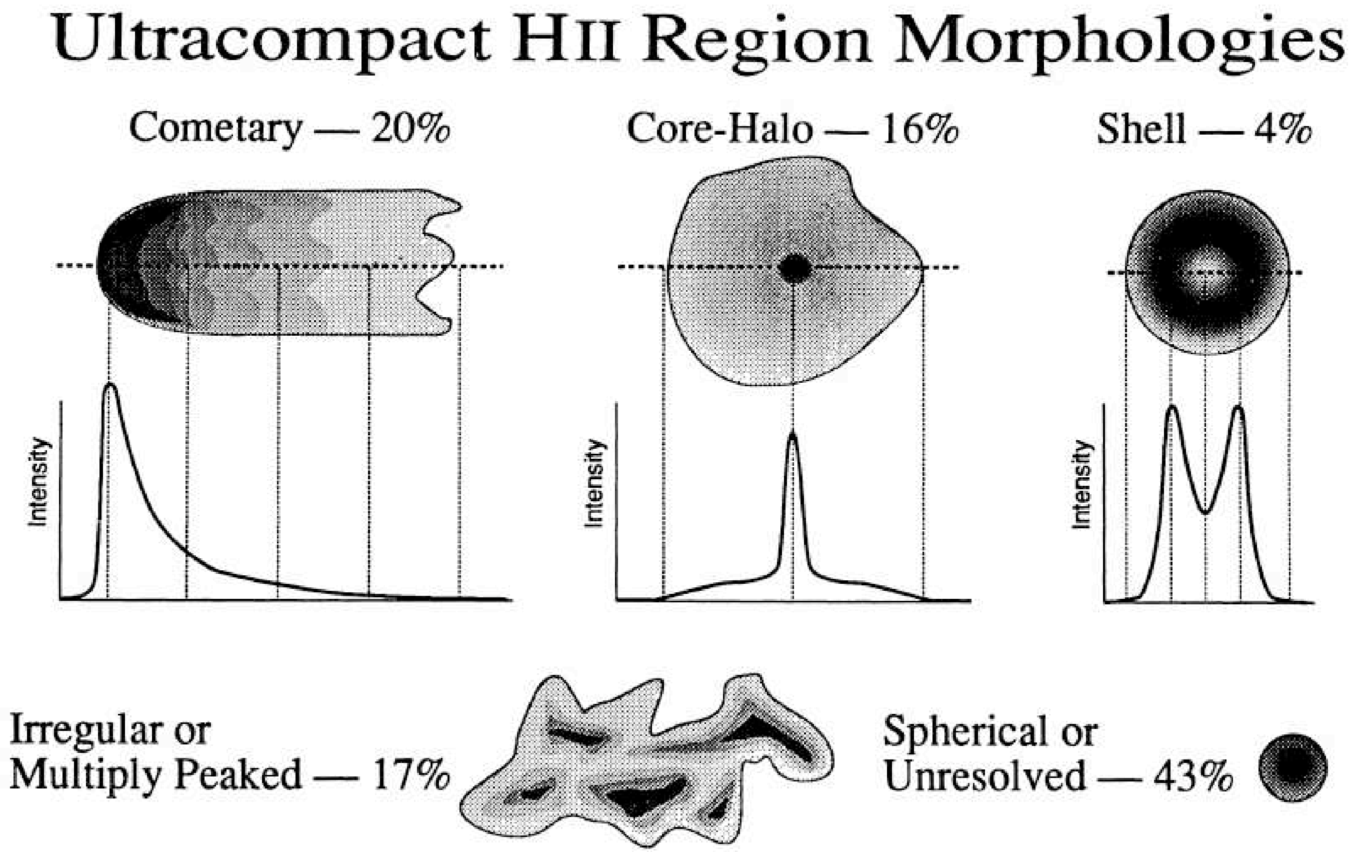

- Wood & Churchwell 1989 classification of UC H II regions
- Question: What is the origin of these morphologies?
- UC H II lifetime problem: Too many UC H II regions observed!

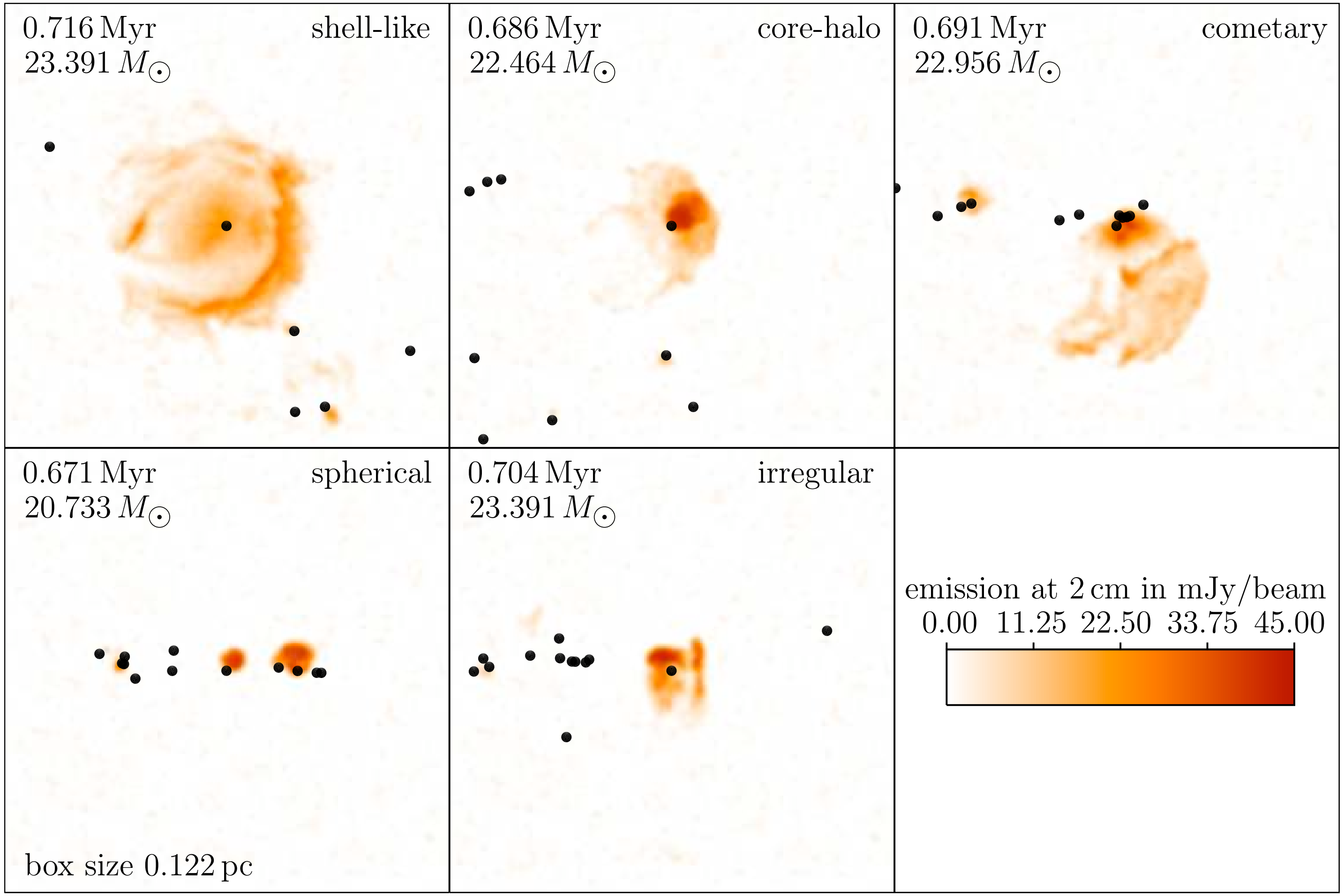

- synthetic VLA observations at $2\,\mathrm{cm}$ of simulation data
- interaction of ionizing radiation with accretion flow creates high variability in time and shape
- flickering resolves the lifetime paradox!

Peters et al. (2010a,b,c)

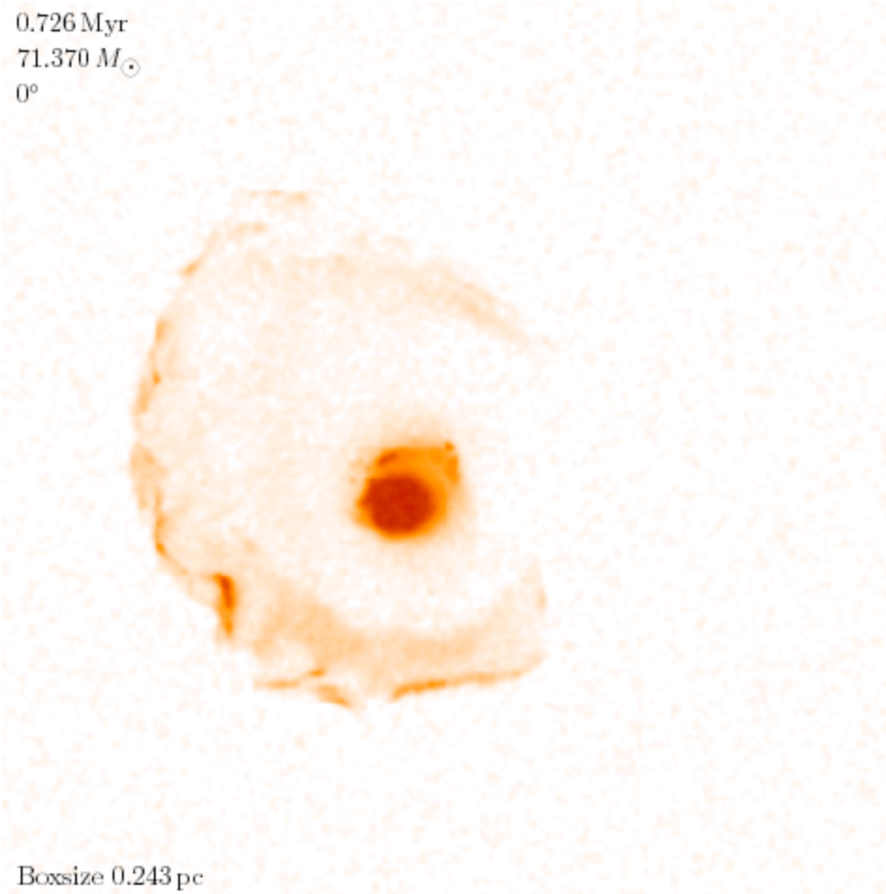

Morphology of HII region depends on viewing angle

Peters et al. (2010a,b,c)

Type	WC89	K94	single	multiple
Spherical/Unresolved	43	55	19	60 ± 5
Cometary	20	16	7	10 ± 5
Core-halo	16	9	15	4 ± 2
Shell-like	4	1	3	5 ± 1
Irregular	17	19	57	21 ± 5

WC89: Wood & Churchwell 1989, K94: Kurtz et al. 1994

- statistics over 25 simulation snapshots and 20 viewing angles
- statistics can be used to distinguish between different models
- single sink simulation does not reproduce lifetime problem

Peters et al. (2010a,b,c)

time variability

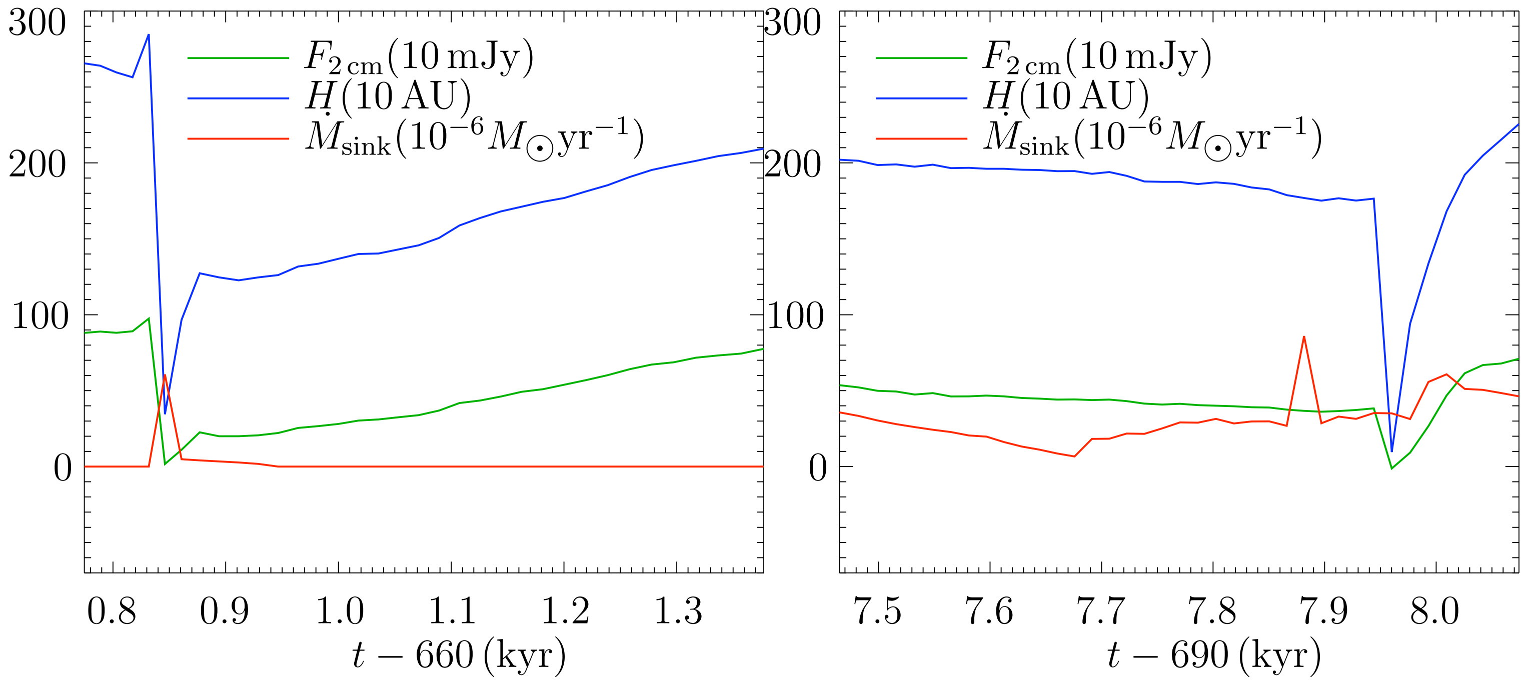

- correlation between accretion events and H II region changes
- time variations in size and flux have been observed
- changes of size and flux of $5\text{–}7\%\mathrm{yr}^{-1}$ match observations

  Franco-Hernández et al. 2004, Rodríguez et al. 2007, Galván-Madrid et al. 2008

(Galvan-Madrid et al. 2011, submitted)

Some results

- Ionization feedback cannot stop accretion
- Ionization drives bipolar outflow
- H II region shows high variability in time and shape
- All classified morphologies can be observed in one run
- Lifetime of H II region determined by accretion time scale
- Rapid accretion through dense, unstable flows
- Fragmentation-induced mass limits of massive stars

Peters et al. (2010a, ApJ, 711, 1017), Peters et al. (2010b, ApJ, 719, 831), Peters et al. (2010c, ApJ, 725, 134), Peters et al. (2011, ApJ, 729, 72

agenda

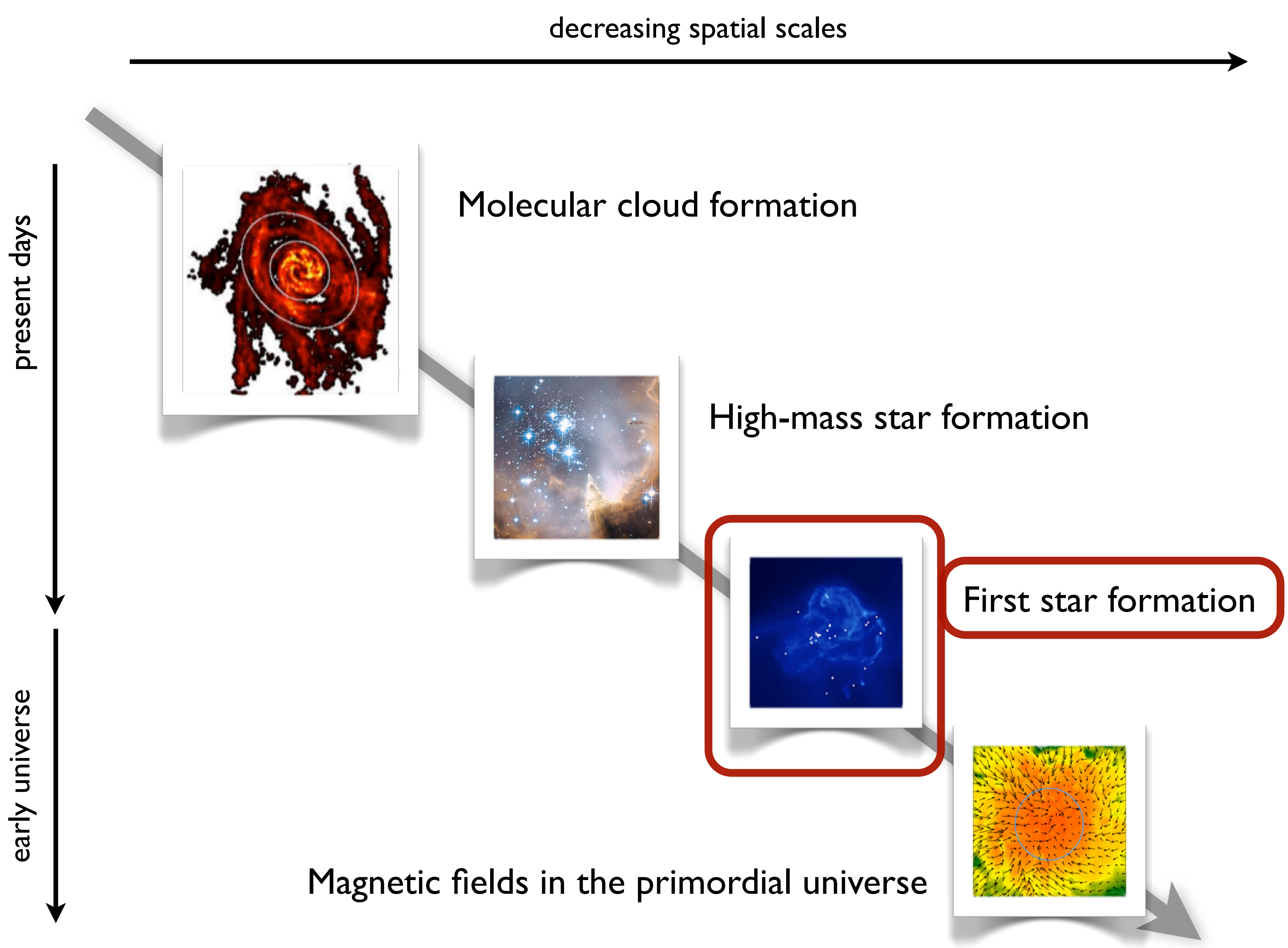
decreasing spatial scales
present days
early universe
Molecular cloud formation
High-mass star formation
First star formation
Magnetic fields in the primordial universe

stellar masses

- distribution of stellar masses depends on
  - turbulent initial conditions
    --> mass spectrum of prestellar cloud cores
  - collapse and interaction of prestellar cores
    --> accretion and *N*-body effects
  - thermodynamic properties of gas
    --> balance between heating and cooling
    --> EOS (determines which cores go into collapse)
  - (proto) stellar feedback terminates star formation
    ionizing radiation, bipolar outflows, winds, SN

(Kroupa 2002)

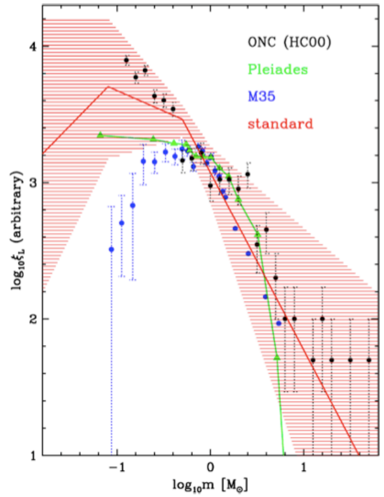

stellar masses

- distribution of stellar masses depends on
  - turbulent initial conditions
    --> mass spectrum of prestellar cloud cores
  - collapse and interaction of prestellar cores
    --> accretion and *N*-body effects
  - thermodynamic properties of gas
    --> balance between heating and cooling
    --> EOS (determines which cores go into collapse)
  - (proto) stellar feedback terminates star formation
    ionizing radiation, bipolar outflows, winds, SN

(Kroupa 2002)

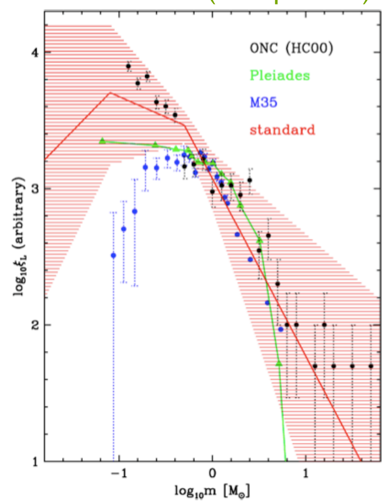

example: model of Orion cloud

„model“ of Orion cloud:
15.000.000 SPH particles,
10^4 M_{sun} in 10 pc, mass resolution 0,02 M_{sun}, forms ~2.500 „stars“ (sink particles)

isothermal EOS, top bound, bottom unbound

has clustered as well as distributed „star“ formation

efficiency varies from 1% to 20%

develops full IMF
(distribution of sink particle masses)

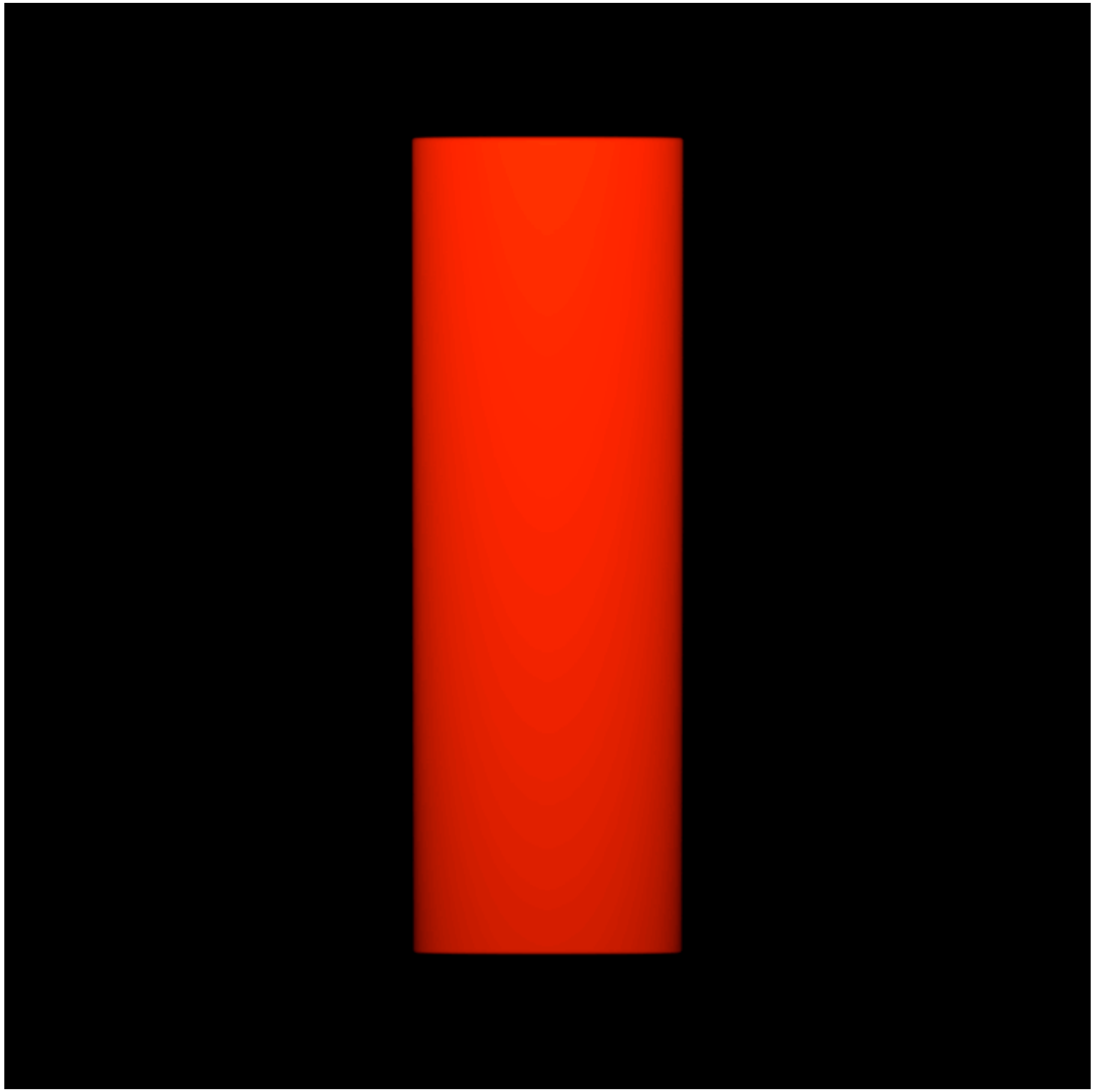

(Bonnell & Clark 2008)

example: model of Orion cloud

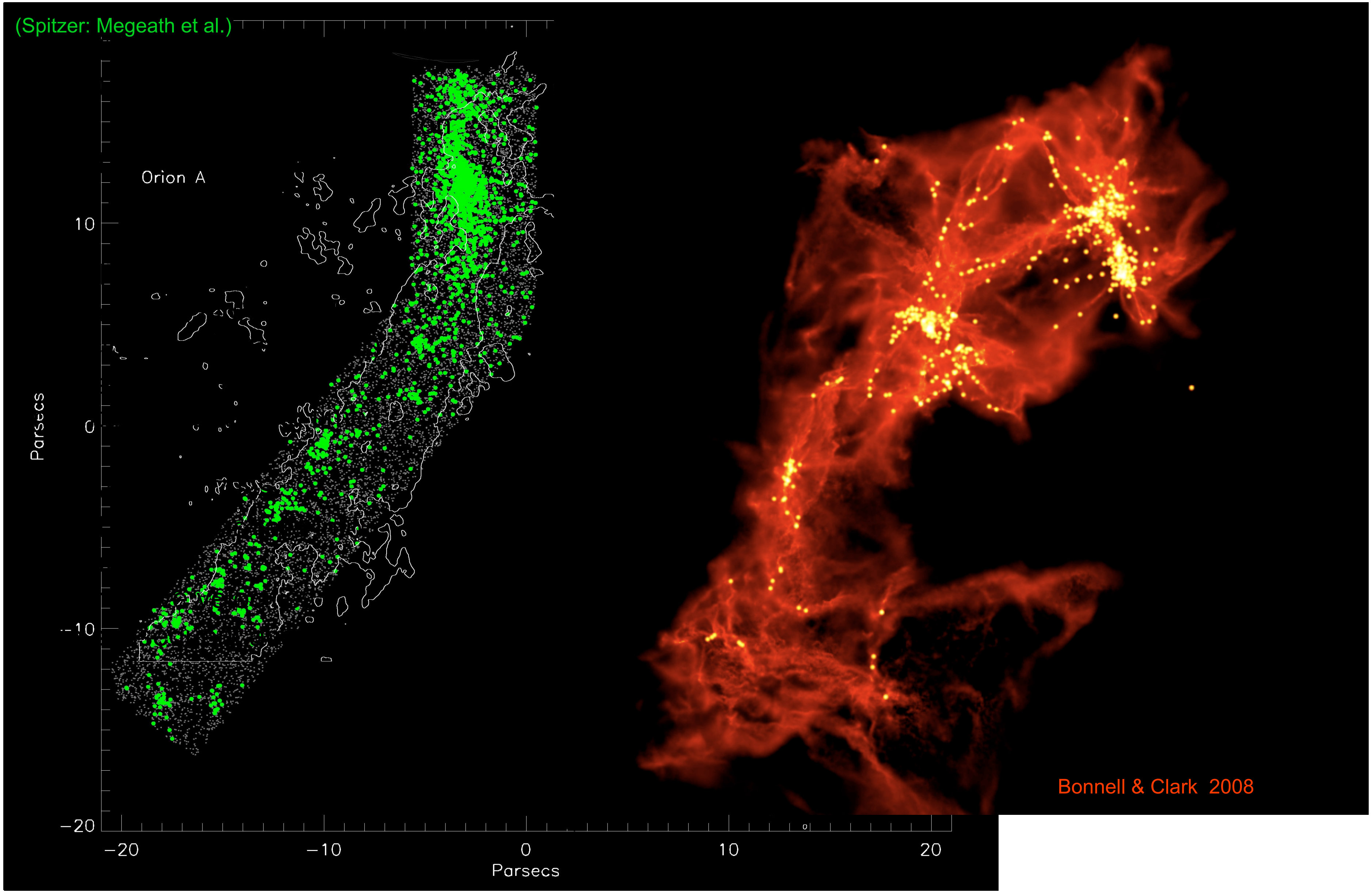

dynamics of nascent star cluster

in dense clusters protostellar interaction may be come important!

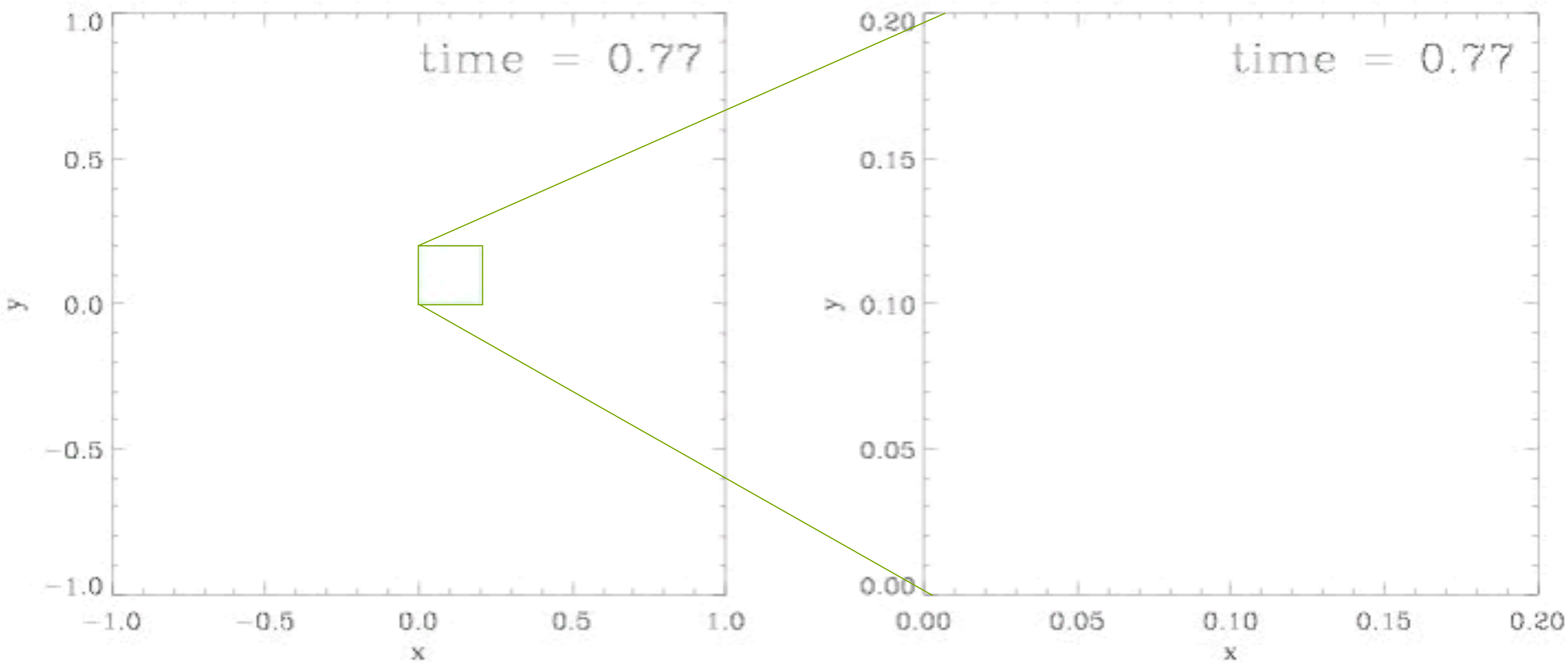

Trajectories of protostars in a nascent dense cluster created by gravoturbulent fragmentation
(from Klessen & Burkert 2000, ApJS, 128, 287)

Dynamics of nascent star cluster

in dense clusters protostellar interaction may be come important!

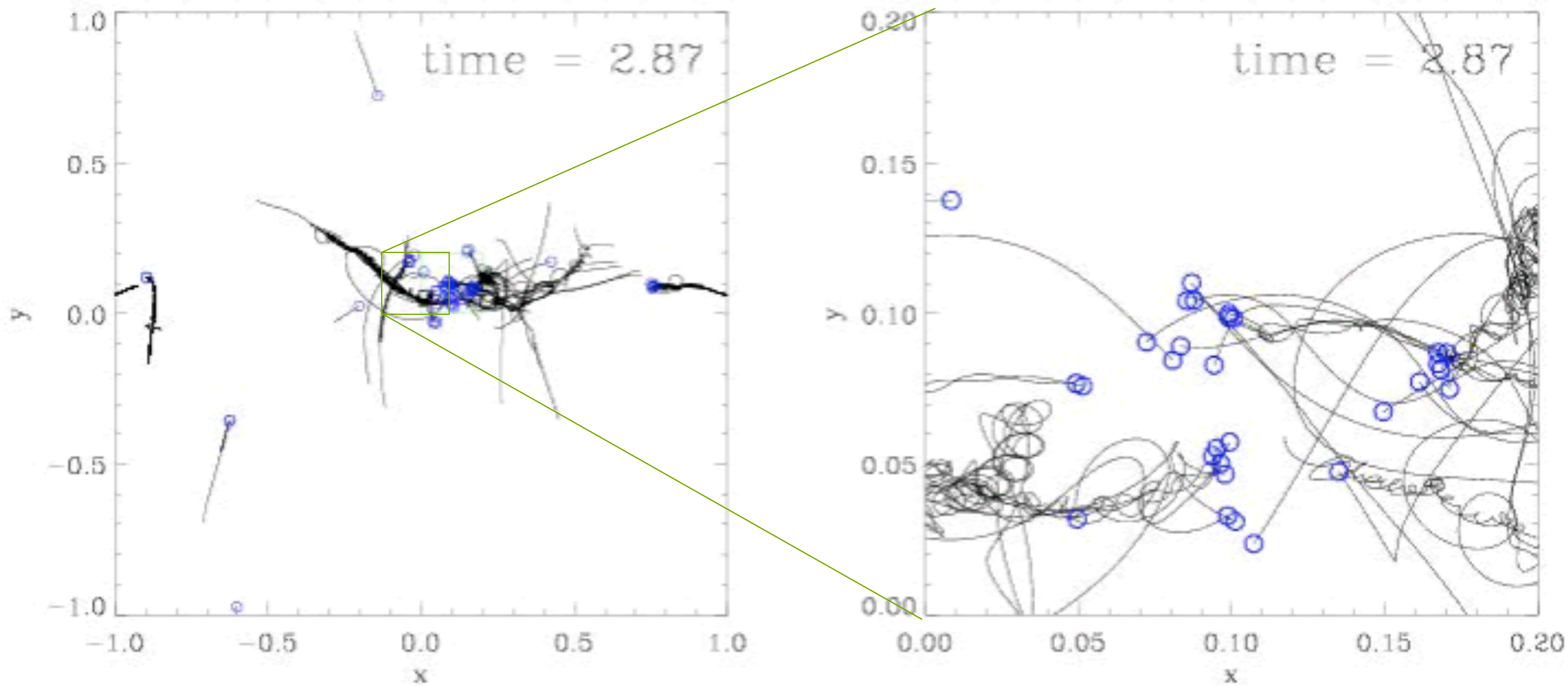

Trajectories of protostars in a nascent dense cluster created by gravoturbulent fragmentation
(from Klessen & Burkert 2000, ApJS, 128, 287)

accretion rates in clust

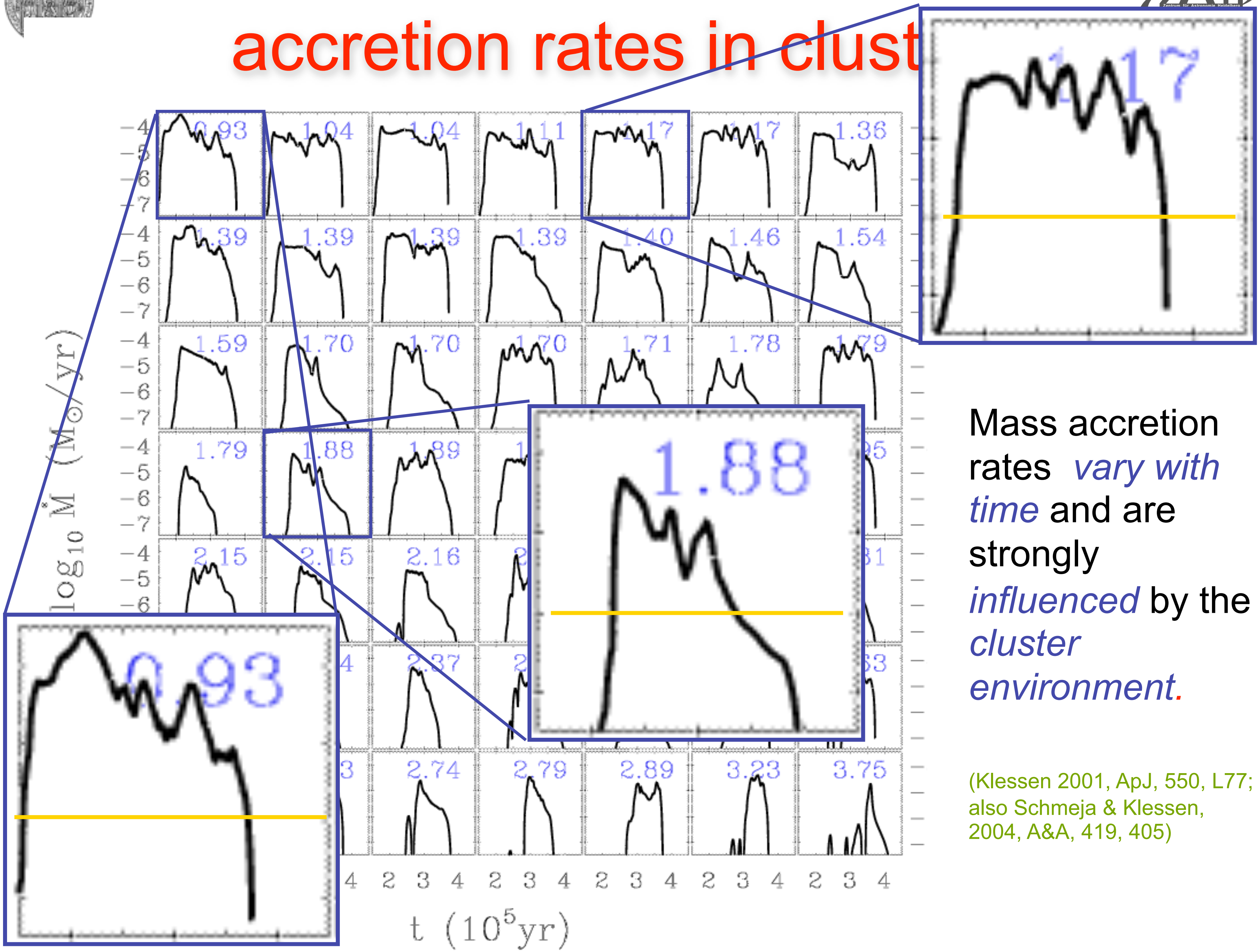

Mass accretion rates *vary with time* and are strongly *influenced* by the *cluster environment*.

(Klessen 2001, ApJ, 550, L77; also Schmeja & Klessen, 2004, A&A, 419, 405)

stellar masses

- distribution of stellar masses depends on
  - turbulent initial conditions
    --> mass spectrum of prestellar cloud cores
  - collapse and interaction of prestellar cores
    --> accretion and *N*-body effects
  - thermodynamic properties of gas
    --> balance between heating and cooling
    --> EOS (determines which cores go into collapse)
  - (proto) stellar feedback terminates star formation
    ionizing radiation, bipolar outflows, winds, SN

(Kroupa 2002)

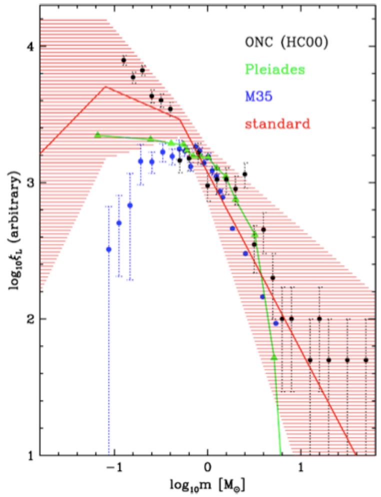

stellar masses

- distribution of stellar masses depends on
  - turbulent initial conditions
    --> mass spectrum of prestellar cloud cores
  - collapse and interaction of prestellar cores
    --> accretion and *N*-body effects
  - thermodynamic properties of gas
    --> balance between heating and cooling
    --> EOS (determines which cores go into collapse)
  - (proto) stellar feedback terminates star formation
    ionizing radiation, bipolar outflows, winds, SN

(Kroupa 2002)

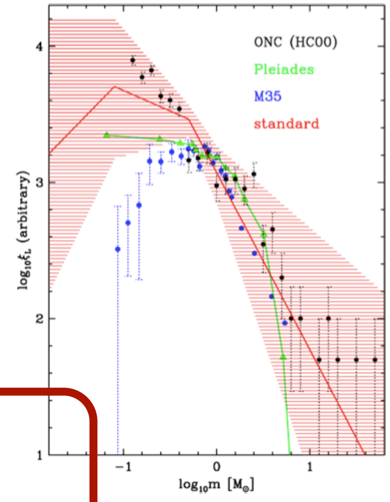

application to first star formation

EOS as function of metallicity

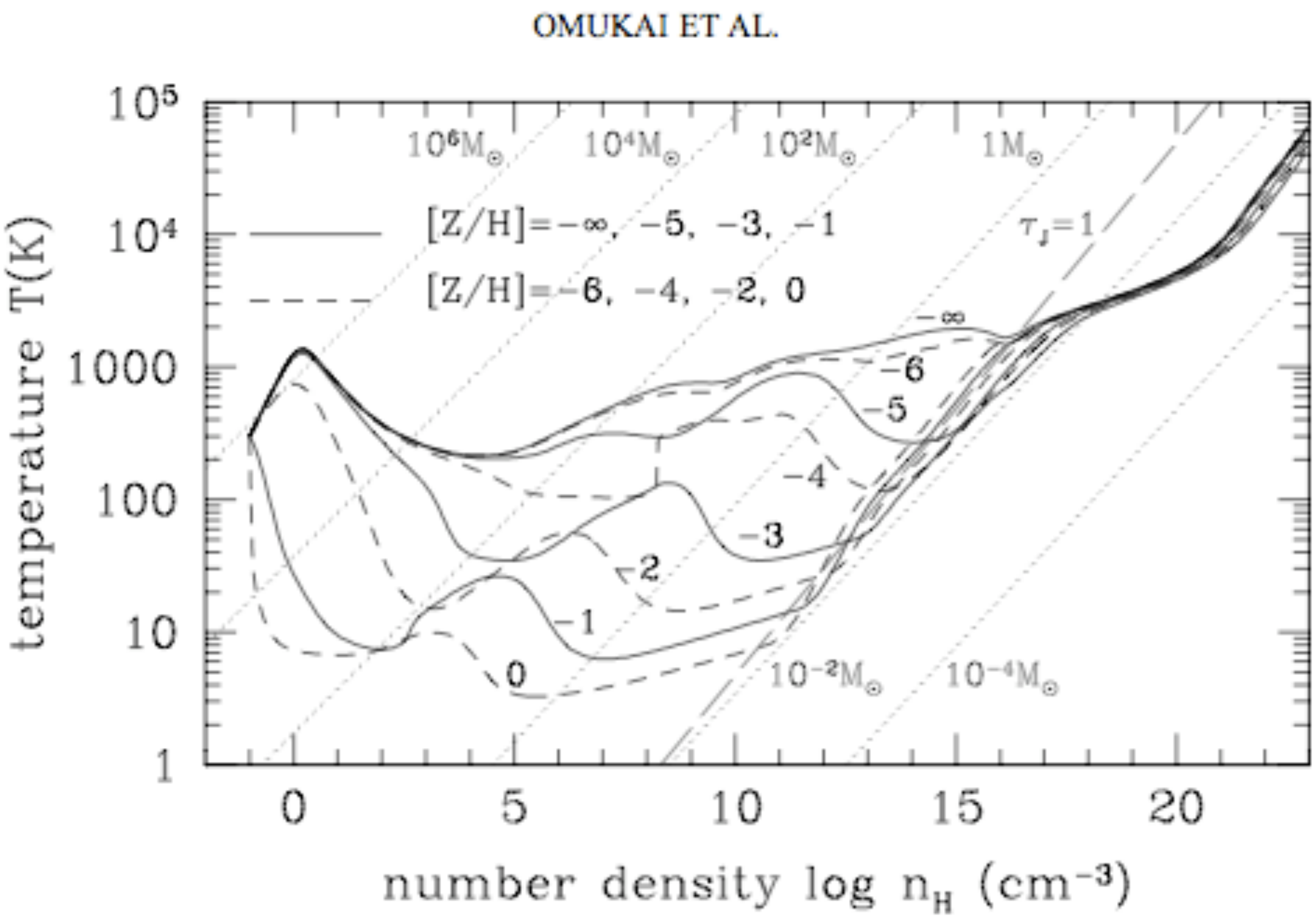

(Omukai et al. 2005)

EOS as function of metallicity

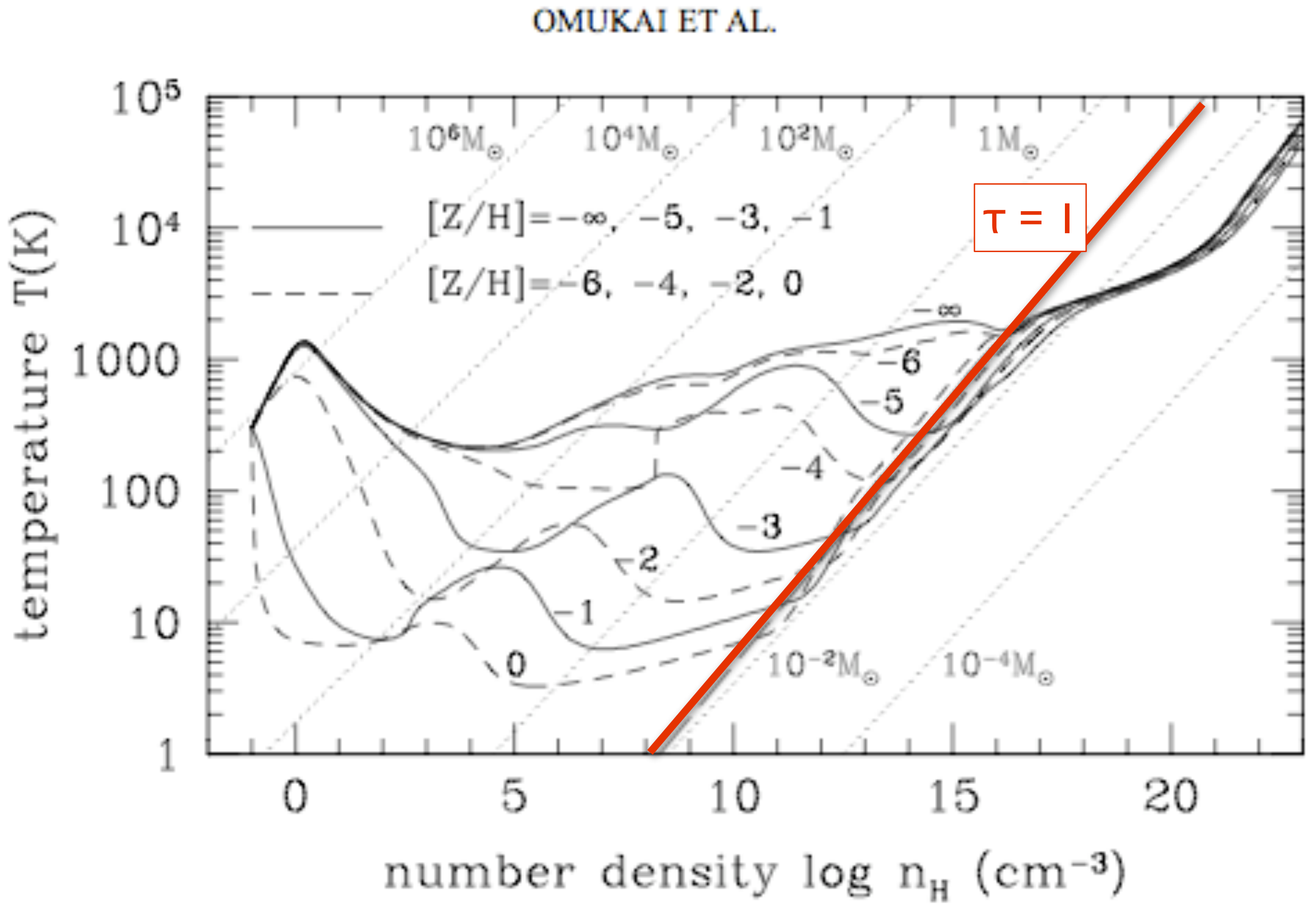

(Omukai et al. 2005)

EOS as function of metallicity

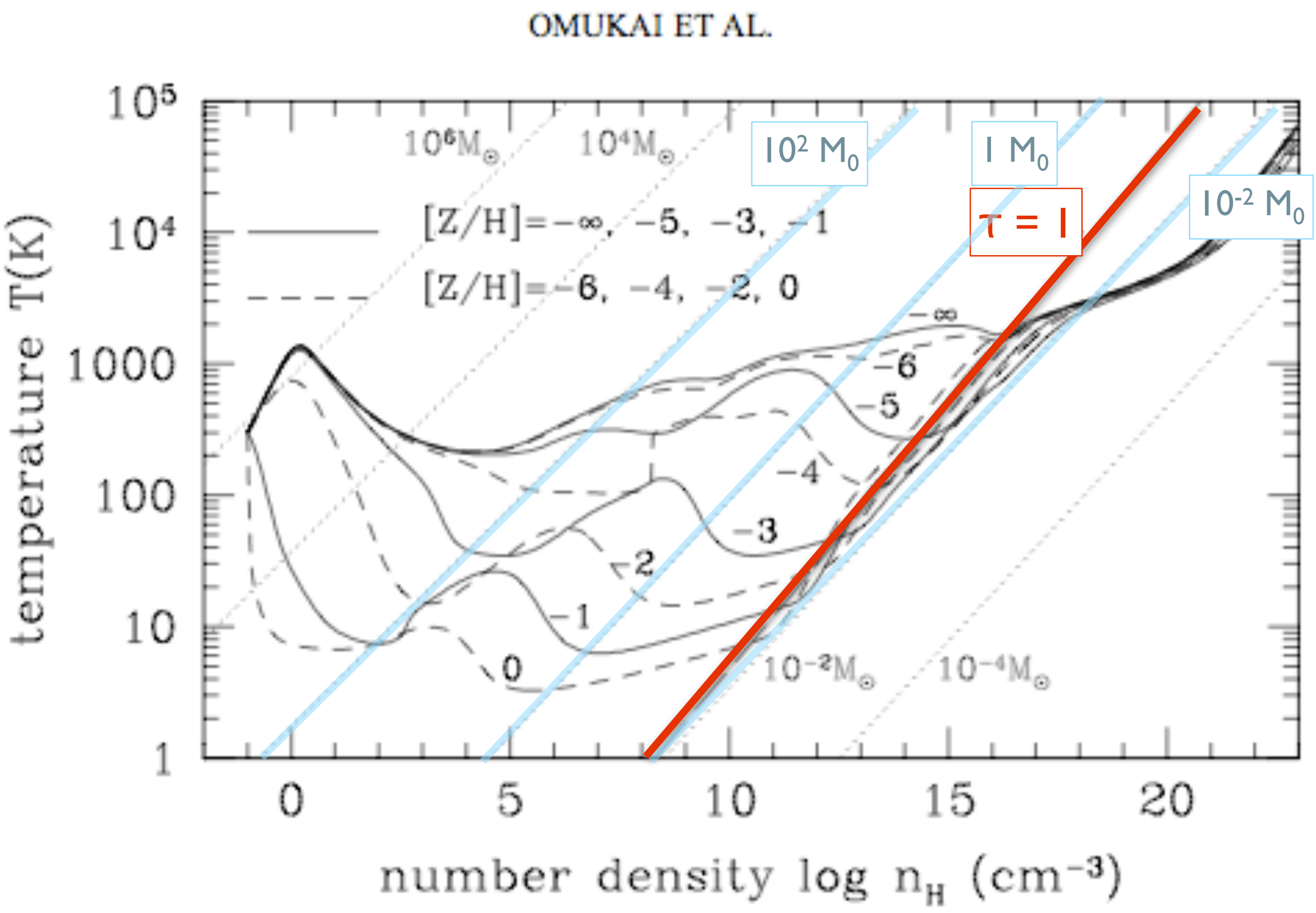

(Omukai et al. 2005)

present-day star formation

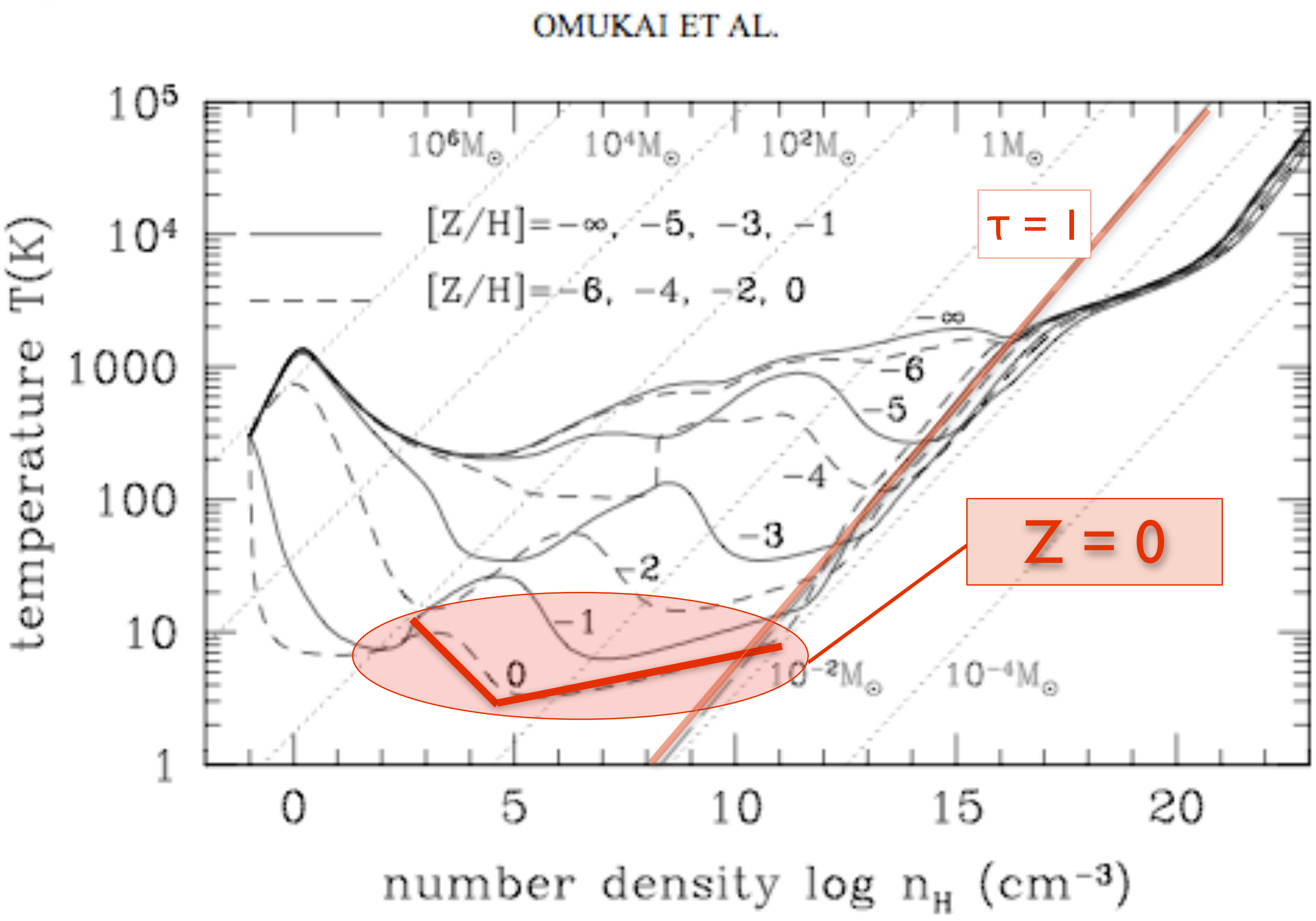

(Omukai et al. 2005, Jappsen et al. 2005, Larson 2005)

present-day star formation

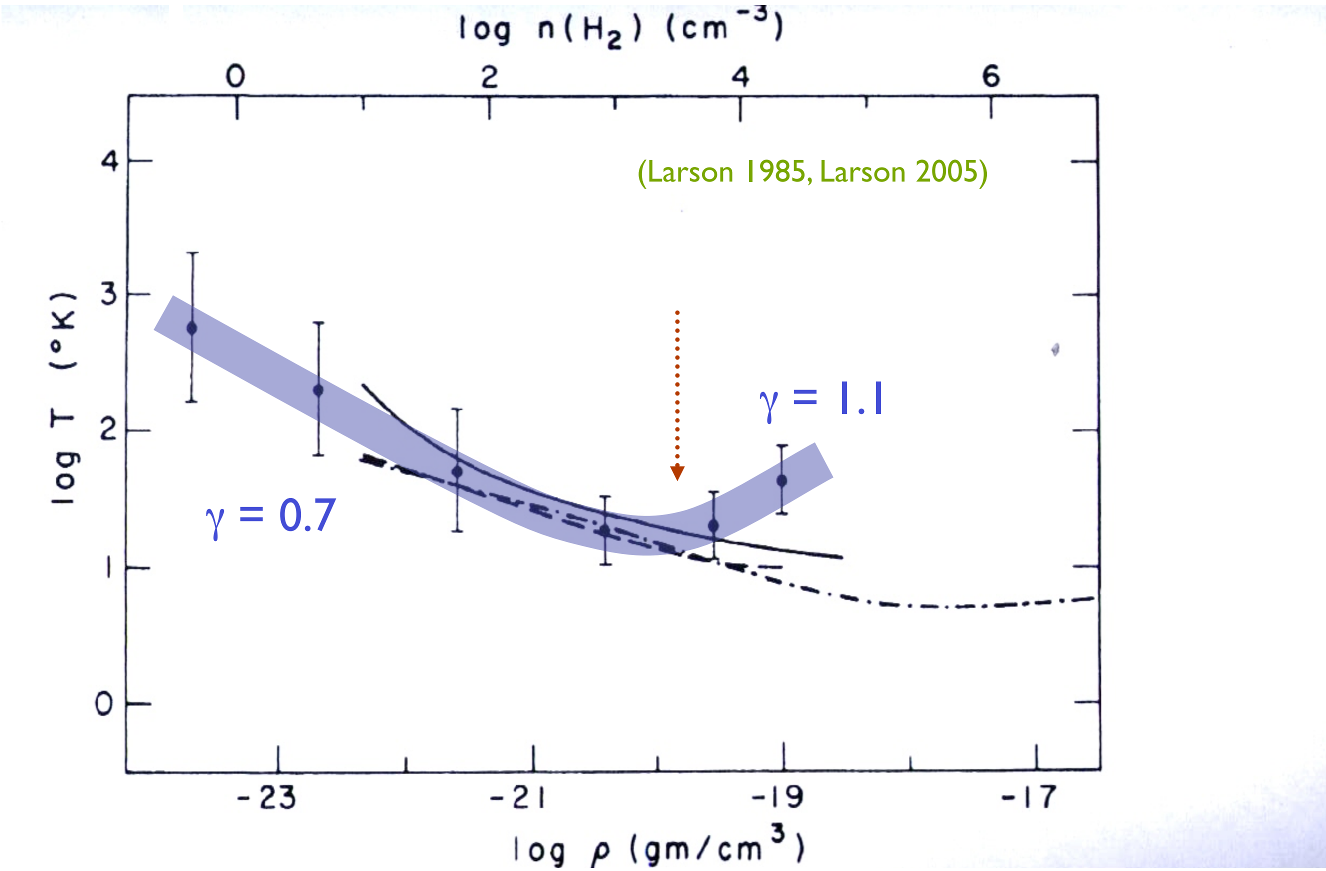

present-day star formation

This kink in EOS is very insensitive to environmental conditions such as ambient radiation field
--> reason for universal for of the IMF? (Elmegreen et al. 2008)

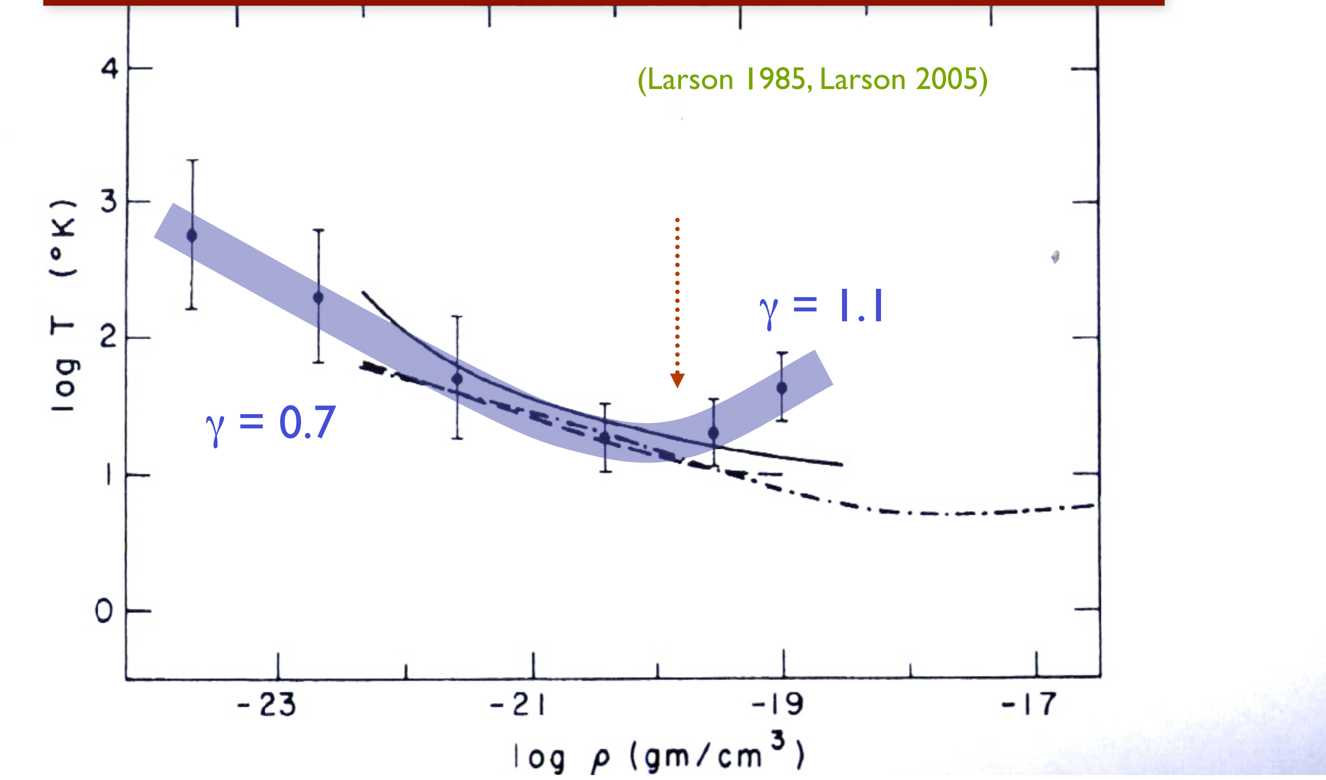

IMF in nearby molecular clouds

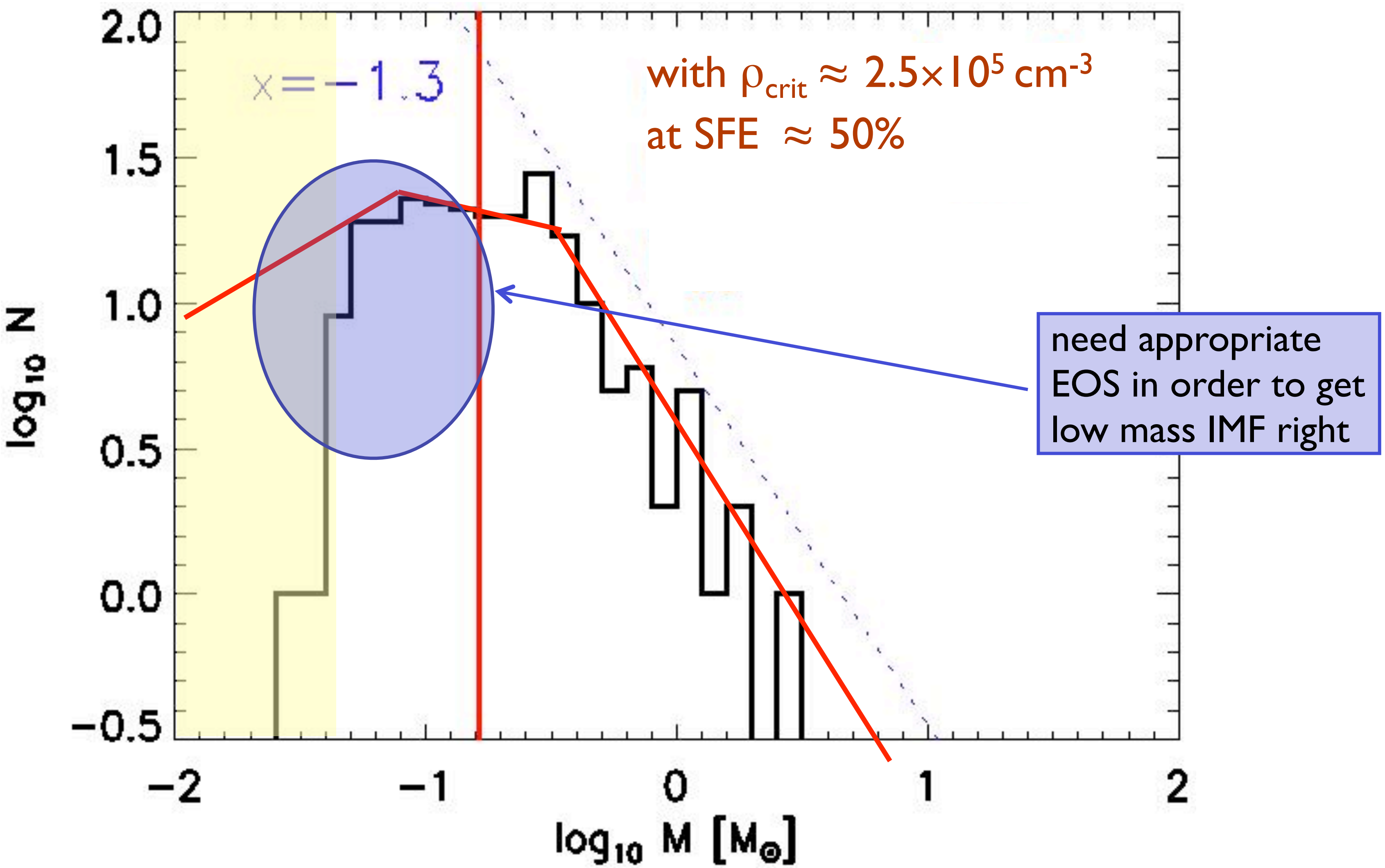

(Jappsen et al. 2005, A&A, 435, 611)

transition: Pop III to Pop II.5

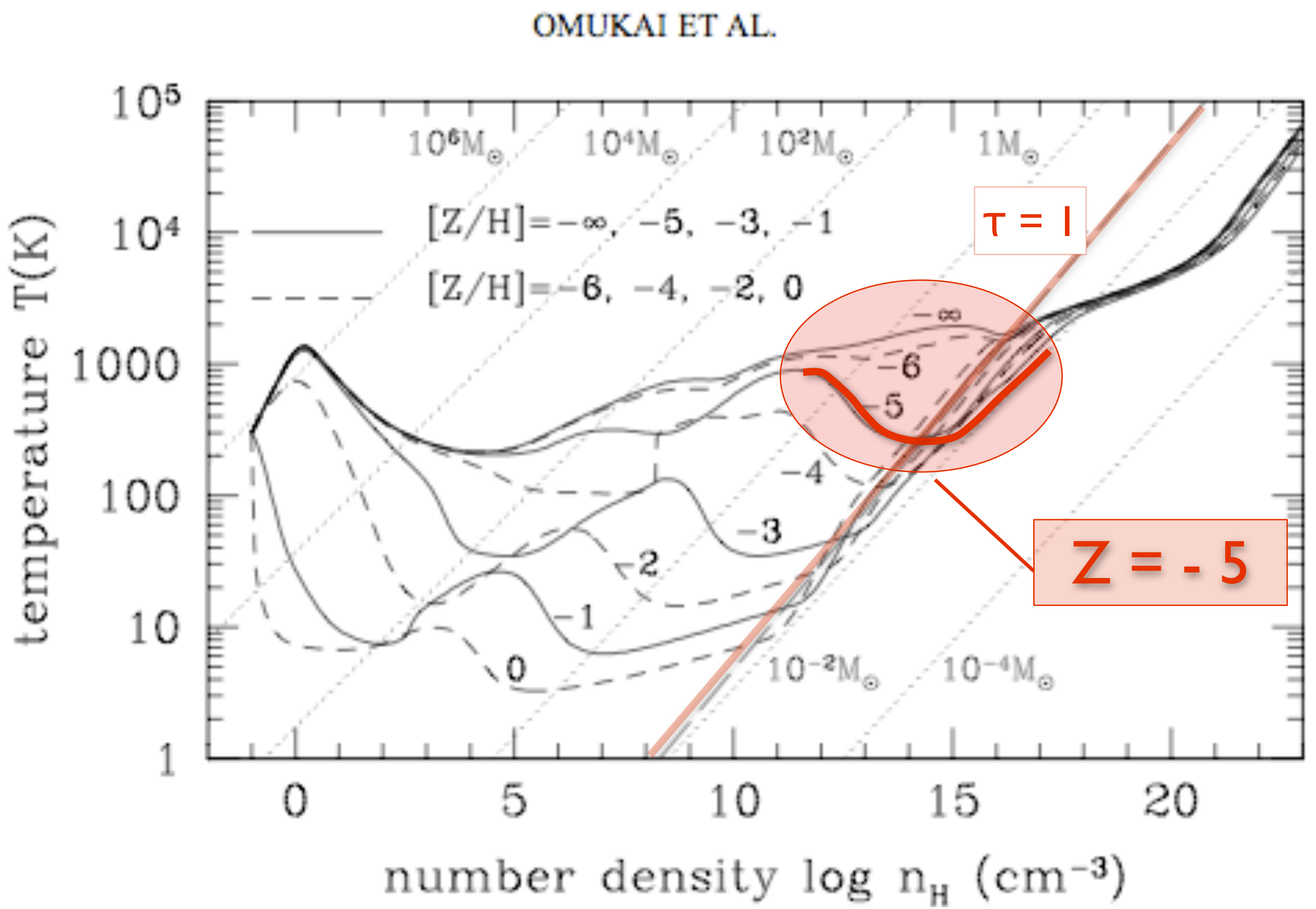

(Omukai et al. 2005)

transition: Pop III to Pop II.5

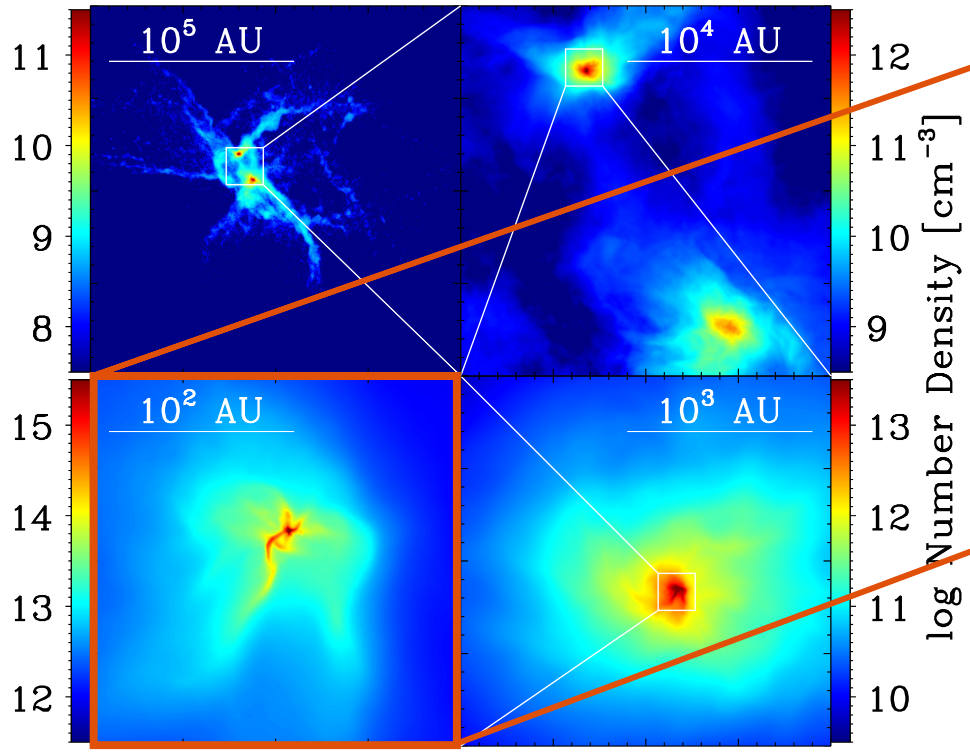

FIG. 2.— Number density maps for a slice through the high density region. The image shows a sequence of zooms in the density structure in the gas immediately before the formation of the first protostar.

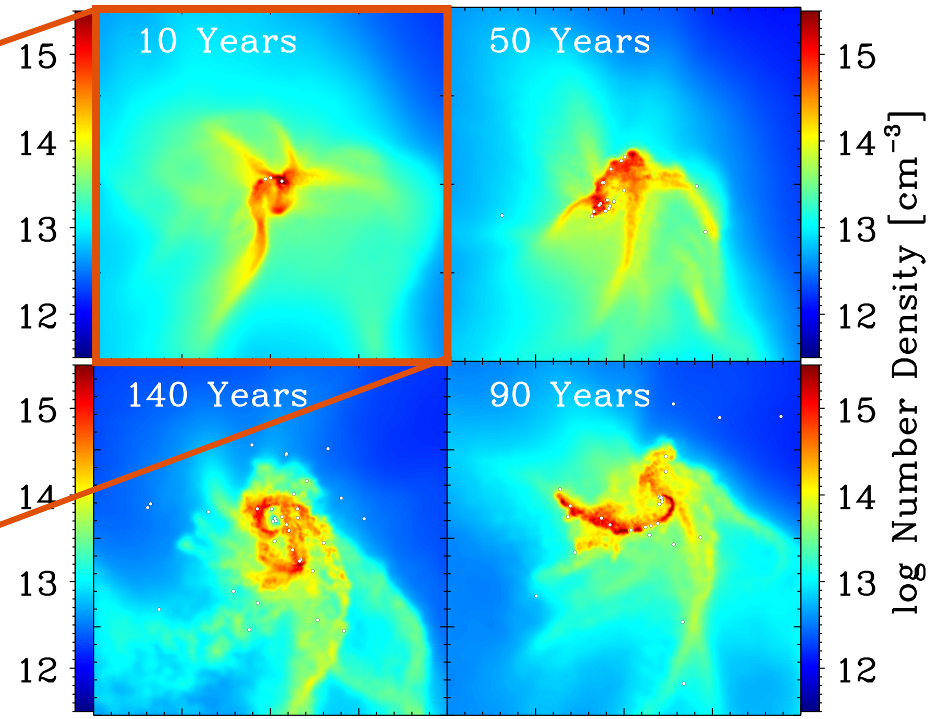

FIG. 3.— Number density map showing a slice in the densest clump, and the sink formation time evolution, for the 40 million particles simulation, and Z = $10^{-4} Z_{\odot}$. The box is 100AU x 100AU and the time is measured from the formation of the first sink particle.

Dopcke et al. (2011, ApJ 729, L3)

transition: Pop III to Pop II.5

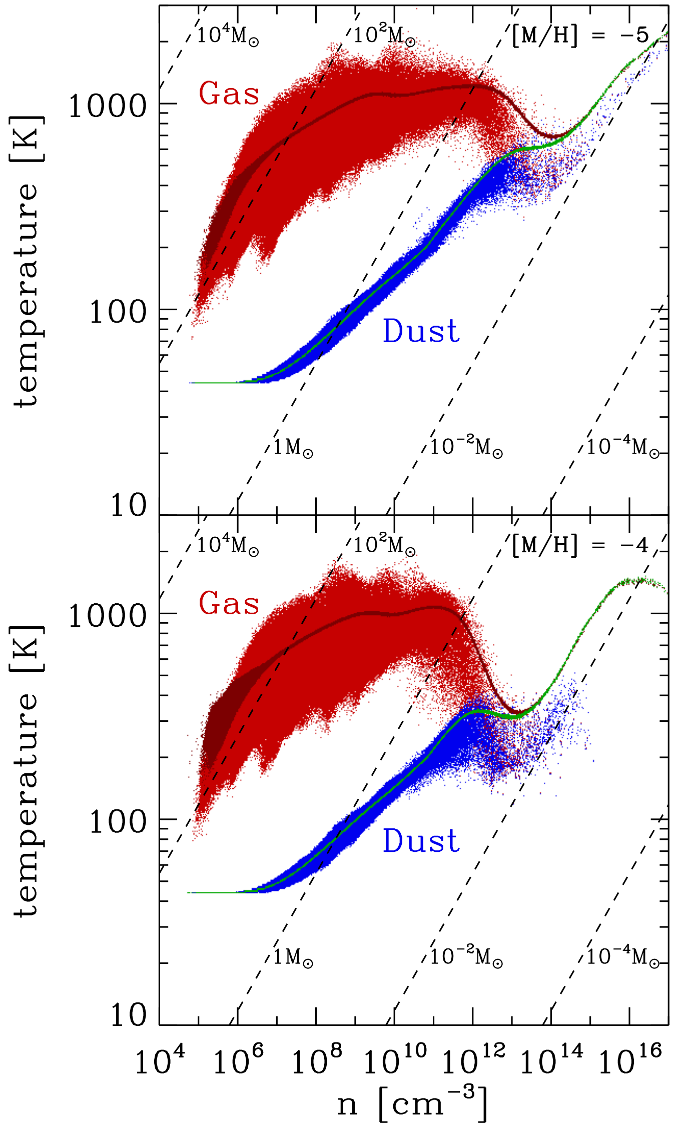

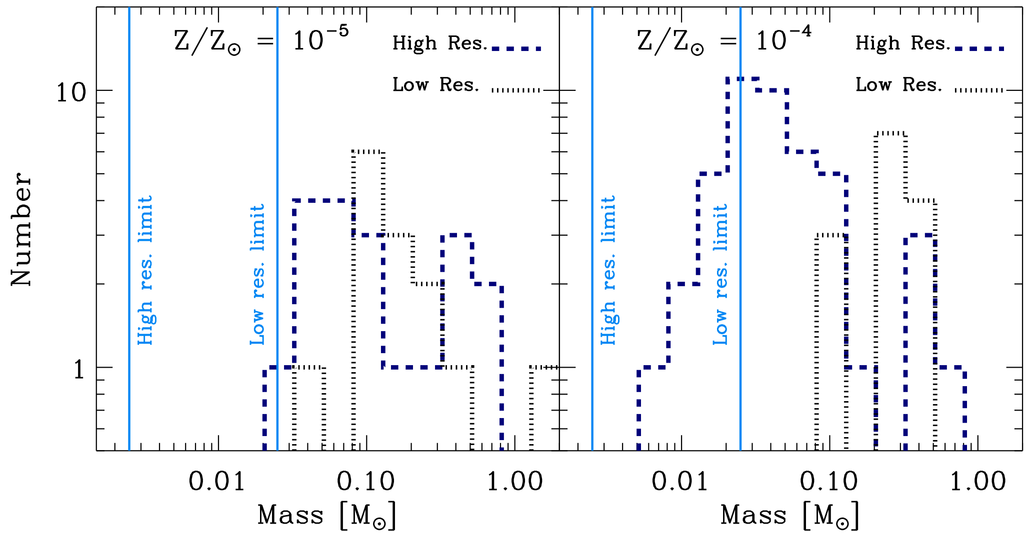

FIG. 4.— Sink particle mass function at the end of the simulations. High and low resolution results and corresponding resolution limits are shown. To resolve the fragmentation, the mass resolution should be smaller than the Jeans mass at the point in the temperature-density diagram where dust and gas couple and the compressional heating starts to dominate over the dust cooling. At the time shown, around 5 $M_\odot$ of gas had been accreted by the sink particles in each simulation.

red / blue: turbulence and rotation
dark red / green: simple collapse

Dopcke et al. (2011, ApJ 729, L3)

dust induced fragmentation at $Z=10^{-5}$

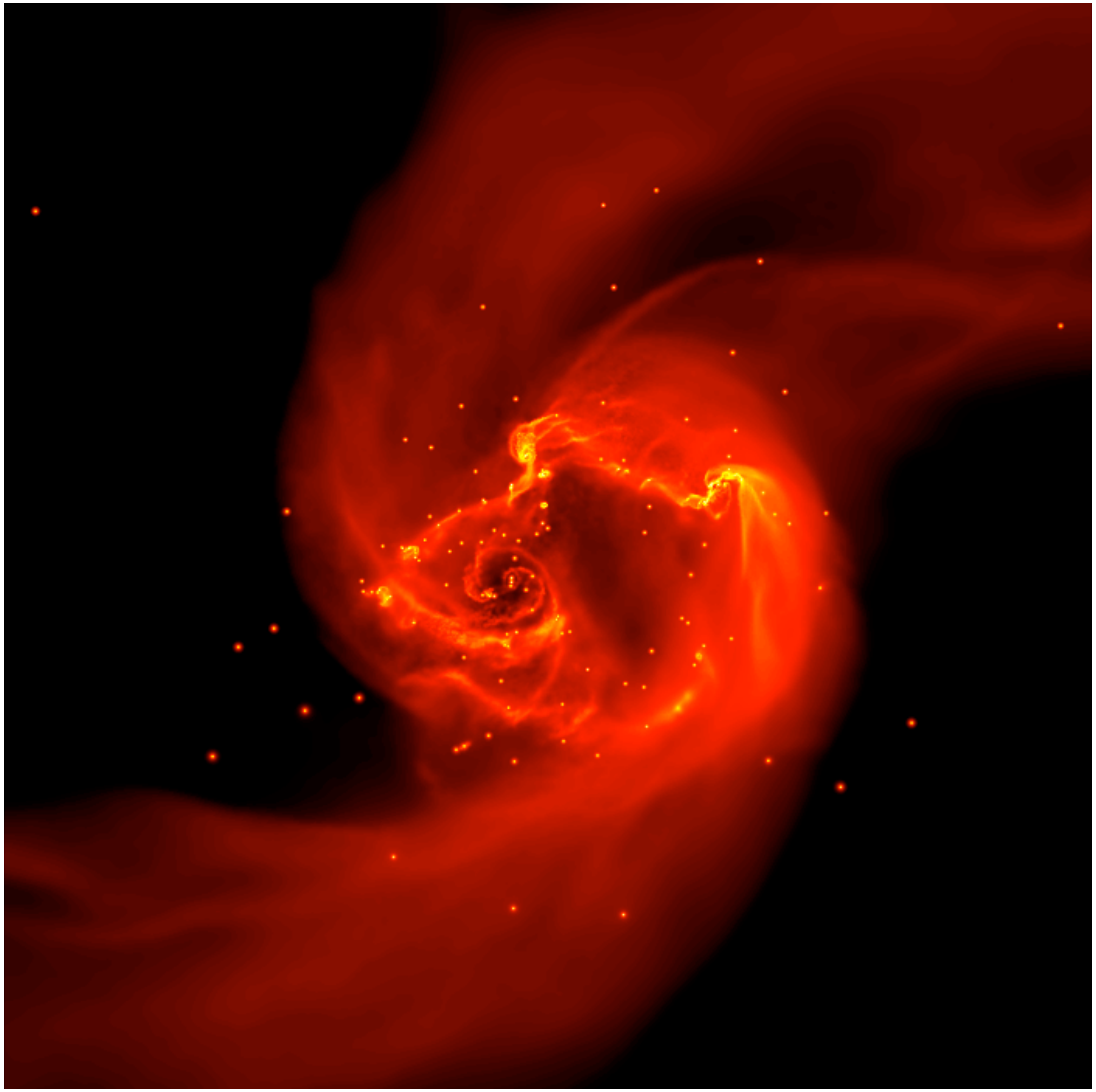

dense cluster of low-mass protostars builds up:

- mass spectrum peaks *below* $1\ M_{sun}$
- cluster VERY dense $n_{stars} = 2.5 \times 10^9\ pc^{-3}$
- fragmentation at density $n_{gas} = 10^{12} - 10^{13}\ cm^{-3}$

(Clark et al. 2008, ApJ 672, 757)

dust induced fragmentation at $Z=10^{-5}$

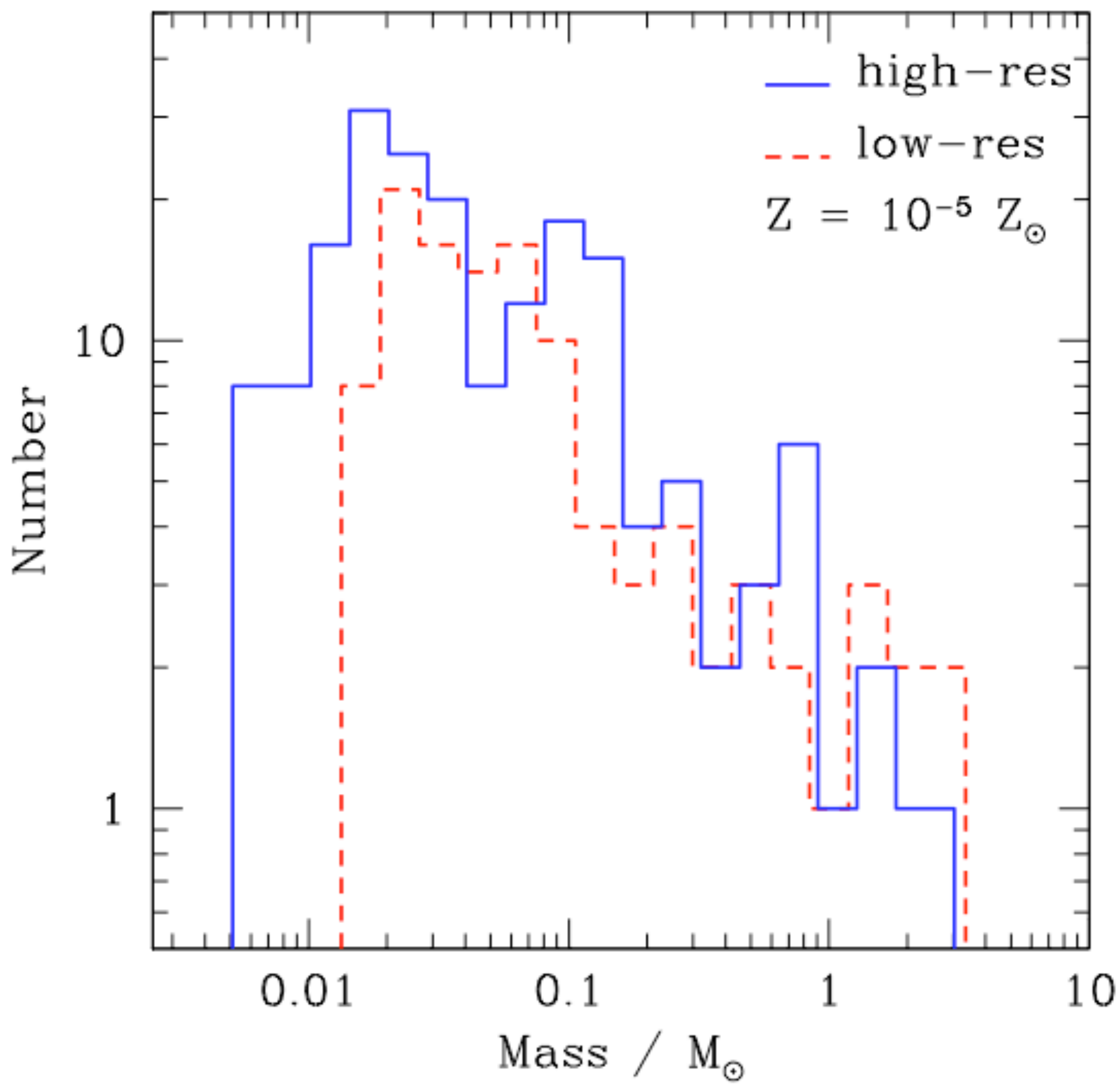

dense cluster of low-mass protostars builds up:

- mass spectrum peaks below 1 M_{sun}
- cluster VERY dense $n_{stars} = 2.5 \times 10^9 \ pc^{-3}$

- *predictions:*
  * low-mass stars with [Fe/H] ~ 10^{-5}
  * high binary fraction

(Clark et al. 2008)

dust induced fragmentation at $Z=10^{-5}$

2 extremely metal deficient stars with masses below 1 Msun.

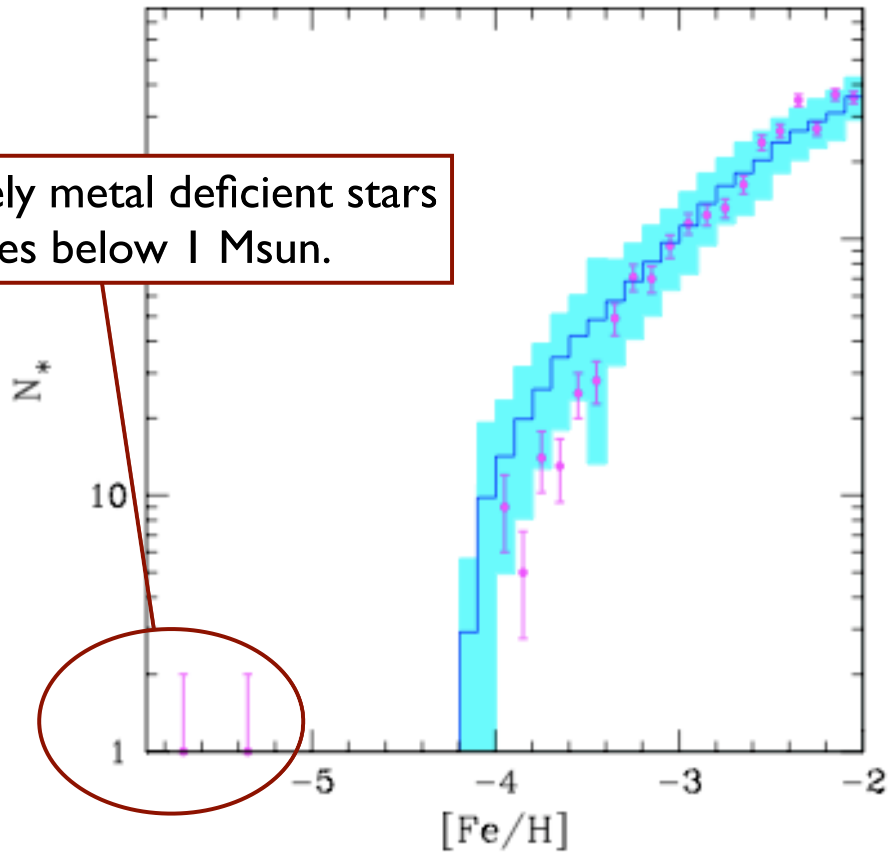

(plot from Salvadori et al. 2006, data from Frebel et al. 2005)

dense cluster of low-mass protostars builds up:

- mass spectrum peaks below 1 M_{sun}
- cluster VERY dense $n_{stars} = 2.5 \times 10^9 \, pc^{-3}$

- *predictions:*
  * low-mass stars with [Fe/H] ~ 10^{-5}
  * high binary fraction

(Clark et al. 2008)

metal-free star formation

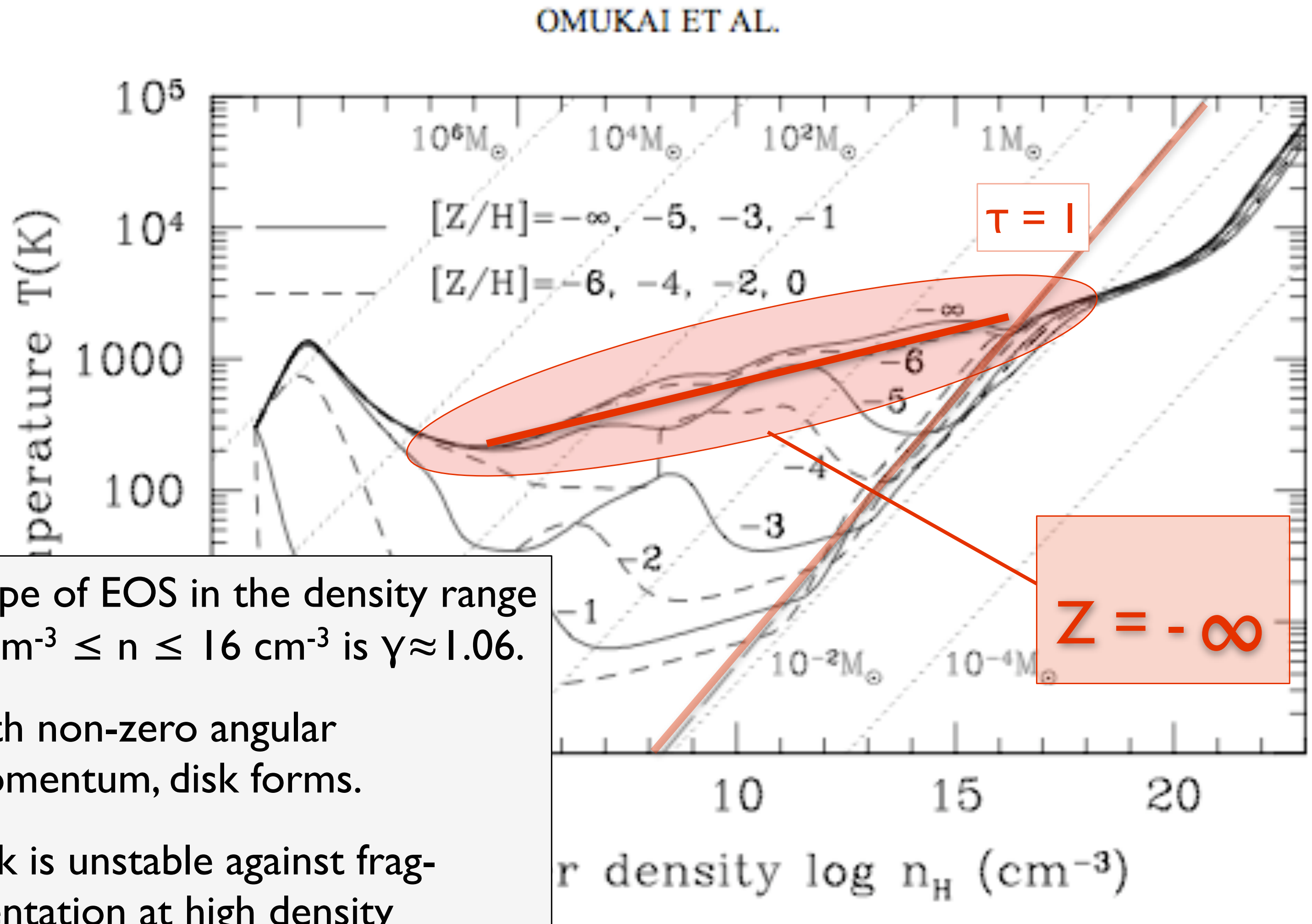

- slope of EOS in the density range 5 cm^{-3} ≤ n ≤ 16 cm^{-3} is $\gamma \approx 1.06$.
- with non-zero angular momentum, disk forms.
- disk is unstable against frag-mentation at high density

(Omukai et al. 2005)

turbulence in Pop III halos

- star formation will depend on *degree of turbulence* in protogalactic halo
- speculation: *differences in stellar mass function*, just like in present-day star formation

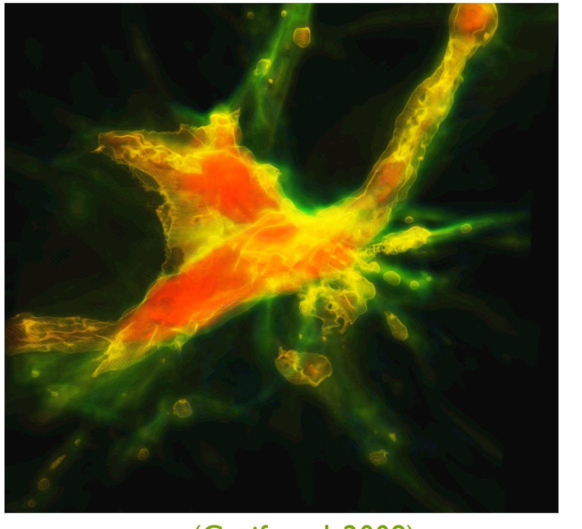

(Greif et al. 2008)

turbulence in Pop III halos

- star formation will depend on *degree of turbulence* in protogalactic halo
- speculation: *differences in stellar mass function*, just like in present-day star formation

turbulence developing in an atomic cooling halo

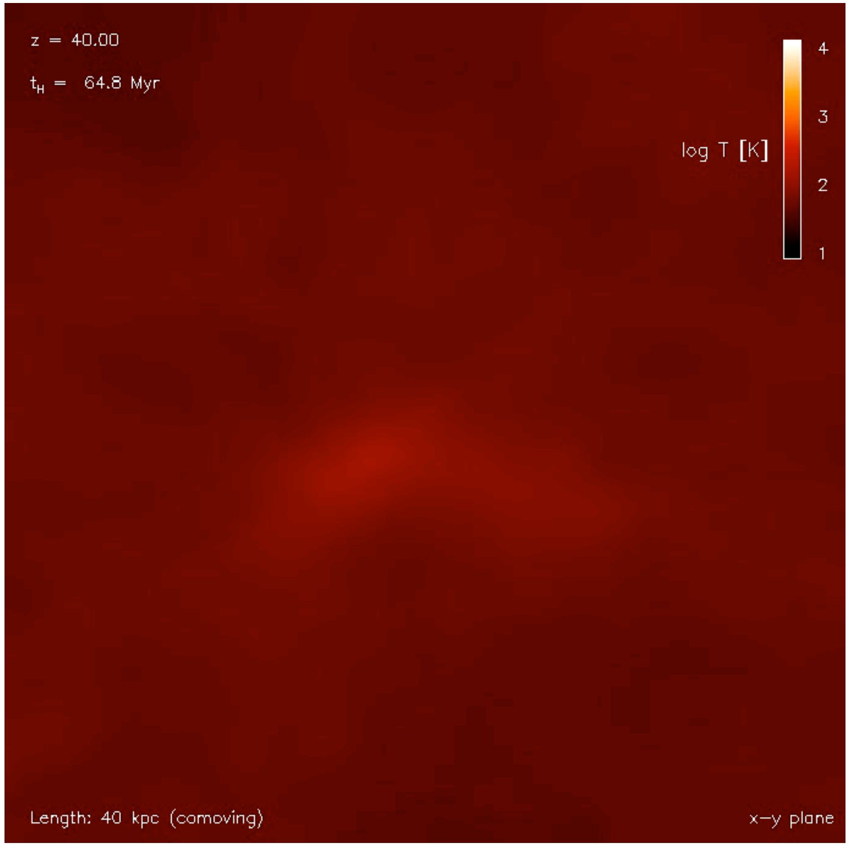

(Greif et al. 2008)

multiple Pop III stars in halo

- parameter study with different strength of turbulence using SPH: study Pop III.1 and Pop III.2 case (Clark et al., 2011a, ApJ, 727, 110)
- 2 very high resolution studies of Pop III star formation in cosmological context
  - SPH: Clark et al. 2011b, Science, 311, 1040
  - Arepo: Greif et al. 2011a, ApJ, submitted (arXiv:1101.5491)
  - complementary approaches with interesting similarities and differences....

SPH study: face on look at accretion disk

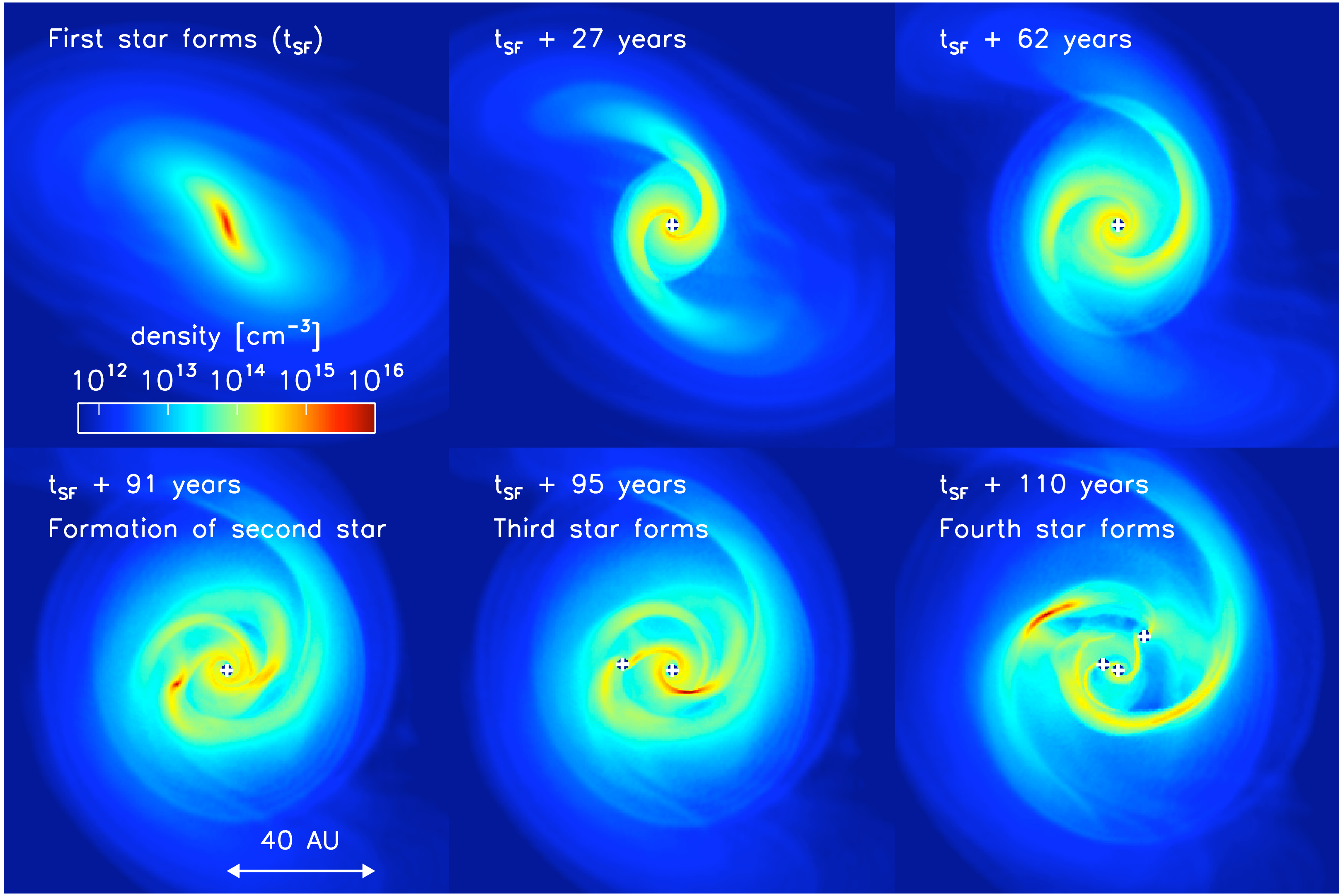

Figure 1: Density evolution in a 120 AU region around the first protostar, showing the build-up of the protostellar disk and its eventual fragmentation. We also see ‘wakes’ in the low-density regions, produced by the previous passage of the spiral arms.

(Clark et al. 2011b, Science, 331, 1040)

SPH study: some disk parameters

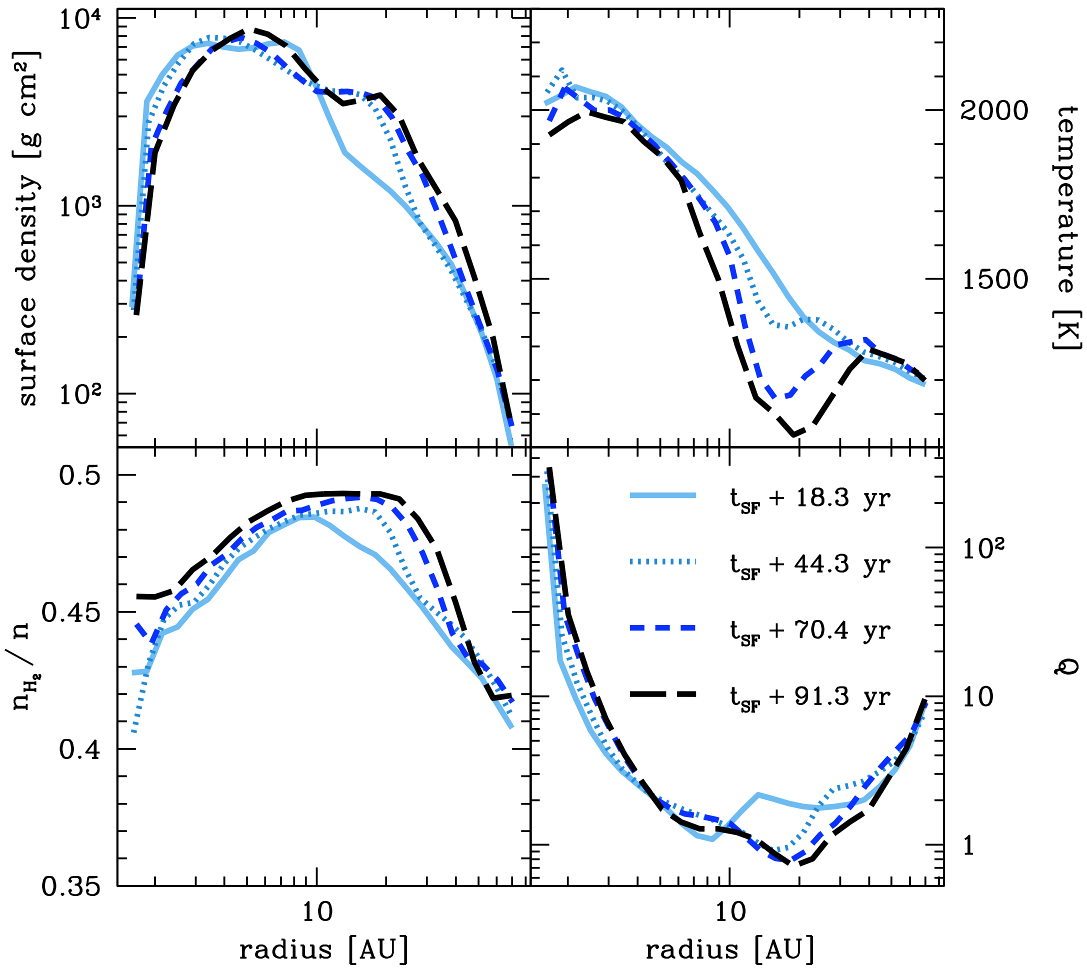

Figure 2: Radial profiles of the disk's physical properties, centered on the first protostellar core to form. The quantities are mass-weighted and taken from a slice through the midplane of the disk. In the lower right-hand plot we show the radial distribution of the disk's Toomre parameter, $Q = c_s\kappa/\pi G\Sigma$, where c_s is the sound speed and κ is the epicyclic frequency. Beause our disk is Keplerian, we adopted the standard simplification, and replaced κ with the orbital frequency. The molecular fraction is defined as the number density of hydrogen molecules (n_{H_2}), divided by the number density of hydrogen nuclei (n), such that fully molecular gas has a value of 0.5

(Clark et al. 2011b, Science, 331, 1040)

SPH study: mass accretion onto disk and onto protostars

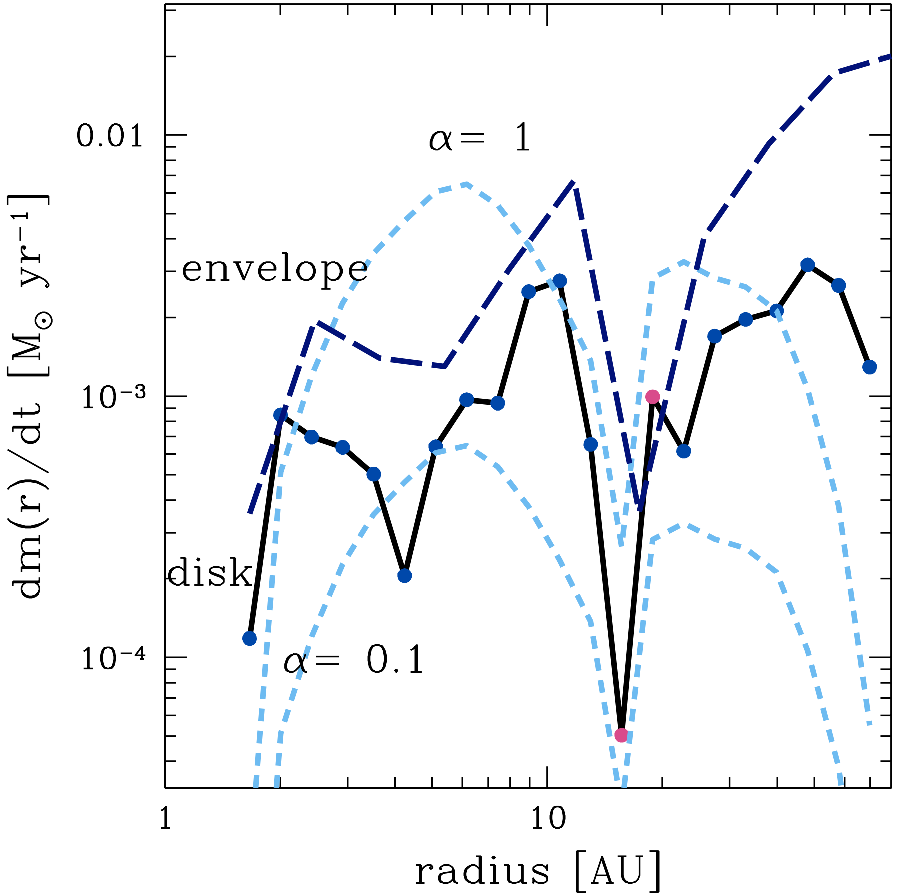

Figure 3: The mass transfer rate through the disk is denoted by the solid black line, while the mass infall rate through spherical shells with the specified radius is shown by the dark blue dashed line. The latter represents the total amount of material flowing through a given radius, and is thus a measure of the material flowing through *and onto* the disk at each radius. Both are shown at the onset of disk fragmentation. In the case of the disk accretion we have denoted annuli that are moving towards the protostar with blue dots, and those moving away in pink (further details can be found in Section 6 of the online material). The light blue dashed lines show the accretion rates expected from an 'alpha' (thin) disk model, where $\dot{M}(r) = 3\,\pi\,\alpha\,c_{\rm s}(r)\,\Sigma(r)\,H(r)$, with two global values of alpha and where $c_{\rm s}(r)$, $\Sigma(r)$, and $H(r)$ are (respectively) the sound speed, surface density and disk thickness at radius r.

(Clark et al. 2011b, Science, 331, 1040)

SPH study: comparison of all relevant heating and cooling processes

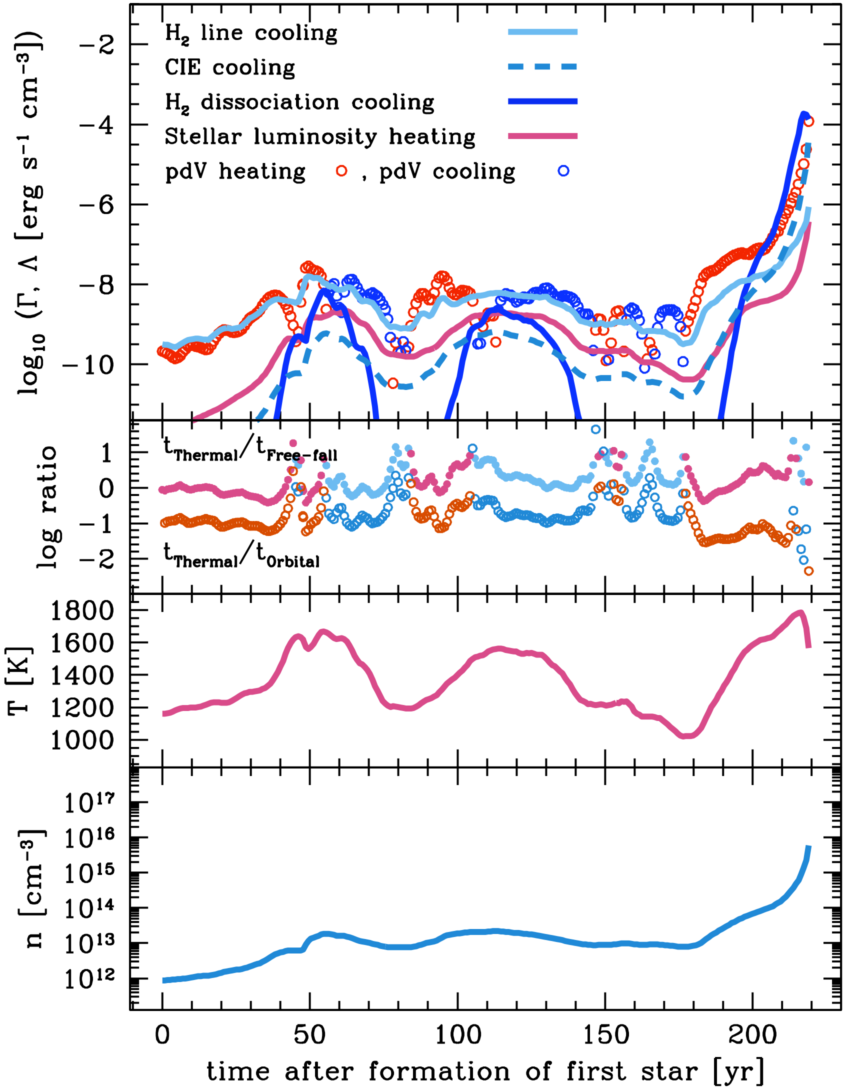

Figure 7: (a) Dominant heating and cooling processes in the gas that forms the second sink particle. (b) Upper line: ratio of the thermal timescale, $t_{\rm thermal}$, to the free-fall timescale, $t_{\rm ff}$, for the gas that forms the second sink particle. Periods when the gas is cooling are indicated in blue, while periods when the gas is heating are indicated in red. Lower line: ratio of $t_{\rm thermal}$ to the orbital timescale, $t_{\rm orbital}$, for the same set of SPH particles (c) Temperature evolution of the gas that forms the second sink (d) Density evolution of the gas that forms the second sink

(Clark et al. 2011b, Science, 331, 1040)

Arepo study: surface density at different times

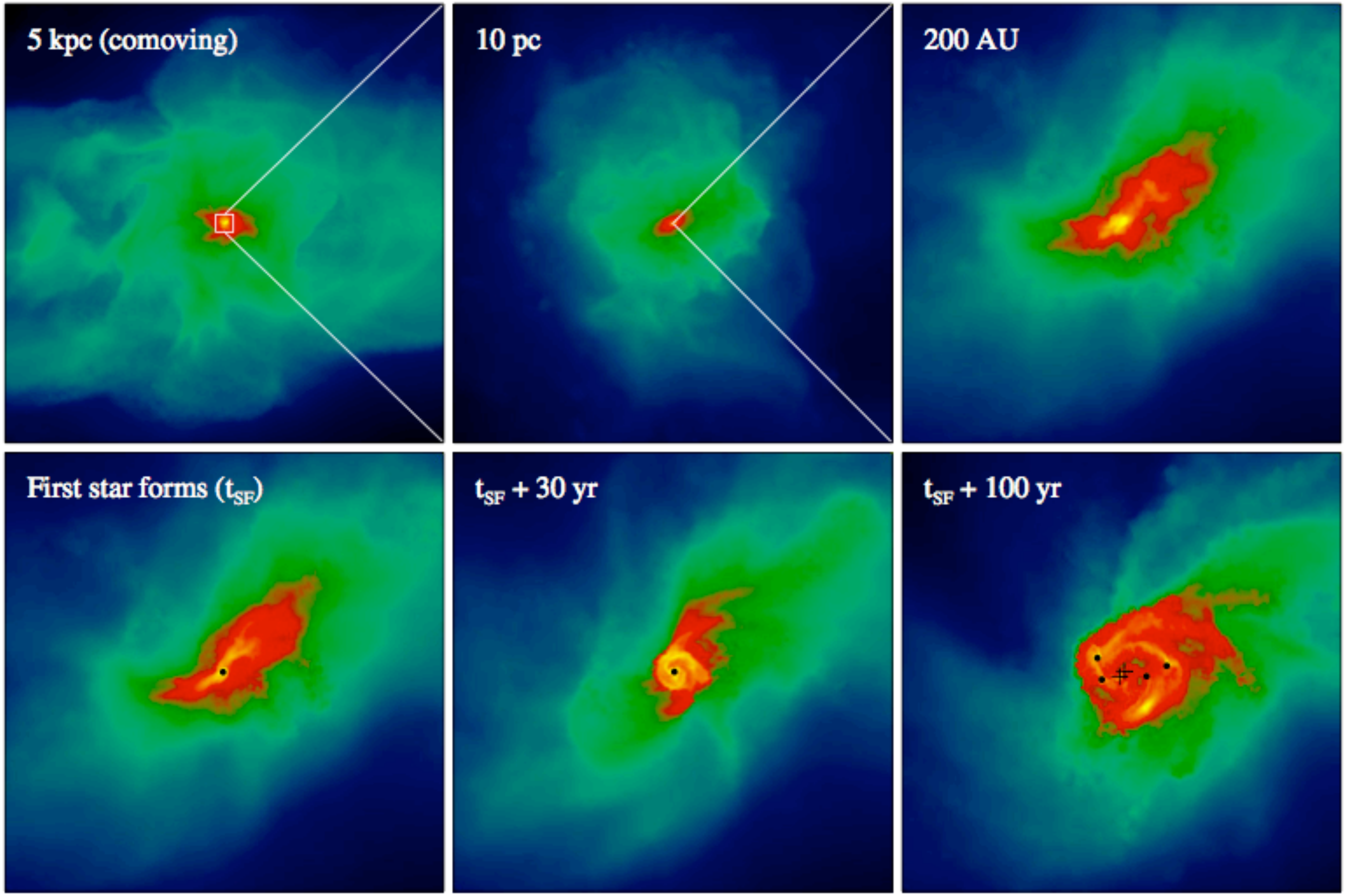

one out of five halos

(Greif et al. 2011a, submitted)

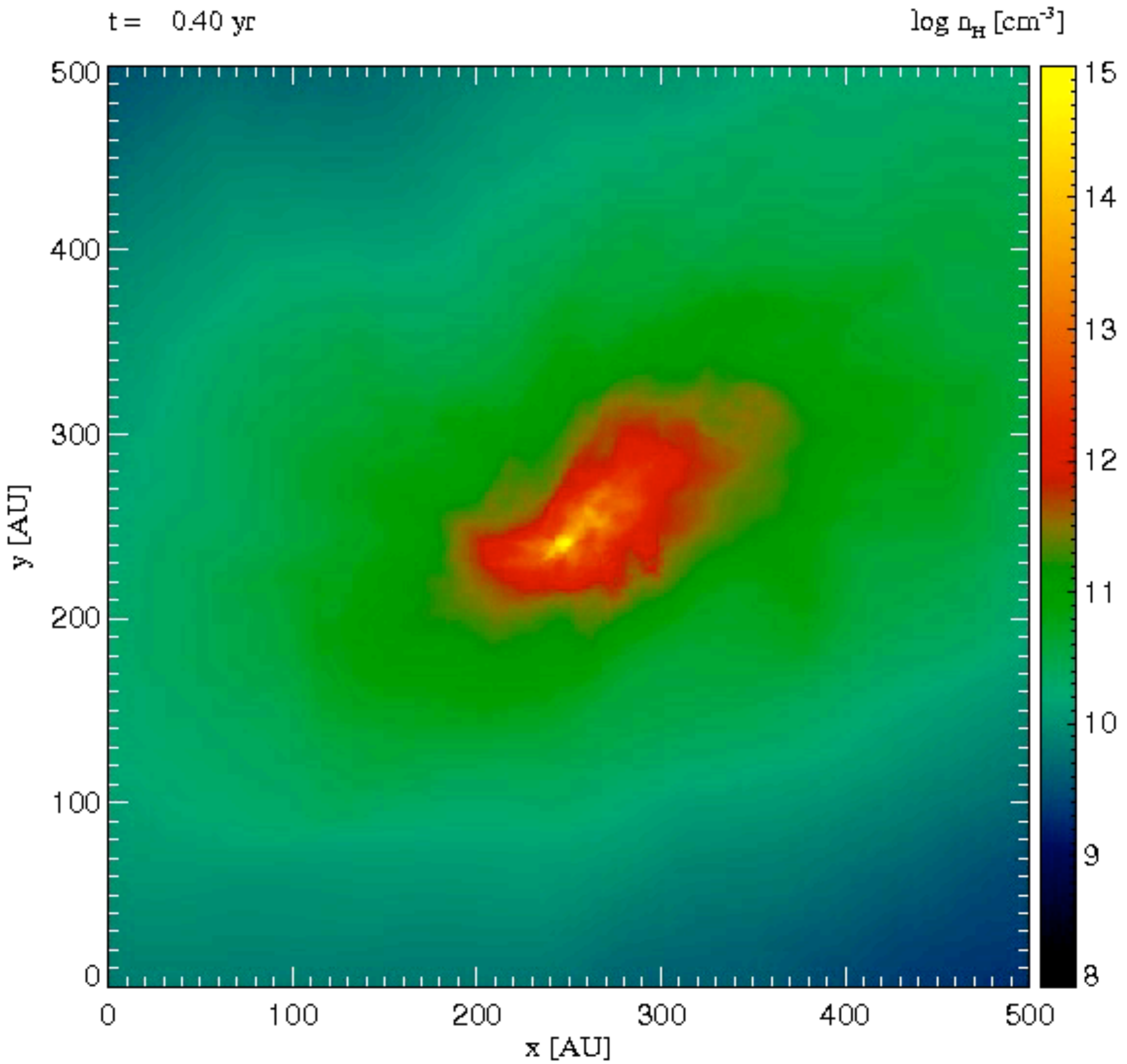

(Greif et al. 2011a, submitted)

Arepo study: mass spectrum of fragments

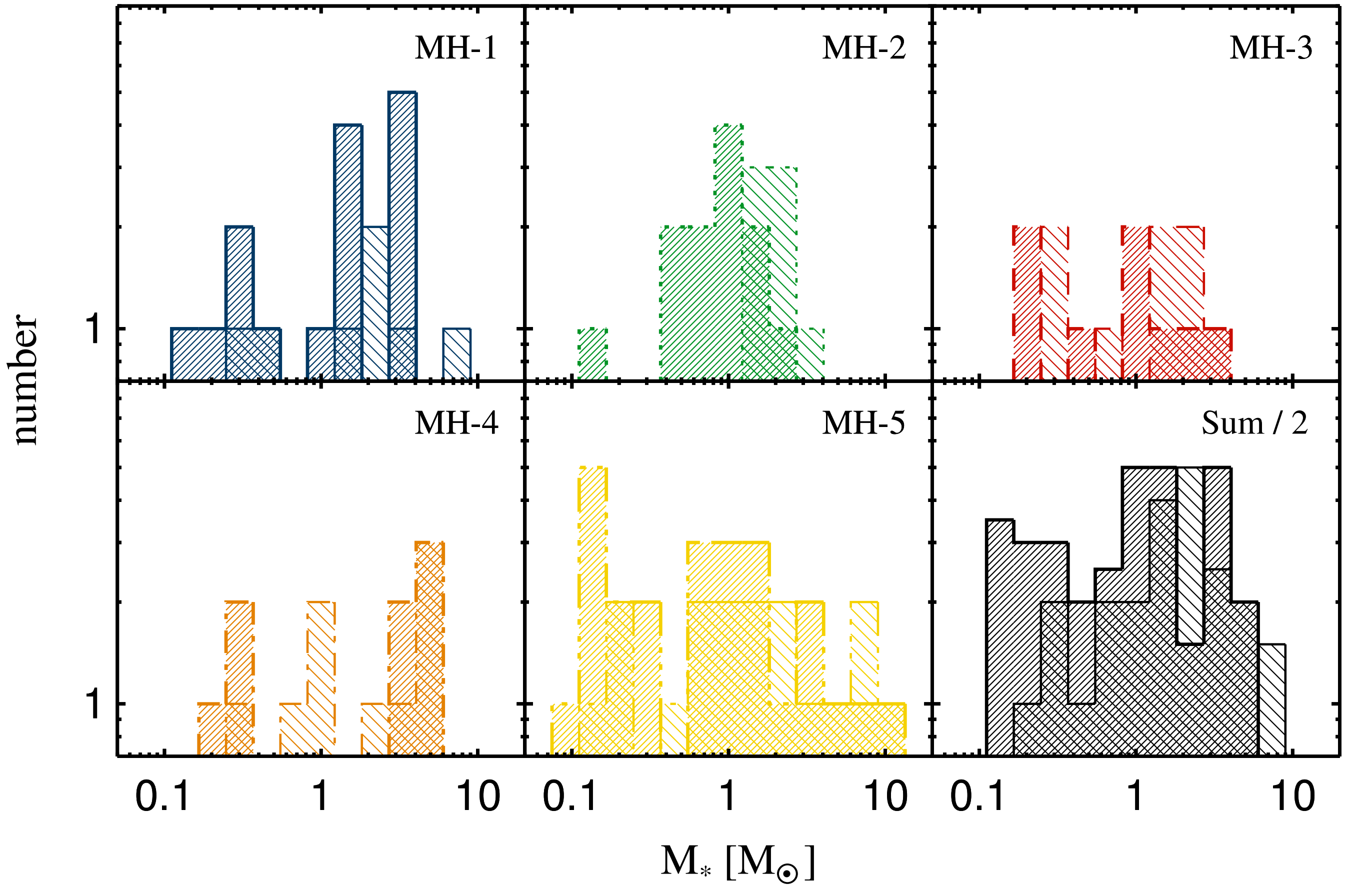

(Greif et al. 2011a, submitted)

primordial star formation

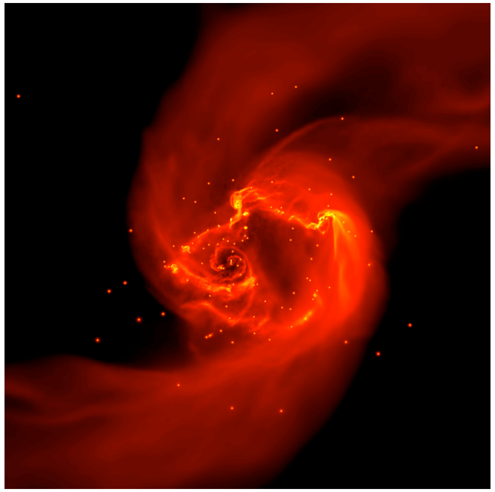

- just like in present-day SF, we expect
  - *turbulence*
  - *thermodynamics*
  - *feedback*
  - *magnetic fields*

  to influence Pop III/II star formation.
- masses of Pop III stars still *uncertain* (surprises from new generation of high-resolution calculations that go beyond first collapse)
- disks unstable: Pop III stars should be *binaries* or *part of small clusters*
- effects of feedback less important than in present-day SF

questions

- is claim of Pop III stars with $M \sim 0.5\ M_\odot$ really justified?
  - stellar collisions
  - magnetic fields
  - radiative feedback
- how would we find them?
  - spectral features
- where should we look?
- what about magnetic fields?

agenda

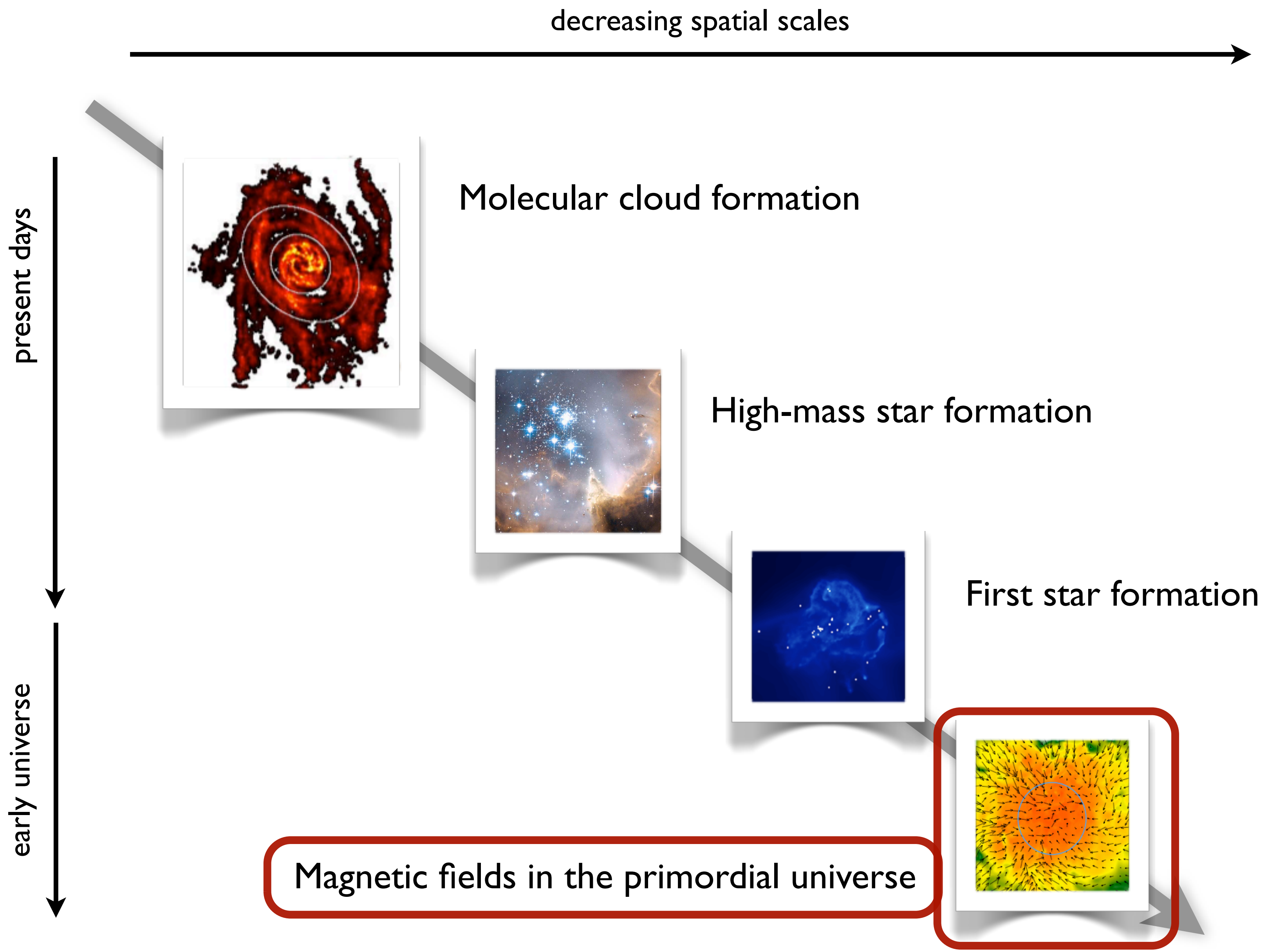
decreasing spatial scales
present days
early universe
Molecular cloud formation
High-mass star formation
First star formation
Magnetic fields in the primordial universe

B fields in the early universe?

- we know the universe is magnetized (now)
- knowledge about B-fields in the high-redshift universe is extremely uncertain
  - inflation / QCD phase transition / Biermann battery / Weibel instability
- they are thought to be extremely small
- however, *THIS MAY BE WRONG*!

small-scale turbulent dynamo

- *idea:* the small-scale turbulent dynamo can generate strong magnetic fields from very small seed fields
- *approach:* model collapse of primordial gas ---> formation of the first stars in low-mass halo at redshift z ~ 20
- *method:* solve ideal MHD equations with very high resolution
  - grid-based AMR code FLASH (effective resolution 65536^3)

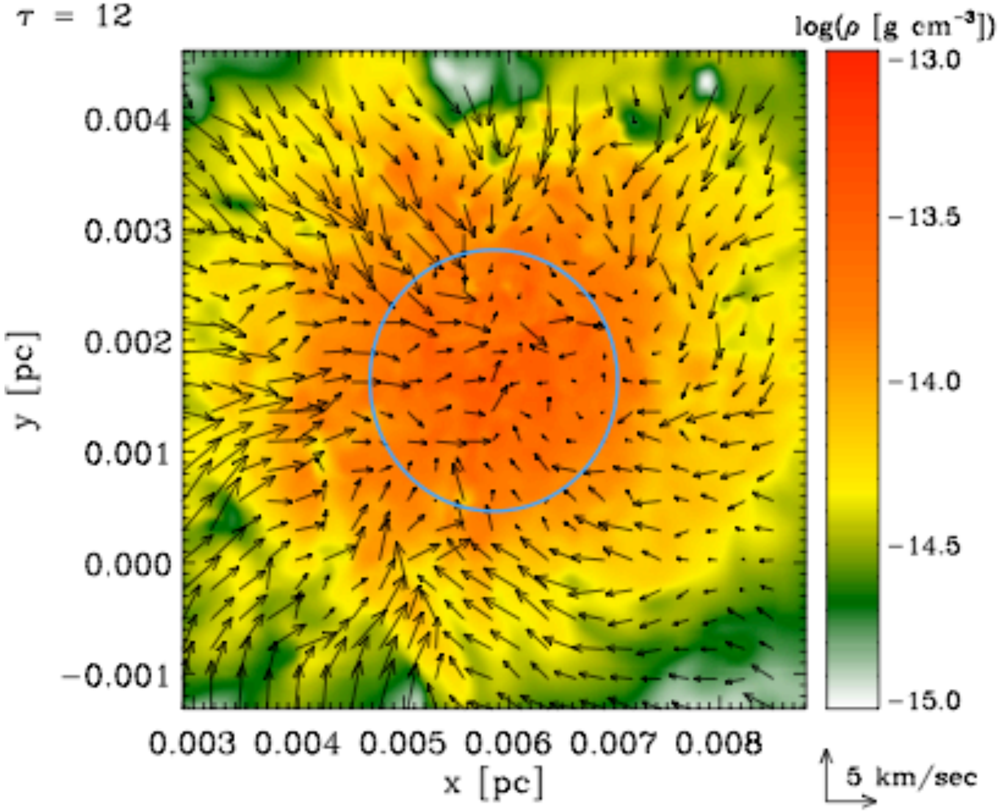

magnetic field structure

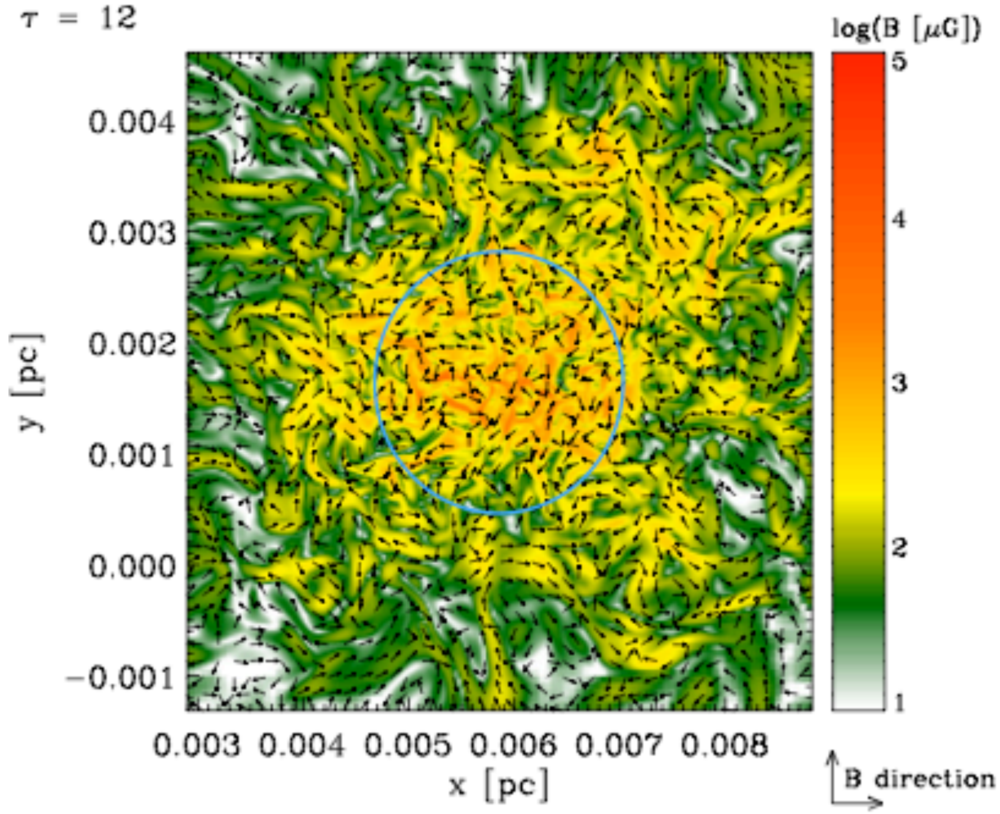

density structure

(Sur et al. 2010, ApJ, 721, L734)

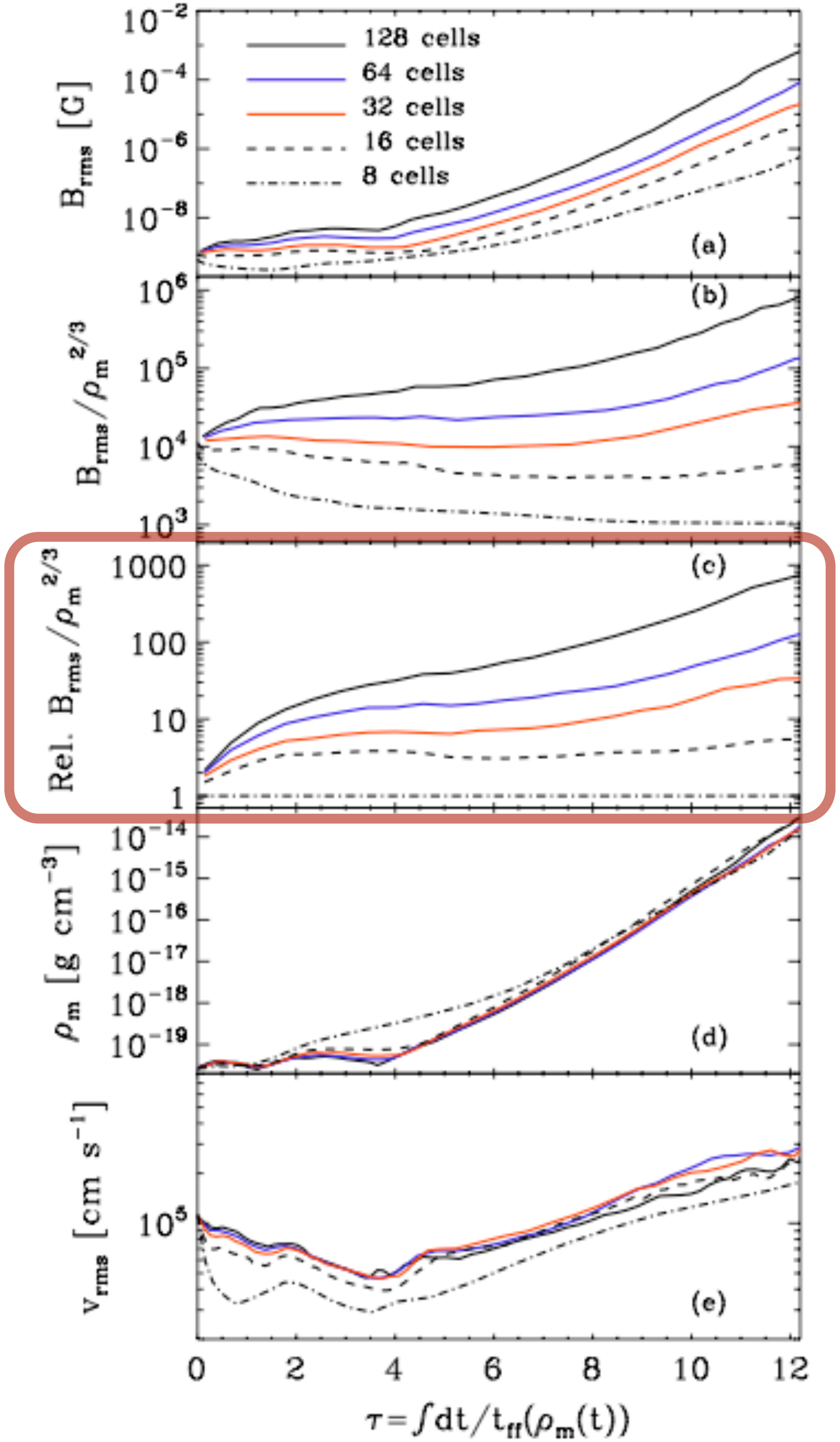

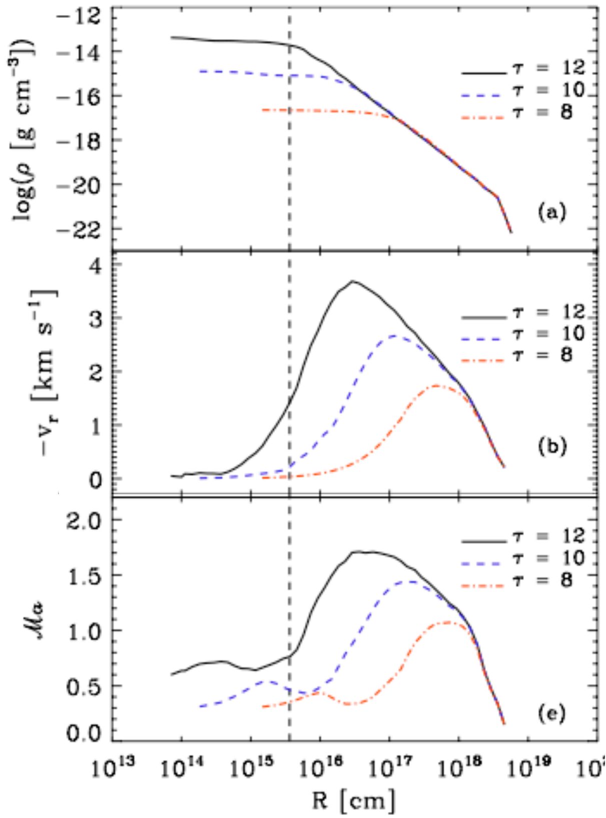

radial density profile

radial velocity profile

Mach number profile

Field amplification during first collapse seems unavoidable.

QUESTIONS:

- Is it really the small scale dynamo?
- What is the saturation value? Can the field reach dynamically important strength?

(Sur et al. 2010, ApJ, 721, L734)

analysis of magnetic field spectra

Slope +3/2 of
Kazantsev theory

(e.g. Brandenburg & Subramanian, 2005, Phys. Rep., 417, 1)

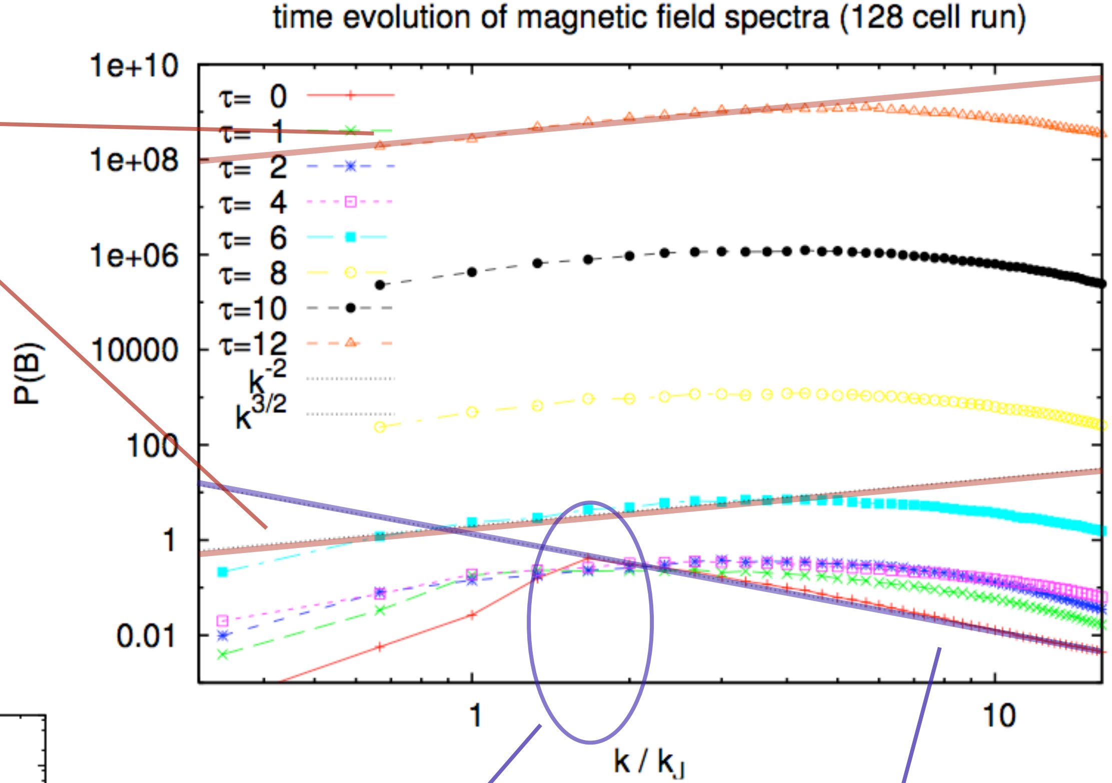

initial peak of
B fluctuation
spectrum

initial slope of
B fluctuations

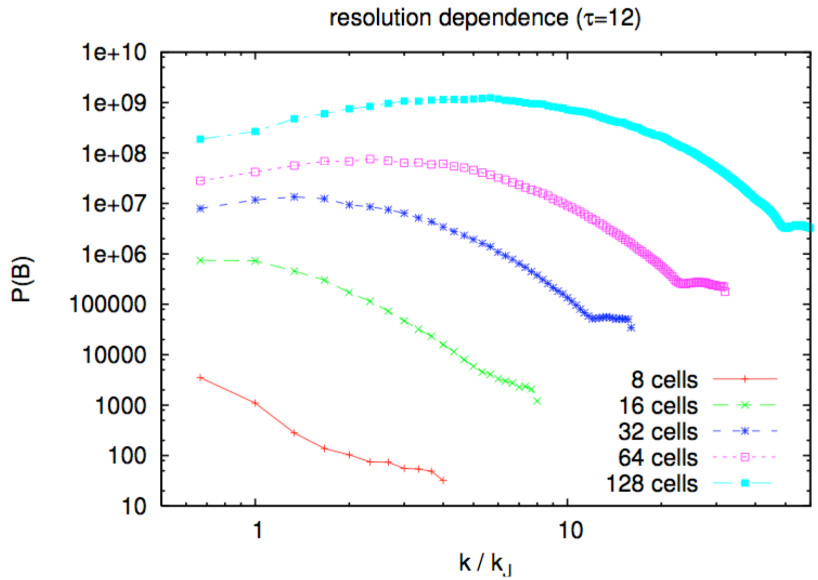

(Federrath et al., 2010, ApJ)

analysis of magnetic field spectra

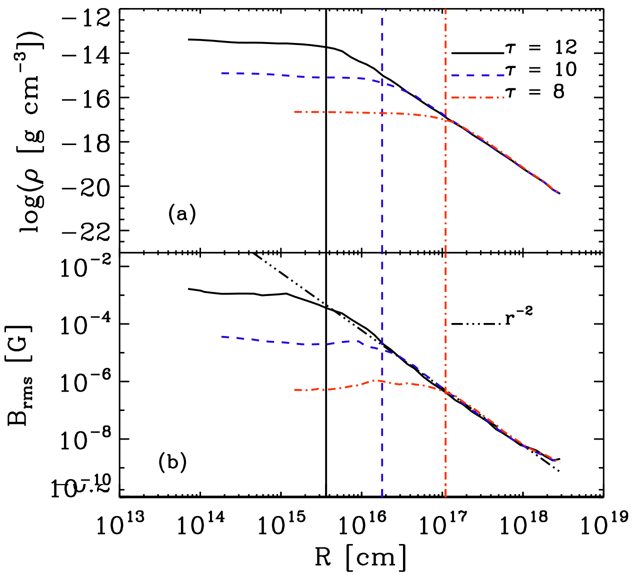

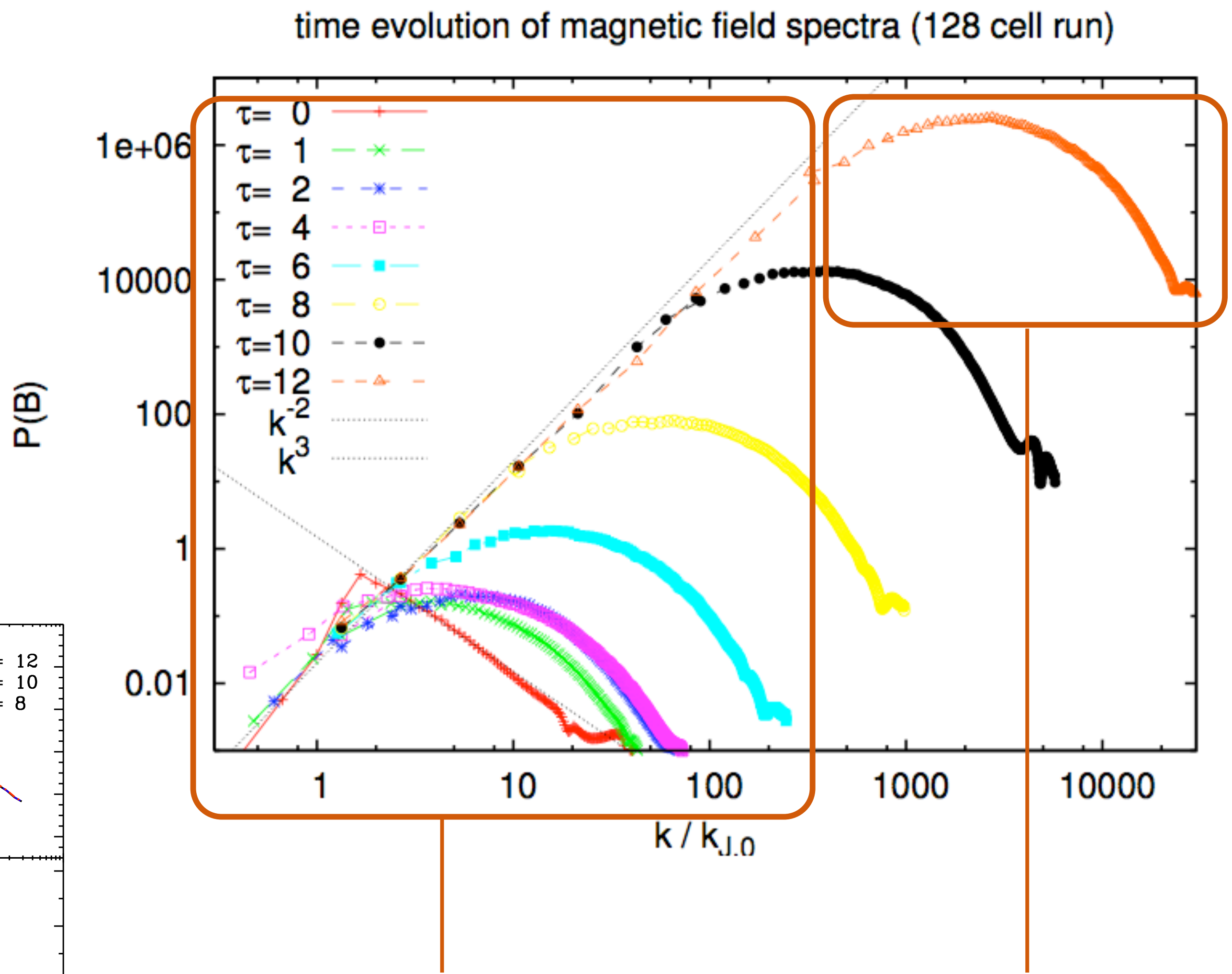

B fluctuation spectrum in $1/r^2$ fall-off

B fluctuation spectrum in flat inner core

(Federrath et al., 2010, ApJ)

first attempts to calculate the saturation level.

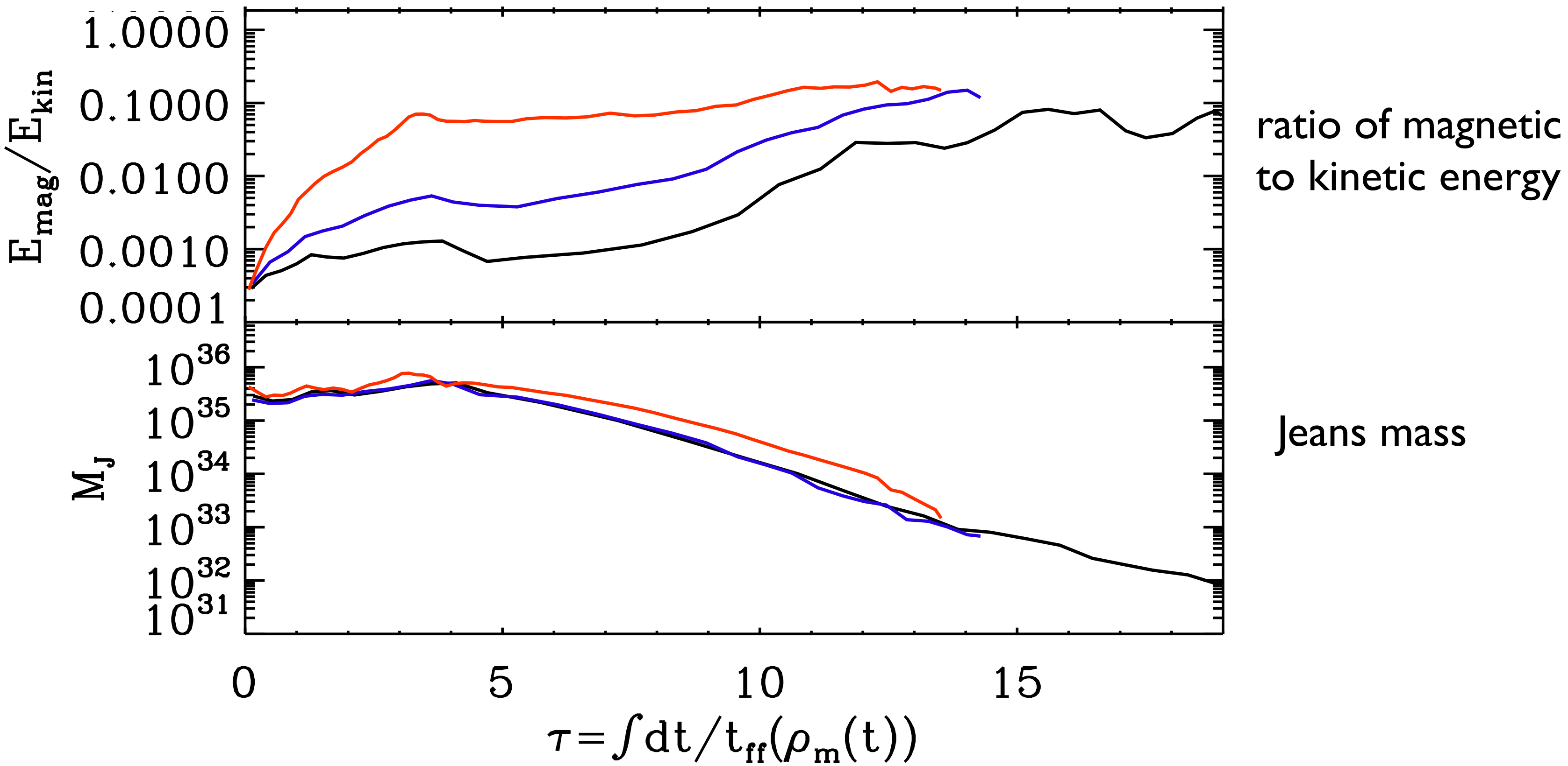

We seem to get a saturation level of ~10% (see, e.g., Subramanian 1997, or Brandenburg & Subramanian 2005)

QUESTIONS:
- Is this true in a proper cosmological context?
- What does it mean for the formation of the first stars

(Sur et al., in prep.)

questions

- *small-scale turbulent dynamo* is expected to operate during Pop III star formation
- process is *fast* (10^4 x t_{ff}), so primordial halos may collapse with B-field at *saturation level!*
- simple models indicate *saturation levels of ~10%* --> larger values via αΩ dynamo?
- *QUESTIONS:*
  - does this hold for "proper" halo calculations (with chemistry and cosmological context)?
  - what is the strength of the seed magnetic field?

summary

decreasing spatial scales

present days

early universe

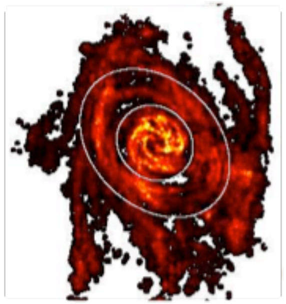

Galactic scale star formation

High-mass star formation

First star formation

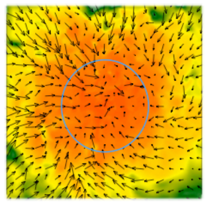

Magnetic fields in the primordial universe

(Sur et al., in prep.)

summary

decreasing spatial scales

present days

early universe

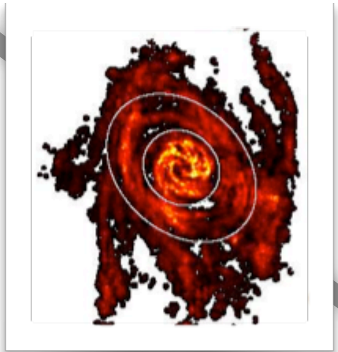

Molecular cloud formation

What are the initial conditions for MC formation?

How do star clusters form inside?

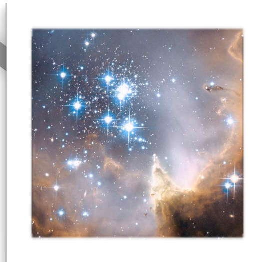

High-mass star formation:

What set upper stellar mass limit?

Can we see UC HII regions flicker?

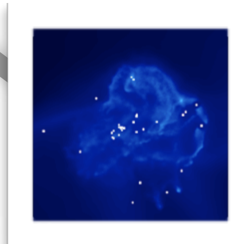

First star formation:

Are there still Pop III stars around?

How can we see them? And where?

Magnetic fields in the primordial universe:

Is there a minimum primordial field?

What is the influence of B on Pop III star?